UNIVERSITY OF CALIFORNIA, SAN DIEGO

TISSUE ENGINEERING OF CARTILAGINOUS GRAFTS WITH MECHANICALLY FUNCTIONAL AGGRECAN

A dissertation submitted in partial satisfaction of the

requirements for the degree Doctor of Philosophy

in

Bioengineering

by

EunHee Han

Committee in charge:

Professor Robert L. Sah, Chair
Professor David A. Gough
Professor Michael J. Heller
Professor Koichi Masuda
Professor Shyni Varghese

2011

The dissertation of EunHee Han is approved, and it is acceptable in quality and form for publication on microfilm and electronically:

_____

_____

_____

_____

_____

_____

Chair

University of California, San Diego

2011

DEDICATION

To the loving memory of appa

EPIGRAPH

We must not forget that when radium was discovered no one knew that it would prove useful in hospitals. The work was one of pure science. And this is a proof that scientific work must not be considered from the point of view of the direct usefulness of it. It must be done for itself, for the beauty of science, and then there is always the chance that a scientific discovery may become like the radium a benefit for humanity.

I am among those who think that science has great beauty. A scientist in his laboratory is not only a technician: he is also a child placed before natural phenomena which impress him like a fairy tale.

-Marie Curie

TABLE OF CONTENTS

Signature Page ..... **iii**

Dedication ..... **iv**

Epigraph ..... **v**

Table of Contents ..... **vi**

List of Figures ..... **xii**

List of Tables ..... **xv**

Acknowledgments ..... **xvi**

Vita ..... **xxi**

Abstract of the Dissertation ..... **xxiii**

Chapter 1 Introduction **1**

1.1 Composition, Structure, and Function of Articular Cartilage 1

1.2 Proteoglycan Aggregates in Articular Cartilage 7

1.3 Cartilage Tissue Engineering 19

1.4 Dissertation Objectives and Overview 26

1.5 References 29

Chapter 2 Shaped, Stratified, Scaffold-free Grafts for Articular Cartilage Defects 37

2.1 Abstract 37

2.2 Introduction 39

2.3 Materials and Methods 42

2.4 Results 49

2.5 Discussion 58

2.6 Acknowledgments 63

2.7 References 64

Chapter 3 Proteoglycan Osmotic Swelling Pressure Contribution to Compressive Properties of Articular Cartilage 68

3.1 Abstract 68

3.2 Introduction 70

3.3 Materials and Methods 73

3.4 Results 80

3.5 Discussion 92

3.6 Acknowledgments 98

3.7 References 99

Chapter 4 Tissue Engineering by Molecular Disassembly and Reassembly: Biomimetic Retention of Mechanically Functional Aggrecan in Hydrogel 103

4.1 Abstract 103

4.2 Introduction 105

4.3 Materials and Methods 108

4.4 Results 115

4.5 Discussion 124

4.6 Acknowledgments 130

4.7 References 131

Chapter 5 Compaction Enhances Extracellular Matrix Content and Mechanical Properties of Tissue-Engineered Cartilaginous Constructs 136

5.1 Abstract 136

5.2 Introduction 138

5.3 Materials and Methods 141

5.4 Results 148

5.5 Discussion 160

5.6 Acknowledgments 166

5.7 References 167

Chapter 6 Conclusions 172

6.1 Summary of Findings 172

6.2 Future Directions 176

6.3 References 181

Appendix A Determination of FCD and True CS and KS Values from Biochemical Assays 183

A.1 Introduction 183

A.2 Adjustments for DMMB Assay 184

A.3 Adjustments for Uronic Acid Assay 187

A.4 References 190

Appendix B Analysis of FCD_{EF}, π_{PG}, and σ_{CN} of Bovine Patello-Femoral Groove Cartilage 191

B.1 Materials and Methods 191

B.2 Results 191

B.3 Discussion..... 192

B.4 Reference..... 195

Appendix C Effect of Depth in Human Cartilage on Total and Extrafibrillar Water Content..... 196

C.1 Results..... 196

C.2 Discussion..... 196

Appendix D Analysis of Released HA Content in PBS..... 198

D.1 Materials and Methods..... 198

D.2 Results and Discussion..... 198

D.3 Reference..... 200

Appendix E Analysis of Confined Compression Testing Set-up..... 201

E.1 Materials and Methods..... 201

E.2 Results and Discussion..... 202

Appendix F Analysis of Retention of Initial Matrix Content After Compaction..... 204

F.1 Materials and Methods..... 204

F.2 Results and Discussion..... 204

F.3 References 207

LIST OF FIGURES

Figure 1.1: Articular cartilage: length scales 4

Figure 1.2: Zonal variations in articular cartilage 5

Figure 1.3: Proteoglycan and collagen contribution to cartilage mechanical properties 6

Figure 1.4: Proteoglycan aggregate 9

Figure 1.5: Structure of chondroitin sulfate and keratan sulfate 18

Figure 1.6: Articular cartilage defects 24

Figure 1.7: Cartilage repair strategies 25

Figure 2.1: Schematic of fabrication of shaped, scaffold-free cartilaginous constructs 48

Figure 2.2: Macroscopic images of shaped cartilaginous constructs 51

Figure 2.3: 3D surface contours of half of constructs 52

Figure 2.4: Biochemical content of constructs 54

Figure 2.5: Safranin-O histochemical sections of constructs 55

Figure 2.6: Fluorescence and phase micrographs of stratified constructs 56

Figure 2.7: Quantification of stratification in constructs 57

Figure 3.1: Biochemical data for bovine and human cartilage 84

Figure 3.2: FCD-π_{PG} curve fit 85

Figure 3.3: FCD and π_{PG} with EF water 86

Figure 3.4: FCD_{EF} for bovine and human cartilage 87

Figure 3.5: π_{PG}, σ_{EQ}, and σ_{CN} for bovine cartilage 88

Figure 3.6: π_{PG}, σ_{EQ}, and σ_{CN} for human cartilage 89

Figure 3.7: CN pre-stress and compression level at σ_{CN}=0 90

Figure 3.8: Strain, FCD_{EF}, π_{PG}, and σ_{CN} for human cartilage with depth 91

Figure 4.1: S-1000 chromatograms of % sGAG content 118

Figure 4.2: Biochemical analysis on release and retention of PG components 119

Figure 4.3: Visualization of SDS PAGE for LP 120

Figure 4.4: Histological staining on constructs at day 3 for PG components 121

Figure 4.5: Compression properties of day 3 constructs 122

Figure 4.6: Histo- and immuno-chemical staining on constructs with chondrocytes after 2 days of culture 123

Figure 5.1: Macroscopic construct images 152

Figure 5.2: Dimension of constructs 153

Figure 5.3: Biochemical content of constructs 154

Figure 5.4: Staining of constructs for sGAG and collagen type II 155

Figure 5.5: Compressive properties of the constructs during and after compaction .. 156

Figure 5.6: Stress-compression relationship of the constructs during and after compaction 157

Figure 5.7: Prediction of PG contribution to compressive properties by π_{PG} 158

Figure 5.8: Live/dead staining of chondrocytes in compacted constructs 159

Figure 5.9: Schematic of application of matrix assembly, compaction, and shaping cartilaginous constructs 165

Figure 6.1: Schematic of cartilage tissue engineering by assembly 180

Figure B.1: Biochemical analysis of bovine PFG cartilage 193

Figure B.2: FCD_{EF}, π_{PG}, σ_{EQ}, and σ_{CN} of bovine PFG cartilage 194

Figure C.1: Total water and extrafibrillar water content with depth of human cartilage 197

Figure D.1: HA content analysis 199

Figure E.1: Analysis of confined compression tests 203

Figure F.1: Matrix content of day 0 constructs and final compacted constructs 206

LIST OF TABLES

Table 2.1: Quantification of shape of constructs 53

Table 3.1: Constants for the 4-segment quadratic equation fit to FCD–π_{PG} data 79

Table 4.1: Experimental groups 114

Table 5.1: Experimental groups 147

Table A.1: Chondroitin sulfate and keratan sulfate information..... 189

ACKNOWLEDGMENTS

This dissertation has been one of the most challenging and rewarding things I have accomplished. Needless to say, this would not have been possible without the help and encouragements of many people along the way. It truly does take a village!

First and foremost, I would like to thank Dr. Sah for his guidance and mentorship these past 9 years, starting when he allowed me to join the lab as a sophomore and then when he became my BMES advisor, professor, and now thesis advisor. I first was amazed by his devotion to education, especially for the undergraduates, and now by his scientific vision, dedication, patience, and generosity with time. He allowed me the freedom to take a histology class at the School of Medicine, to meander into the wonderful world of electron microscopy, although not used in this dissertation, and to "play around in the lab." While they made my life more difficult at times, I am immensely thankful for his uncompromising, meticulous, and rigorous approach to research and demand for excellence. They have challenged me to become a better bioengineer in research and in communication, and this dissertation certainly would not be what it is today without them. I finish here with the knowledge that I am well trained for whatever my future steps will be.

I also would like to thank Dr. Koichi Masuda for his valuable insights and feedback on this thesis, especially with alginate recovered chondrocyte method and proteoglycan biochemistry, which was instrumental for a major part of this dissertation. I would like to acknowledge Dr. Shyni Varghese for her helpful discussions and suggestions about hydrogels during development of the methods

described in Chapter 4. I thank my other committee members, Dr. David Gough and Dr. Michael Heller, for their input to this dissertation.

Chapter 2, in full, is reproduced from Clinical Orthopaedics and Related Research, volume 466, issue 8, 2008 with permission from Springer. The dissertation author is the primary investigator and thanks co-authors, Drs. Won C. Bae and Nancy D. Hsieh-Bonassera, Mr. Van W. Wong, Mrs. Barbara L. Schumacher, and Drs. Simon Görtz, Koichi Masuda, William D. Bugbee, and Robert L. Sah for their contributions to this work.

Chapter 4, in full, is reproduced from Tissue Engineering Part C Methods with permission from Mary Ann Liebert, Inc. The dissertation author is the primary investigator and thanks co-authors, Ms. Lissette Wilensky, Mrs. Barbara Schumacher, and Drs. Koichi Masuda and Robert Sah for their contributions to this work.

Chapters 3 and 5 are being prepared for publication. The dissertation author is the primary author and thanks co-authors Drs. Silvia Chen, Stephen Klisch, and Robert Sah for their contribution to the work in Chapter 3 and Mr. Chenghao "Charles" Ge, Mrs. Barbara Schumacher, and Drs. Albert Chen, and Robert Sah for their contribution to the work in Chapter 5.

My teachers in my formative years were crucial in getting this girl interested in science and fostering that interest. Mrs. KoongJa Lauridsen, my 5th and 6th grade teacher, showed me that science is fascinating and important even when I hardly knew any English. The unabashed enthusiasm of my 8th grade science teacher, Mrs. Edwina Williams, for all things science has left an indelible mark in my life and career path. My McNair Program coordinator Dr. Norienne Saign was instrumental in getting me

into Dr. Sah's lab and encouraging this first-generation college student to strive for graduate/professional school. To these women, thank you so much for all your investment in me. I am truly a product of the educational programs designed to encourage girls and under-privileged students in science and higher degrees.

A very special and huge thank-you to Barb Schumacher, the "lab mom". Barb taught me how to dissect my first bovine calf knee when I was a sophomore, and her scientific knowledge and willingness to answer my many cartilage biochemistry and proteoglycan questions has been invaluable. I've learned from her that "this is why it's called re-re-search!" Beyond science, I am thankful for her ever-ready warm words of support and encouragement, especially these past two years.

Much thanks goes to the two undergrads who worked with me: Lissette Wilensky, who kept me company with irresistible enthusiasm through hundreds of DMMB plates and numerous S-1000 columns, and Charles Ge, who helped with not-so-glamorous collagen and proteoglycan preparations. They have bright futures ahead of them, and I hope I was able to contribute to their growth.

CTE is a very special place because of all the wonderful, creative, generous people who make up this unit. I have benefited tremendously from working along side them. Thank you to Dr. Albert Chen, who is an immense resource for all things compression test- and dynastat-related. Dr. Michele Temple-Wong has been a valuable resource on biochemical plate assays and statistical analysis. I am very grateful to the lab staff who kept and keep the lab running in tip-top shape, including Dr. Michael Voegtline (and his chocolate mint patties), Tae Kim, Carrie Wirt, Leo Schumacher, Johnny Du, and most importantly Van Wong with his technical wizardry

of every machine and program in lab, answers to my numerous questions about where equipments and supplies are, and random sports/news/Lego conversations. To Van's army of lab assistants (Jason, Dorinda, Gina, Jeff, Christella, Jesse, Joannah, Alina, Nitin, Daniel), thanks for keeping the lab well-stocked.

There are many graduate students from (way) past and present to acknowledge during my long stay in the CTE lab. I am grateful to Dr. Tannin Schmidt, my graduate student mentor during my undergraduate years for showing me the ropes. Thank you to the older grad students who I was too scared to talk to as an undergrad but eventually learned to talk to and gain valuable insights from: Drs. Won Bae, Michele Temple-Wong, Travis Klein, Kevin McGowan, Kyle Jadin, Gayle Nugent, Kanika Chawla, Anya Asanbaeva, Ken Gratz, Megan Blewis, Nancy Hsieh-Bonassera, Ben Wong, and Greg Williams. I also have been privileged to spend my time with these recent and present CTErs who have shared their insights, food creations, and laughs: Dr. Jen Hwang, Jen Antonacci, Hoa Nguyen, Andrea Pallante, Bill McCarty, Elaine Chan, Brad Hansen, Alex Hui, Jerome Hollenstein, Felix Hsu, and Neil Chang. Thanks to the two "corners" in the lab and in the office pod, with Hoa, Andrea, Elaine, and Jen A, for the times of sharing, encouragements, and laughter. Because of my experience as a shy, scared undergrad, I made it a point to introduce myself to the new lab undergrads; I hope I've made a difference with that. :)

Thank you to Jessica Yuen, Denise Bogard Lindberg, and Clare Huang, my dear college friends and roommates, for cheering me along the way with our get-togethers and rounds of emails. To my roommates, Dr. Joyce Chuang and soon-to-be

Dr. Maika Onishi, thanks for sampling my cooking and baking experiments and for the late night chats.

My Lighthouse Bible Church family has been there from the beginning of my grad school journey, and I thank them for their constant encouragements, support, prayers, and love, especially in the most difficult and trying times. To Kaitlyn Oh Tou, Elaine Lau Sarmiento, Karen Ngai Fong, Lillian To, Tina Huyhn, Jen Shih, Andrea Lem, Ada Shao, and Jen Park: thanks for snapping me out of the grad school bubble and into a more balanced life with the eternal perspective. I am very much looking forward to the time I'll now have to bake, cook, brunch, watch Jane Austen, golf, laugh, maybe even run, and grow with you all!

My parents, Peter Dong Keun and Susan Myung Sook Han, sacrificed so much and worked tirelessly in a new country where they did not speak the language so that their daughters would have better lives. My dad's cirrhosis was the reason for my interest in tissue engineering, introduced to me through the pages of the *Los Angeles Times*. He has been my inspiration and driving force for this journey. Appa, I know that you were immensely proud of me, and I hope you are proud today as well even though you are no longer with me here. Umma, thank you for telling me time and time again to take it "차근 차근히", one step at a time, and for your love, encouragements, and many sacrifices for my education. To my sister EunSook, thank you so much for the perspectives, reassurances, and sacrificed days and weekends to run errands for mom and dad to the hospital so that I can stay in SD to work. To my family, you have been the steadying force in this turbulent journey, and I love you. 고맙고 사랑해요!

And lastly and most importantly, Soli Deo Gloria.

VITA

2004	B.S., Bioengineering: Biotechnology University of California-San Diego, La Jolla, California
2004-2011	Graduate Student Researcher Cartilage Tissue Engineering Laboratory University of California-San Diego, La Jolla, California
2007	M.S., Bioengineering University of California-San Diego, La Jolla, California
2011	Ph.D., Bioengineering University of California-San Diego, La Jolla, California

Book Chapter

Schmidt TA, Schumacher BL, **Han EH**, Klein TJ, Voegtline MS, Sah RL: Chemo-mechanical coupling in articular cartilage: IL-1 alpha and TGF-beta 1 regulate chondrocyte synthesis and secretion of lubricin/superficial zone protein. Physical Regulation of Skeletal Repair, ed by RK Aaron and ME Bolander, American Academy of Orthopaedic Surgeons, Chicago, 2005.

Journal Articles

Han EH, Chen SS, Klisch SM, Sah RL. Proteoglycan osmotic swelling pressure contribution to compressive properties of articular cartilage. *submitted*.

Han EH, Ge C, Chen AC, Schumacher BL, Sah RL. Enhancement of extracellular matrix content and mechanical properties of tissue engineered cartilaginous constructs by mechanical compaction. *submitted*.

Falcovitz Degrassi Y, Shieh AK, **Han EH**, Nguyen QT, Chen SS, Maroudas A, Sah RL. Compressive properties of normal human articular cartilage: Age, depth, and compositional dependencies. *submitted*.

Han EH, Wilensky LM, Schumacher BL, Chen AC, Masuda K, Sah RL. Tissue engineering by molecular disassembly and reassembly: biomimetic retention of mechanically functional aggrecan in hydrogel. *Tissue Eng Part C Methods*, 2010 Dec; 16(6): 1471-9.

Han EH, Bae WC, Hsieh-Bonassera ND, Wong VW, Schumacher BL, Gortz S, Masuda K, Bugbee WD, Sah RL. Shaped, stratified, scaffold-free grafts for articular cartilage defects. *Clin Orthop Relat Res*, 2008 Aug; 466(8):1912-20.

Schmidt TA, Gasteulm NS, **Han EH**, Nugent GE, Schumacher BL, Sah RL.

Differential regulation of proteoglycan 4 metabolism in cartilage by IL-1 alpha, IGF-I, and TGF-beta 1. *Osteoarthritis Cartilage*, 2008 Jan;16(1):90-7.

Conference Abstracts

Han EH, Sah RL. Incorporation of CS:KS ratio and collagen extrafibrillar water content into osmotic pressure model to study compressive properties of articular cartilage. *Trans Orthop Res Soc* 57:0163, 2011.

Han EH, Chen AC, Sah RL: Prediction of aggrecan osmotic pressure accounting for CS:KS ratio and collagen extrafibrillar water content. *Am Soc Matrix Bio* :107, 2010

Han EH, Wilensky LM, Schumacher BL, Masuda K, Sah RL. Tissue engineering by molecular disassembly and reassembly: biomimetic aggregation to tune the retention of mechanically-functional aggrecan. *Trans Orthop Res Soc*, 35:258, 2010.

Han EH, Wilensky LM, Schumacher BL, Masuda K, Sah RL. Biomimetic reassembly of proteoglycan aggregate for natural enhancement of tissue-engineered hydrogel. *Trans Tiss Eng Regen Med Intnl Soc-World Congress*, 2:1023, 2009.

Han EH, Bae WC, Wong VW, Masuda K, Bugbee WD, Sah RL. Shaped, scaffold-free cartilaginous constructs for articular cartilage defects. *Trans Orthop Res Soc*, 32:1529, 2007.

Han EH, Bae WC, Wong VW, Hsieh-Bonassera ND, Masuda K, Bugbee WD, Sah RL. Shaped, scaffold-free cartilaginous constructs for articular cartilage defects. *California Tissue Engineering Meeting*, Davis, CA, 2006.

Chawla K, Jadin KD, Schumacher BL, **Han EH**, Hwang J, Huynh NT, Bae WC, Lewis CL, Kitahara S, Masuda K, Sah RL. Effects of stratification of cartilaginous tissue implants on early in vivo repair of articular defects. *Int Cart Repair*, 6:3-55, 2006.

Schmidt TA, Schumacher BL, **Han EH**, Klein TJ, Voegtline MS, Sah RL. Synthesis and secretion of lubricin/superficial zone protein by chondrocytes in cartilage explants modulated by TGF-b1 and IL-1a. Trans Orthop Res Soc, 29:577, 2004.

ABSTRACT OF THE DISSERTATION

TISSUE ENGINEERING OF CARTILAGINOUS GRAFTS WITH MECHANICALLY FUNCTIONAL AGGRECAN

by

EunHee Han

Doctor of Philosophy in Bioengineering

University of California, San Diego, 2011

Professor Robert L. Sah, Chair

The main extracellular matrix components of articular cartilage, proteoglycans (PG) and collagens (COL), and their interaction with each other provide the unique biomechanical properties that vary with development, aging, and depth from the articular surface. Negatively-charged aggrecan (AGC), composing ~90% of PG, is mainly responsible for the compressive resistance, the fixed charge density (FCD), and the high osmotic pressure (π_{PG}) within the tissue. The COL network (CN) provides the restraint that counterbalances π_{PG} at rest or in compression. This dissertation analyzes the engineering of mechanically functional aggrecan-laden cartilaginous grafts by elucidating the role of PG and its interaction with COL in the compressive properties

of articular cartilage and by developing rapid novel methods for shaping, assembling, and concentrating matrix-laden constructs.

The application of a refined FCD–π_{PG} relationship to native cartilage demonstrated that extrafibrillar FCD and π_{PG} change with growth, age and depth of the tissue. Mature cartilage from bovine calf, adult and human young sources had higher FCD_{EF} and π_{PG} than immature (bovine fetal) or aged (human old) tissue due to COL content variations. Depth-related variations in the strain, FCD_{EF}, π_{PG}, and σ_{CN} profiles for human cartilage revealed the loss of a functional superficial layer in aged cartilage. These findings in native tissue provided guidance for engineered constructs and novel methods for the assembly cells and matrix components in engineered constructs to modulate shape, AGC retention, and matrix content. Molding of chondrocyte-based constructs resulted in shaping on one, two, or neither construct surfaces in combination with biomimetic layering of the chondrocyte subpopulations. Addition of PG aggregates, consisting of AGC with hyaluronan and link proteins, to hydrogel constructs resulted in rapid assembly, enhanced AGC retention, and increased the construct compressive stiffness. Further, the addition of COL to PG-hydrogel constructs increased the compressive properties, highlighting the importance of PG-COL interaction in mechanical function. Finally, the mechanical compaction of these constructs rapidly increased the matrix concentrations and material properties.

These results may be useful in rapidly engineering mechanically functional cartilaginous grafts and facilitate for more rapid application of the grafts into the mechanical demanding environment of an *in vivo* joint.

CHAPTER 1

INTRODUCTION

1.1 Composition, Structure, and Function of Articular Cartilage

Articular cartilage is a glossy, smooth connective tissue found at the ends of long bones (Fig. 1.1). This load-bearing, low-friction, and wear-resistant material in articulating joints, such as the knee and the hip, are designed to last a lifetime [17]. Adult articular cartilage consists of chondrocytes, which contribute less than 5% of the total wet weight (WW), and various extracellular matrix (ECM) components, including collagens (10-20% WW) and proteoglycans (5-10% WW) [64]. Fibrillar collagens, composed mostly of type II collagen (>90%), form a tight network that contains the chondrocytes and proteoglycans. The core of the fibril contains type XI collagen surrounded by type II collagen with type IX collagen on the surface of the fibrils [15]. About 90% of the proteoglycan mass comes from large aggregating proteoglycans, primarily aggrecan in articular cartilage [17]. Aggrecan monomers, each with large numbers of negatively-charged glycosaminoglycan (GAG) chains, non-covalently associate with a hyaluronan (HA) chain and link proteins (LP) to form proteoglycan aggregates. In addition to aggrecans, there are various small leucine-rich

proteoglycans, such as decorin, fibromodulin, biglycan, and lumican, which may have important roles in matrix organization [73].

The chondrocytes and ECM in articular cartilage are organized in an inhomogeneous fashion, from the articular surface toward the bone as well as from the chondrocyte to out into the interterritorial matrix (Fig. 1.2). The top 10-20% of full-thickness cartilage from the surface, the superficial zone, is most cellular region with a highly compacted and uniform population of thin collagen fibrils that are organized parallel to the articular surface, which help to resist the shear forces during joint articulation. The middle zone, occupying 50-60% of the overall thickness below superficial zone, contains more randomly organized collagen fibrils that have a larger average diameter. Proteoglycan content increases in the middle and deep zone with depth of cartilage. Just above the calcified cartilage, the deep zone contains chondrocytes arranged in columns along with mostly thick, vertical collagen fibrils and a subpopulation of thinner collagen fibrils that are arranged more isotropically [17]. The matrix also varies with distance from the chondrocytes. The pericellular matrix that surrounds the chondrocytes contains thin fibril collagen with diameters <20 nm and without any remarkable banding pattern observed under transmission electron microscope. These fibrils tend to be short and appear to form a nest of fibrils around the chondrocyte. Farther away from the cell, the territorial and interterritorial matrix contains collagen fibrils that gradually increase in diameter and contain the d-band pattern, characteristic of collagen fibrils [45].

The organization of matrix imparts mechanical function to normal articular cartilage. The osmotic swelling pressure resulting from the high fixed charge density

from the carboxyl and sulfate groups of GAGs provides the compressive resistance in cartilage (Fig. 1.3). The collagen network counterbalances this swelling pressure of GAGs with the restraining force while providing tensile resistance [56]. The sum of the contributions from PG and collagen network provides the unique biomechanical properties of cartilage that is much stiffer in tension than in compression. Due to the variations in biochemical content and organization, the mechanical properties of articular cartilage vary with depth from the articular surface [77] and distance from the chondrocytes [1]. ECM organization within the tissue imparts the higher shear tensile strength in the superficial zone and higher compressive strength in the deeper zones of cartilage [64]. The thin collagen fibrils in pericellular matrix running parallel to the cell surface protect the chondrocytes from mechanical force while the larger collagen fibrils in the interterritorial matrix provide the mechanical strength of the tissue [15].

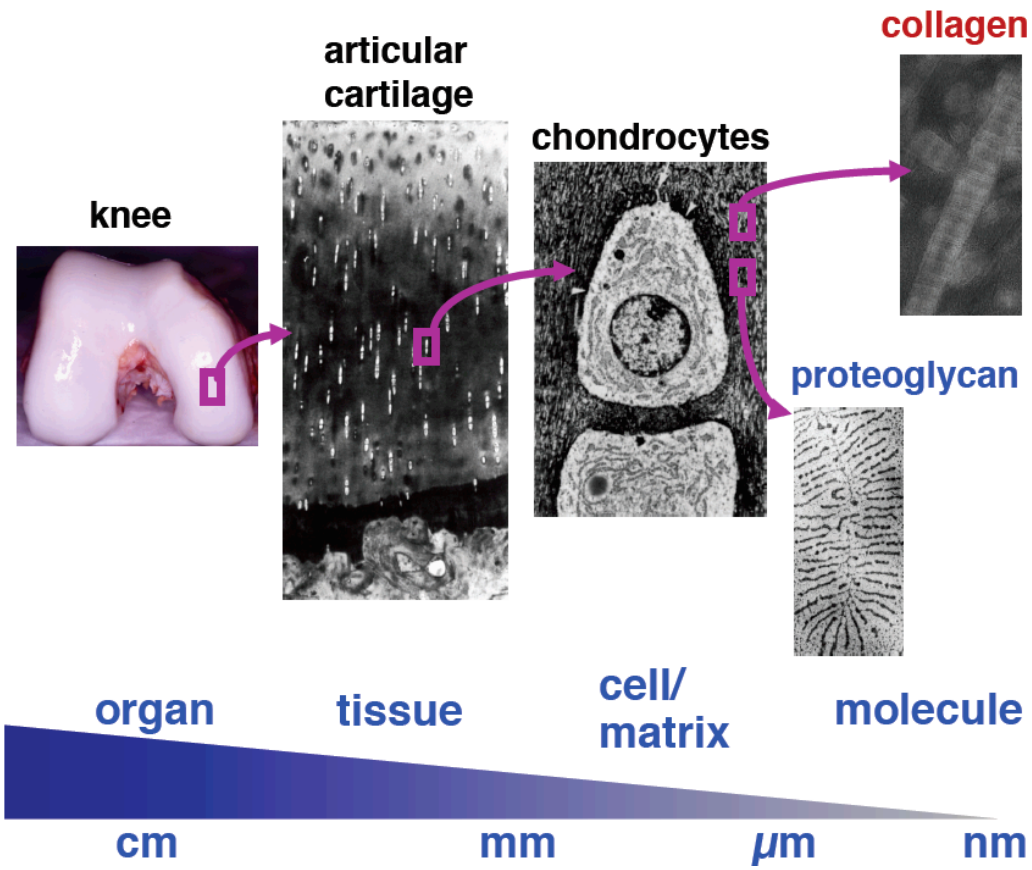

Figure 1.1: Articular cartilage: length scales. Human knee joints are covered with articular cartilage, which is comprised of chondrocytes sparsely embedded in extracellular matrix, largely consisting of proteoglycan aggregates and a network of collagens. (Micrographs adapted from [18, 42]).

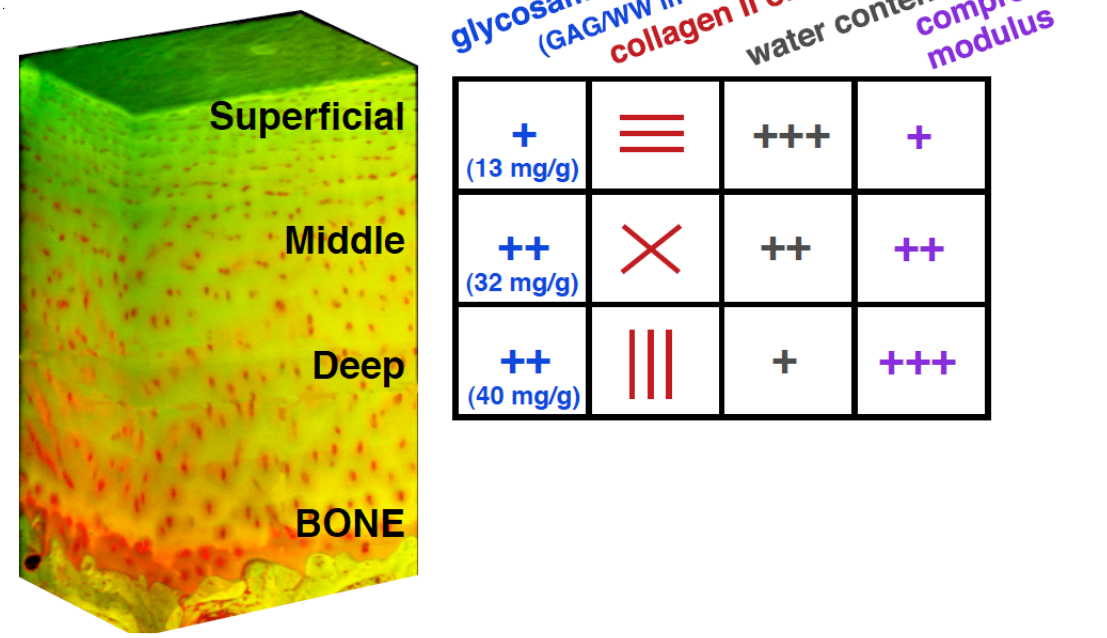

Figure 1.2: Zonal variations in composition, structure, and function of articular cartilage. Glycosaminoglycan content increases while collagen orientation varies from parallel to surface to perpendicular to surface with depth. The water content decreases while compressive modulus increases with depth.

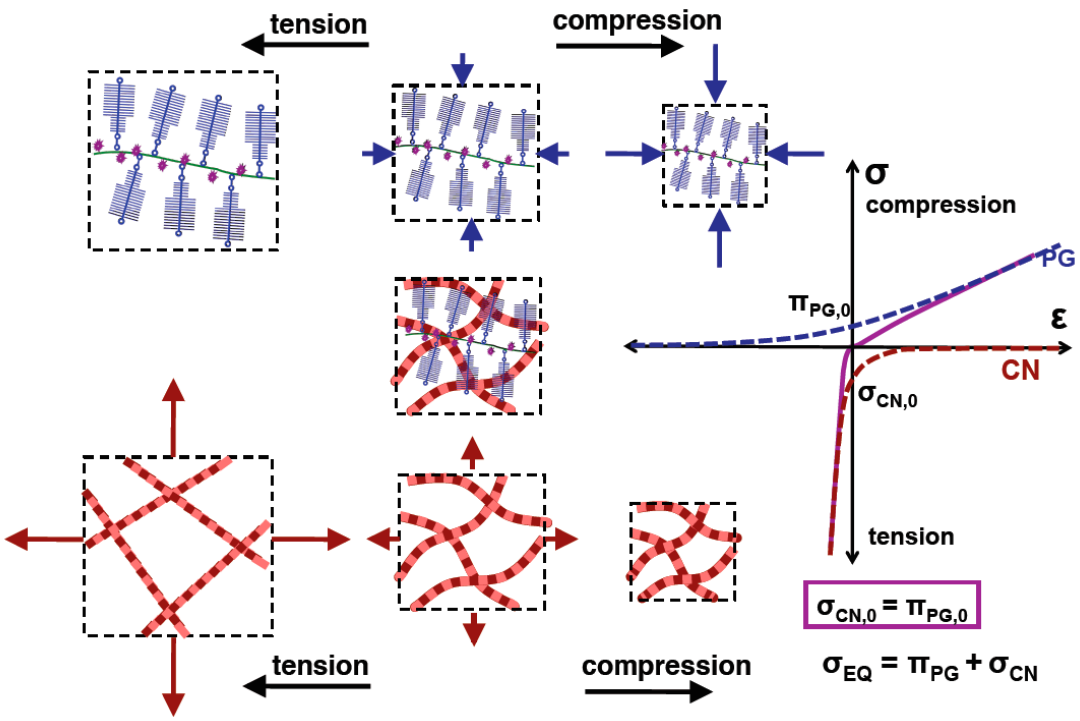

Figure 1.3: Proteoglycan and collagen contribution to cartilage mechanical properties. Proteoglycans contribute mostly in compression and at zero strain while collagen contributes mainly in tension and also at zero strain to restrain the swelling PG.

1.2 Proteoglycan Aggregates in Articular Cartilage

1.2.1. Proteoglycan Aggregate Components

Proteoglycans are present at high concentrations in articular cartilage, ~50-100 mg/ml [63] in humans and about 30 mg/ml in bovine [88]. Approximately 90% of the total proteoglycan mass comes from large aggregating proteoglycan such as aggrecan (M_r 1-3.5x10^6 Da) (Fig. 1.4). Many GAG chains covalently attach along the length of a protein core filament to form the aggrecan monomer; the GAG chains of each monomer include ~100 chains of chondroitin sulfate (CS) and ~30 chains of keratan sulfate (KS), and are accompanied by shorter oligosaccharides [63]. The core protein (M_r ~2x10^5 Da) contains three globular domains, G1, G2, and G3, with the region between G2 and G3 being the KS and CS attachment domains [73]. G1 domain of the protein core contains the hyaluronan biding region (HABR) and non-covalently binds with a hyaluronan (HA) chain, an association stabilized by link protein [73].

Link proteins are glycoproteins with high homology to the G1 domain of core protein. They are found in cartilage in two molecular forms, LP1 (4.8x10^4 Da) and LP2 (4.4x10^4 Da), with either two or one oligosaccharide chains on the N-terminal region respectively. LP3 (4.1x10^4 Da), a proteolytically cleaved form, and other proteolytic LP fragments are also present in cartilage [6]. Link protein is able to bind to both aggrecan G1 domain and hyaluronan to stabilize their interaction, allowing for formation of more uniformly packed aggregate [24]. Link protein aids in the conformational change of G1 domain of a newly synthesized aggrecan from a lower HA affinity form into more mature form with higher HA affinity, more suitable for aggregate formation [62].

Hyaluronan is a long, unbranched, non-sulfated GAG formed from a repeating disaccharide unit of D-glucuronic acid and N-acetylglucosamine. HA has a widely varying molecular weight [34]. It is essential for the aggregation of proteoglycans, and up to about 100 aggrecan monomers interact with a single HA molecule along its length to form the large proteoglycan aggregates with molecular weight of approximately 10^8-10^9 Da [34, 73].

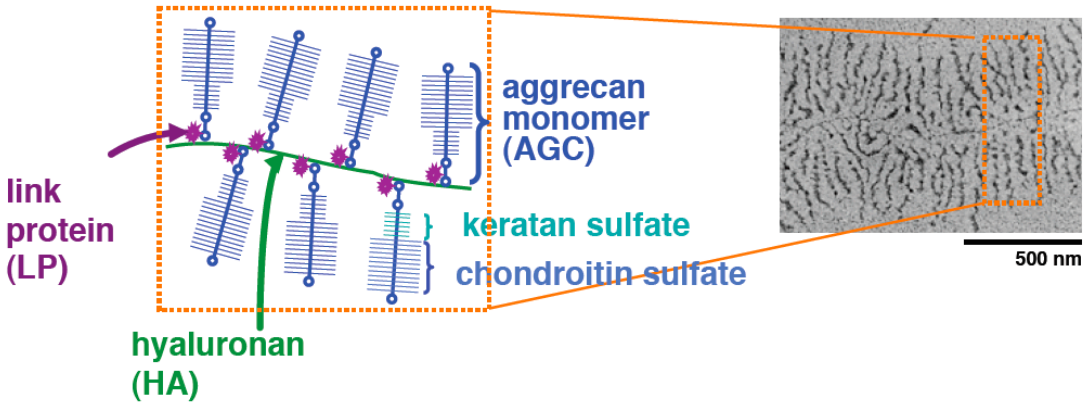

Figure 1.3: A proteoglycan aggregate is composed of aggrecan monomers that are non-covalently bound to hyaluronan and link proteins. The aggrecan monomers contain long chains of chondroitin sulfate and keratan sulfate. (Micrograph adapted from [16])

1.2.2. Proteoglycan Aggregation in Articular Cartilage

The separate sites of synthesis of HA and aggrecan monomers help to ensure that their aggregation occurs outside of the cell. Once translated by the ribosomes, the aggrecan core proteins are transported to Golgi apparatus for glycosylation with addition of GAG chains. The new aggrecan monomers are then secreted rapidly into the pericellular space. Likewise, the link proteins are glycosylated in the Golgi apparatus with either one or two N-linked oligosaccharide chains after translation. HA chains are synthesized and elongated by hyaluronan synthase on the plasma membrane and extruded directly out into the extracellular matrix [24].

The mechanisms by which proteoglycans move into interterritorial matrix far away from their point of synthesis and form aggregates remain to be fully elucidated. When first released from chondrocytes, the aggrecan monomers have low affinity for HA. The delayed aggregation of aggrecan to HA may be due to slow formation of the disulfide bonds in the G1 domain [10]. However, link protein appears to accelerate this conformational change in the G1 domain to higher affinity state for HA [62]. Link protein also stabilizes this aggregating interaction between an aggrecan monomer and HA by preventing its dissociation. In purified aggregates, link protein is present in 1:1 ratio to aggrecan monomers, possibly indicating that each aggrecan monomer interacts with only one link protein [63]. Link protein preferentially localizes throughout the extracellular matrix of superficial zone and the pericellular and interterritorial matrix of middle and deep zones of articular cartilage, as assessed by immunohistology [69]. The differential distribution of link protein as well as the presence of low HA-affinity

form of aggrecan may allow aggrecan monomers to diffuse out into the interterritorial matrix before forming a very stable proteoglycan aggregate with HA and link protein.

1.2.3. Kinetics of Proteoglycan Metabolism in Cartilage

Kinetics of proteoglycan metabolism varies depending on the culture system used. A small number of *in vivo* studies found the half life of proteoglycans to be about 150 days in adult dog articular cartilage [54] and 60-70 days in guinea pig costal cartilage [55]. In *in vitro* explant culture studies, the half life of proteoglycans ranges from 10-30 days in bovine articular cartilage [87]. After depletion of proteoglycans by enzymatic digestion and subsequent culture, articular cartilage was able to restore the GAG content within 4-10 days by increasing the rate of proteoglycan synthesis [4] although the newly synthesized proteoglycans may be of smaller size and lower chondroitin sulfate content initially [38]. *In vitro*, extracted aggrecan monomers were able to convert from the low HA affinity state to the higher HA affinity state with a half life of about 5.7 hours, and this conversion is slowed by increasing levels of static compression and decreased (acidic) pH [75].

1.2.4. Biochemical Methods of Cartilage Proteoglycan Extraction and Purification

Aggrecan from articular cartilage can be extracted by various methods, including a disruptive procedure and a dissociative procedure. In the disruptive procedure, the articular cartilage is homogenized at a high speed in a low ionic strength solution, such as 0.15M sodium chloride. The homogenization may be

subsequently purified for proteoglycans by precipitation with cetylpyridinium chloride or by high speed centrifugation [41, 76]. In the dissociative procedure, the aggrecan from articular cartilage is first extracted in a high ionic strength solution with chaotropic ability, such as 4M guanidine hydrochloride solution. This extract can be dialyzed to an associative condition (i.e. 0.4 M guanidine hydrochloride), and then purified using equilibrium density gradient centrifugation with cesium chloride (CsCl). The disruptive method subjects the aggrecan molecules to high shear forces, resulting in smaller aggregates than those obtained by dissociative extraction. The recovery by disruptive method is only 50-60% of the aggregates in cartilage compared to 85% from guanidine extraction after reassociation. In order to minimize mechanical fragmentation and to recover more proteoglycan molecules in their native form, the dissociative procedure has been the preferred method [41, 76].

Aggrecan monomers and link proteins can be further purified from the associative equilibrium density gradient centrifugation with cesium chloride (CsCl) after dissociative extraction in guanidine hydrochloride. The bottom third cut from the equilibrium density gradient centrifugation, termed A1 fraction, can be subject to a dissociative equilibrium density gradient centrifugation with CsCl after the addition of guanidine hydrochloride to 4M. The fractions can be cut into sixths where the bottom A1D1 and A1D2 fractions contain most of the aggrecan while the top third fractions, A1D5 and A1D6, contain the link proteins along with hyaluronan. The link protein can be further purified from hyaluronan by gel filtration chromatography [81]. Addition of EDTA can help to decrease the self-aggregation and precipitation of link protein under associative conditions [71]. Upon the removal of the dissociative agent,

the proteoglycan molecules are able to associate to form the large proteoglycan aggregates *in vitro*.

1.2.5. Cartilage Proteoglycan Aggregation In Vitro

Purified aggrecan, HA, and link protein from articular cartilage maintain their ability to form aggregates in solution *in vitro*. Many factors affect this aggregating interaction, including concentrations of each component, pH, and length of HA. Aggrecan in solution forms aggregates with hyaluronan with a dissociation constant (K_d) of about 10^{-8} M [63]. This interaction is optimal at 0.8% (w/w aggrecan) HA and decreases with pH change from 7 to 5 from 58% to 36% of the initial aggrecan monomer content [19, 82].

Link protein is also able to associate with hyaluronan in the absence of aggrecan, with an increasing binding rate as pH decreases from 8 to 5 [72], with a dissociation constant (K_d) similar to that of aggrecan and HA [63]. Link protein is also able to bind to hyaluronan as short as a decasaccharide [72]. HA-bound link protein can protect HA from mild hyaluronidase degradation, indicating a possible HA-protective role of aggrecan and link protein [70].

The extent of interaction between aggrecan and link protein is somewhat less clear. In one study, aggrecan and link protein did not appear to have a strong interaction in the absence of hyaluronan in free solution [13] while another study found that they do interact [25]. However, link protein fraction prepared from equilibrium density gradient centrifugation without further gel filtration may contain HA [81] and may complicate the interpretation of the results.

The addition of link protein to the aggrecan-HA mixture minimizes the pH effect on the aggregate stability, with 6-8% (w/w aggrecan) LP (or 3:1 or 4:1 LP:aggrecan molar ratio) resulting in maximum aggregation of about 80% of initial aggrecan content [19, 82] regardless of pH. The presence of link protein resulted in longer HA filaments in the aggregates, increased aggrecan per aggregate, and more uniform spacing between aggrecan, indicating that it has a key role in the spatial organization of proteoglycan aggregates [82]. The aggrecan-LP complex requires a HA of at least 24-30 saccharides to bind [40]. The zero shear rate viscosity increases nonlinearly with increasing level of aggregation, and this increase is most dramatic at higher aggrecan concentrations of that approaching physiological levels (50 mg/ml) [39].

1.2.6. Aggrecan and Proteoglycan Aggregates Diffusive Transport in Free Solution

The large size of aggrecan monomers, estimated length of ~300 nm and width of ~100 nm along [18], results in low diffusivity that decreases exponentially as the concentration increases near physiological levels. In dilute solutions of aggrecan monomers of various molecular weights, lateral diffusion coefficient ranges from about 4-6 x 10^{-8} cm^2s^{-1} with a strong aggrecan concentration dependence [36, 53, 68]. Proteoglycan aggregates containing about 30 aggrecan monomers exhibit an even lower free lateral diffusion coefficient (6.6 x 10^{-9} cm^2s^{-1}). Thus, aggregation to HA provides a mechanism for aggrecan monomers to be retained within the articular cartilage tissue.

1.2.7. Proteoglycan Aggregates with Aging and Disease

With aging and disease, the proteoglycan aggregate structure is altered. In humans, the CS1 attachment domain on the core protein, one of the two CS domains, varies in length between individuals, which affects the number of CS chains that can bind to the core protein [73]. Truncation of the aggrecan core protein due to proteolytic cleavage by aggrecanases, matrix metalloproteinases, and other enzymes [34], decrease in GAG content [74], decrease in HA size due to degradation [73], and decreased LP1:LP2 ratio [35] have been observed with aging and disease. The age-related changes affect the aggregate size and the anionic charge density of the aggregates, which ultimately has functional consequences with altered compressive properties of the articular cartilage.

1.2.8. Proteoglycan Aggregates in Biomechanical Function of Articular Cartilage

The GAG content of a tissue strongly correlates with compressive biomechanical properties [88]. The formation of large proteoglycan aggregates aids in the retention of the polyanions of aggrecan within the cartilage matrix due to their entrapment within collagen network. The sulfate and carboxyl groups in CS and sulfate groups in KS chains on aggrecan provide a high fixed charge density to the tissue that provide attracts increased concentration of cations to maintain charge neutrality of the tissue (Fig.1.5). This differential of ion concentrations provides the high osmotic pressure (π_{PG}) to the tissue, leading to retention of water, a high resistance to fluid flow and thereby resistance to compression, and pre-stress to the

collagen network [24]. Therefore, the retention of aggrecan in cartilage is crucial to its biomechanical function.

1.2.9 Proteoglycan Osmotic Pressure Models

In order to study the contribution of the proteoglycans to the compressive mechanical properties, several models of the relationship between π_{PG} and PG content, usually expressed in the form of FCD or GAG concentrations have been developed [8, 9, 22, 26]. These π_{PG} models have been used to estimate the contribution of PG from the electrostatic effects to compressive resistance in articular cartilage [8, 9, 22, 26]. These models also can be used to estimate the collagen or other non-electrostatic contribution to compressive resistance in articular cartilage using the idea of "balance of forces" between swelling PG and restraining collagen stresses [8].

Attempts have been made to determine the π_{PG} contribution to the compressive modulus or aggregate modulus of articular cartilage [7, 22, 26], but such comparisons heavily depend on the accuracy and assumptions of the FCD and π_{PG} calculations. The FCD-π_{PG} relationship may be affected by estimation of FCD from GAG or PG concentration and by exclusion of COL intrafibrillar (IF) water to PG. The FCD estimations usually imply but usually do not explicitly account for CS and KS charge differences (z_{CS}=~2, z_{KS}=~1 per disaccharide) and for varying CS:KS ratios, which are known to change with age and depth of the tissue [84]. Additionally, the water closely associated with collagen fibrils in articular cartilage are unavailable to interact with the PG [58]. This exclusion of COL intrafibrillar (IF) water to PG, which varies with external stress applied to the tissue [8, 58], results in higher effective FCD and higher

π_{PG}. This effect was not appreciated or applied as much since the models were developed from PG in solution and not in tissue and did not need to consider the interaction between PG and COL and its effect on π_{PG}. Thus, consideration of these factors into π_{PG} calculation may provide a useful tool in better understanding the relationship between composition and function of articular cartilage by using estimating the π_{PG} from a known PG concentration or FCD at its reference state or under compression.

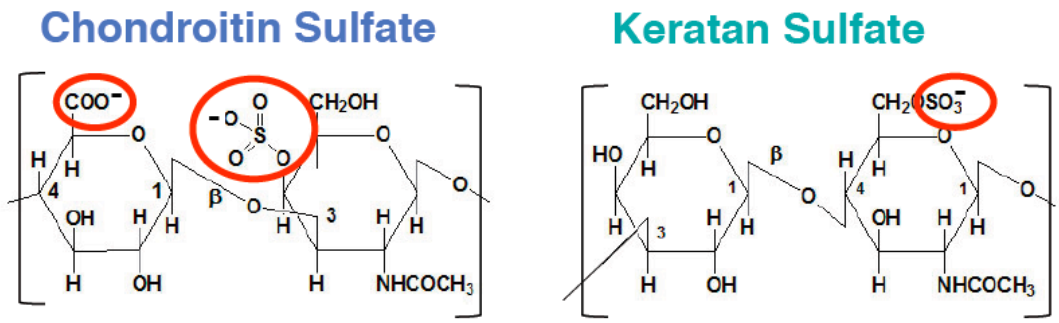

Figure 1.5: Structure of chondroitin sulfate and keratan sulfate with the anionic moieties in circles.

1.3 Cartilage Tissue Engineering

1.3.1. Current Clinical Treatments for Articular Cartilage Defects

Due to its avascular nature, articular cartilage of adults has a poor capacity to regenerate once damaged by trauma or degeneration (Fig. 1.6). Commonly found during arthroscopy [31, 42], focal defects can lead to widespread joint degeneration, which are associated with pain [33] and can impair the ability of cartilage to withstand mechanical demands on the joint [17]. Surface restoration is one of the goals of defect repair with osteochondral allografts [20] and autografts or mosaicplasty [60], as well as with tissue engineering-based, chondral graft treatments, such as autologous cell implantation (ACI) [14] and matrix-guided autologous cell implantation (MACI) [30] (Fig. 1.7). However, these treatments are limited by availability of donor tissue sources, donor site morbidity, and prolonged rehabilitation times. Tissue engineering of cartilaginous grafts has been presented as a potential solution to the problems with current treatments.

1.3.2. Cartilage Tissue Engineering Overview

Tissue engineering has been defined as “the application of principles and methods of engineering and life sciences toward fundamental understanding of structure-function relationships in normal and pathologic mammalian tissues and the development of biological substitutes to restore, maintain, or improve tissue functions” [80]. Using the normal native cartilage as the design paragon, cartilage tissue engineering typically uses a combination of cells, scaffolds, and/or external stimuli to produce cartilaginous grafts that aim to restore function to the joint. The

cells may be from autogenic, allogenic, or xenogenic sources, and may be of various differentiation states ranging from stem cells to progenitor cells or fully differentiated chondrocytes. The biomaterials applied for cartilage tissue engineering include protein-based scaffolds (e.g. collagen, fibrin), polysaccharide-based (e.g. hyaluronan, GAG) and synthetic scaffolds (e.g. PEG derivatives, PLGA, PGA) with various three-dimensional shape and architecture. The external stimuli that have been investigated include chemical factors (e.g. growth factors, cytokines, chemokines), mechanical stimulation (e.g. static and dynamic compression, shear, pressure, perfusion), and other biophysical stimuli (e.g. oxygen tension, electric field) [50, 86].

1.3.3. Shaped Grafts in Cartilage Tissue Engineering

For larger articular cartilage defects, grafts that match the complex surface geometries of the joint are needed to facilitate healing and joint restoration. Surface incongruity of osteochondral grafts to the surrounding native cartilage surface has been shown to result in local mechanical stresses that may be unfavorable for the success of the graft treatment [52].

Previous studies have examined the shaped tissue-engineered constructs for articular cartilage of the patella [44], middle and distal phalanx [46, 78], and mandibular condyle [2]. Fabrication of the shaped cartilaginous constructs can be grouped into two main approaches. In the scaffold prefabrication approach, a scaffold is shaped into the desired geometry, subsequently seeded with cells (chondrocytes, stem cells, etc.), and cultured *ex vivo* or subcutaneously [23, 48]. This approach is commonly used for osteochondral grafts, where most of the scaffold is used for the

bony substance [78]. In the molding approach, a mixture of cell and scaffold is placed together into a mold where the scaffold is polymerized, and the shaped construct is subsequently incubated *in vitro* for some time. Scaffolds for the molding method are commonly hydrogels, including agarose as a model system [44], alginate [27], and photopolymerizable polyethylene glycol derivative [2]. These methods have been used for engineering of elastic and non-articular cartilage such as auricle [23, 47, 89], nose [27, 47], and tympanic membrane [43]. Bone grafts also have been constructed in various shapes, including femoral head and mandible [49]. Many of these previous works rely on scaffolds to provide mechanical stability for the constructs and aid in the maintenance of their shapes. While the results of these studies are promising, the resultant constructs vary from the desired shape due to growth and remodeling, and the surface contours of these constructs have not been analyzed.

1.3.4. Structural Organization of Engineered Cartilaginous Grafts

Biomimetic zonal stratification, an important structural feature of the articular cartilage, has been achieved in tissue-engineered cartilaginous grafts. Cartilaginous constructs have been created with stratification of superficial and middle/deep zone subpopulations [51, 79] and also with deep zone layer and calcified cartilage layer [3]. Some of these constructs maintain some of the zone-specific characteristics of normal articular cartilage, including the synthesis and secretion of proteoglycan 4 by the chondrocytes derived from the superficial zone [51], relatively high levels of matrix production by deep zone chondrocytes [79], and mineralization in the calcified cartilage layer [3]. This structural organization may be important since various cellular

products are correlated with inhomogeneous biochemical and mechanical properties of articular cartilage [57].

1.3.5. Biochemical and Biomechanical Properties of Engineered Cartilaginous Grafts

Many cell-based tissue-engineered cartilaginous constructs are mechanically inferior to native tissue due to an imbalance between its extracellular matrix contents. These constructs usually have a fairly robust proteoglycan content that approaches physiological levels or even surpasses it, but the collagen content is usually substantially below those of native cartilage even after prolonged *in vitro* culture [28, 66]. Due to the limited restraining forces provided by the low collagen content, these constructs tend to be highly hydrated with over 80% water content [65], akin to the increased hydration found in degenerate cartilage [85], with compressive modulus only on the order of tens of kPa [51, 67] and have very little tensile strength.

In normal cartilage, the collagen content is typically ~2-10 times higher that of sGAG content in very immature fetal bovine to adult human cartilage [83, 88]. Typical ratio of collagen: sGAG are 1:1 or less in cell-based, engineered cartilaginous constructs even with a very long-term culture [28, 66]. More recently, there have been efforts to increase the collagen: GAG ratio by selective enzymatic degradation of proteoglycans in cartilage and engineered constructs [5, 11, 65]. The resulting cartilage and constructs have higher tensile stiffness and further highlight the importance of the balance between collagen and proteoglycans in normal function of the tissue and engineered grafts. As collagen plays an important role in restraining the

swelling pressure from proteoglycans, methods to improve collagen content would be important in improving the biochemical composition and function of the grafts. By modulating the accumulation of proteoglycans and collagen molecules with various chemical and mechanical factors [12, 21, 32, 61], there have been efforts to create tissue-engineered cartilaginous constructs with more mature mechanical properties. The fabrication of more mature cartilaginous constructs that more closely approximates that of the normal cartilage with compressive modulus on the order of hundreds or thousands of kPa [29, 88] may allow for more rapid application of the grafts into the mechanical demanding environment of an *in vivo* joint.

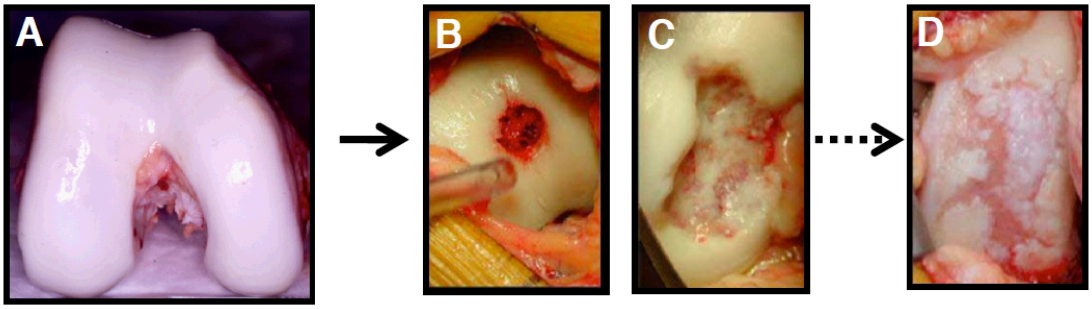

Figure 1.6: Articular cartilage (A) can develop focal defects (B, C) that can lead to widespread joint degeneration (D). (Photo courtesy of Dr. William D. Bugbee)

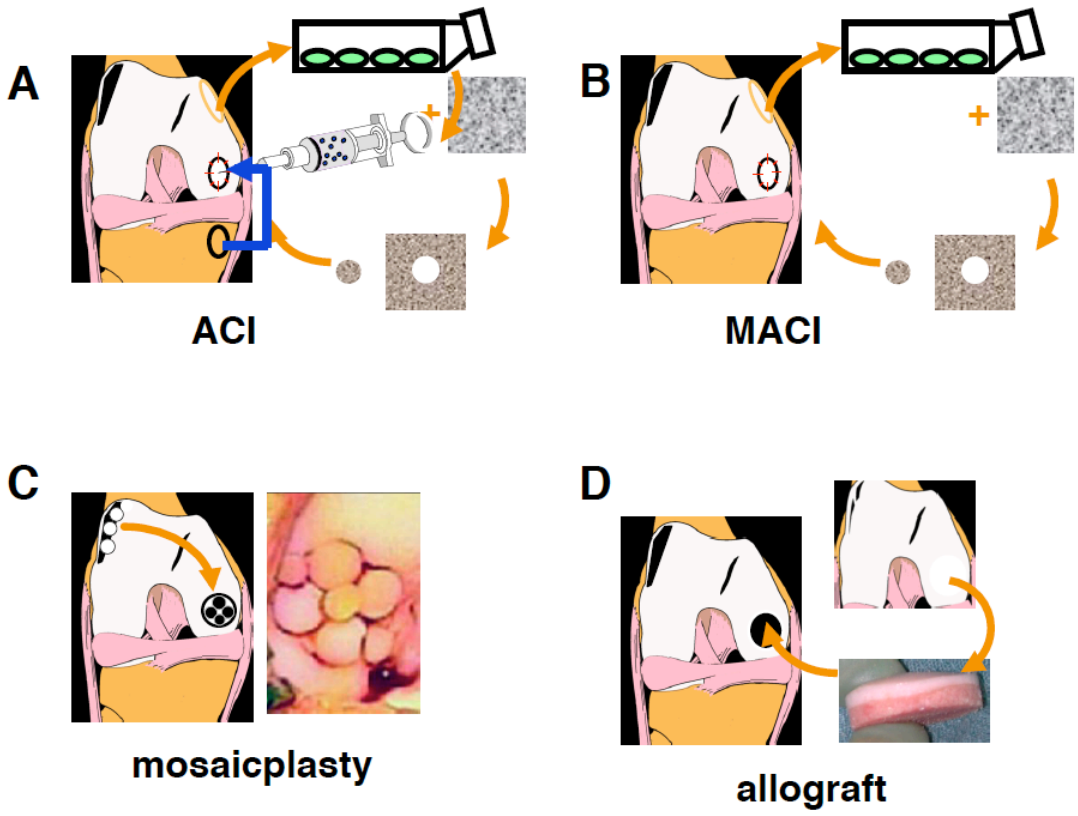

Figure 1.7: Strategies for repair of articular cartilage defects include autologous chondrocyte implantation (ACI) (A), matrix assisted-ACI (B), mosaicplasty of osteochondral autografts (C), or osteochondral allograft implantation (D).

1.4 Dissertation Objectives and Overview

The overall motivation of this dissertation was to contribute to the engineering of mechanically functional aggrecan-laden cartilaginous grafts by (1) elucidating the roles of proteoglycans and its interaction with collagen to the compressive properties of articular cartilage and (2) developing rapid novel methods for shaping, assembling, and concentrating matrix-laden cartilaginous constructs. For large defects in articular cartilage, grafts that match the surface contour of the joint and have load-bearing biomechanical properties are needed to facilitate healing and re-establish joint function. Additionally, many types of tissue-engineered cartilaginous constructs are soft due to a content of proteoglycan and collagen that is substantially below those of native cartilage, even after prolonged *in vitro* culture. Typically, tissue engineered cartilaginous constructs take weeks if not months to culture and fabricate [59]. Thus, the ability to quickly assemble the components, chondrocytes and matrix proteins, into constructs with biomimetically appropriate organization and contour and a more physiological biochemical content may be beneficial in significantly reducing the fabrication time and providing potential off-the-shelf grafts for implantation. Specifically, the objectives of this work were 1) to develop a novel combination of molding and stratification to form a cartilaginous graft of appropriate three-dimensional shape, 2) to quantitatively describe the role of aggrecan and its interaction with collagen in the compressive biomechanical properties of native articular cartilage, as it varies with age and depth, 3) to develop engineered constructs with tunable aggrecan retention by *in vitro* assembly, and 4) to present a mechanical compaction method to enhance the extracellular matrix content of engineered constructs.

Chapter 2, which was published in *Clinical Orthopaedics and Related Research*, describes a novel molding method of shaping scaffold-free cartilaginous constructs that were anatomically shaped and targeting spherically shaped hip joints. Additionally, biomimetic stratification of the anatomically shaped constructs was achieved with appropriate superficial and middle/deep zone chondrocyte subpopulations. This builds on previously described alginate recovered chondrocyte method to fabricate stratified, scaffold-free constructs.

Chapter 3, which was submitted to *Biophysical Journal*, elucidates the π_{PG} model and the interaction of collagen and aggrecan on the compressive mechanics of native articular cartilage, as it varies with age and depth. A new relationship for effective FCD-π_{PG} was described and applied to biomechanical and biochemical data of confined compression tests performed on full-thickness cartilage from bovine fetal, calf, and adult sources, and human young and old sources to determine the FCD, π_{PG}, and collagen network stress. Human young and old cartilages were also analyzed with depth from the articular surface to determine depth-variation in the FCD, π_{PG}, and collagen network stress profiles and any age related changes in the depth-varying properties.

Chapter 4, which was published in *Tissue Engineering, Part C: Methods*, examines the effect of biomimetic molecular reassembly of PG aggregates (native aggrecan (AGC) with hyaluronan (HA) ± link proteins (LP)) on AGC retention kinetics in hydrogel constructs. The compressive properties of such hydrogel constructs were further examined to relate to the content of retained AGC. The

biocompatibility of the reassembly method was verified by a short-term culture of the constructs containing chondrocytes.

Chapter 5, which will be submitted to *Tissue Engineering, Part A*, describes a novel method to enhance the extracellular matrix content of engineered constructs by mechanical compaction of a cartilaginous graft composed of in agarose hydrogel ± PG ± collagen. The increase in biochemical content and maintenance of the compressive mechanical properties of such constructs were examined. In addition, the difference in compressive mechanical properties of PG-containing grafts with or without collagen was explored. This extends the findings from Chapter 3 and 4 by studying the role of collagen in compressive properties of an engineered construct.

Chapter 6 summarizes the major findings of these studies and discusses potential directions for future studies.

Appendix A, B, and C, which will be Supplemental Materials of the submitted manuscript in Chapter 3, provide the rationale and the details of FCD and osmotic pressure model calculations.

Appendix D and E, which were published in *Tissue Engineering, Part C: Methods* as an Electronic Supplement, presents the validation of methods used in Chapter 4. The confined compression testing set up with a stack of two agarose constructs containing proteoglycans was compared to a stack of one construct containing proteoglycans with the same overall thickness. The rationale for pooling of PBS for HA analysis was also presented.

Appendix F, which supplements the submitted manuscript in Chapter 5, presents the retention of matrix content in compacted constructs.

1.5 References

1. Alexopoulos LG, Setton LA, Guilak F: The biomechanical role of the chondrocyte pericellular matrix in articular cartilage. *Acta Biomater* 1:317-25, 2005.

2. Alhadlaq A, Mao JJ: Tissue-engineered osteochondral constructs in the shape of an articular condyle. *J Bone Joint Surg Am* 87:936-44, 2005.

3. Allan KS, Pilliar RM, Wang J, Grynpas MD, Kandel RA: Formation of biphasic constructs containing cartilage with a calcified zone interface. *Tissue Eng* 13:167-77, 2007.

4. Asanbaeva A, Masuda K, Thonar EJ, Klisch SM, Sah RL: Mechanisms of cartilage growth: modulation of balance between proteoglycan and collagen in vitro using chondroitinase ABC. *Arthritis Rheum* 56:188-98, 2007.

5. Asanbaeva A, Tam J, Schumacher BL, Klisch SM, Masuda K, Sah RL: Articular cartilage tensile integrity: Modulation by matrix depletion is maturation-dependent. *Arch Biochem Biophys* 474:175-82, 2008.

6. Baker JR, Neame PJ: Isolation and characterization of the link proteins. *Methods Enzymol* 144:401-12, 1987.

7. Basser PJ, Horkay F: Toward a Constitutive Law of Cartilage: A Polymer Physics Perspective. *Macromol Symp* 227:53-64, 2005.

8. Basser PJ, Schneiderman R, Bank RA, Wachtel E, Maroudas A: Mechanical properties of the collagen network in human articular cartilage as measured by osmotic stress technique. *Arch Biochem Biophys* 351:207-19, 1998.

9. Bathe M, Rutledge GC, Grodzinsky AJ, Tidor B: Osmotic pressure of aqueous chondroitin sulfate solution: a molecular modeling investigation. *Biophys J* 89:2357-71, 2005.

10. Bayliss MT, Ridgway GD, Ali SY: Delayed aggregation of proteoglycans in adult human articular cartilage. *Biosci Rep* 4:827-33, 1984.

11. Bian L, Crivello KM, Ng KW, Xu D, Williams DY, Ateshian GA, Hung CT: Influence of Temporary Chondroitinase ABC-Induced Glycosaminoglycan Suppression on Maturation of Tissue-Engineered Cartilage. *Tissue Eng Part A*, 2009.

12. Blunk T, Sieminski AL, Gooch KJ, Courter DL, Hollander AP, Nahir AM, Langer R, Vunjak-Novakovic G, Freed LE: Differential effects of growth factors on tissue-engineered cartilage. *Tissue Eng* 8:73-84, 2002.

13. Bonnet F, Dunham DG, Hardingham TE: Structure and interactions of cartilage proteoglycan binding region and link protein. *Biochem J* 228:78-85, 1985.

14. Brittberg M, Lindahl A, Nilsson A, Ohlsson C, Isaksson O, Peterson L: Treatment of deep cartilage defects in the knee with autologous chondrocyte transplantation. *N Engl J Med* 331:889-95, 1994.

15. Bruckner P, van der Rest M: Structure and function of cartilage collagens. *Micros Res Tech* 28:378-84, 1994.

16. Buckwalter JA, Mankin HJ: Articular cartilage. Part I: tissue design and chondrocyte-matrix interactions. *J Bone Joint Surg Am* 79-A:600-11, 1997.

17. Buckwalter JA, Mankin HJ: Articular cartilage. Part II: degeneration and osteoarthrosis, repair, regeneration, and transplantation. *J Bone Joint Surg Am* 79-A:612-32, 1997.

18. Buckwalter JA, Rosenberg LC: Electron microscopic studies of cartilage proteoglycans. Direct evidence for the variable length of the chondroitin sulfate-rich region of proteoglycan subunit core protein. *J Biol Chem* 257:9830-9, 1982.

19. Buckwalter JA, Rosenberg LC, Tang L-H: The effect of link protein on proteoglycan aggregate structure: an electron microscopic study of the molecular architecture and dimensions of proteoglycan aggregates reassembled from the proteoglycan monomers and link proteins of bovine fetal epiphyseal cartilage. *J Biol Chem* 259:5361-3, 1984.

20. Bugbee WD, Convery FR: Osteochondral allograft transplantation. *Clin Sports Med* 18:67-75, 1999.

21. Buschmann MD, Gluzband YA, Grodzinsky AJ, Hunziker EB: Mechanical compression modulates matrix biosynthesis in chondrocyte/agarose culture. *J Cell Sci* 108 (Pt 4):1497-508, 1995.

22. Buschmann MD, Grodzinsky AJ: A molecular model of proteoglycan-associated electrostatic forces in cartilage mechanics. *J Biomech Eng* 117:179-92, 1995.

23. Cao Y, Vacanti JP, Paige KT, Upton J, Vacanti CA: Transplantation of chondrocytes utilizing a polymer-cell construct to produce tissue-engineered cartilage in the shape of a human ear. *Plast Reconstr Surg* 100:297-302; discussion 3-4, 1997.

24. Carney SL, Muir H: The structure and function of cartilage proteoglycans. *Physiol Rev* 68:858-910, 1988.

25. Caterson B, Baker J: The interaction of link proteins with proteoglycan monomers in the absence of hyaluronic acid. *Biochem Biophys Res Commun* 80:496-503, 1978.

26. Chahine NO, Chen FH, Hung CT, Ateshian GA: Direct measurement of osmotic pressure of glycosaminoglycan solutions by membrane osmometry at room temperature. *Biophys J* 89:1543-50, 2005.

27. Chang SC, Rowley JA, Tobias G, Genes NG, Roy AK, Mooney DJ, Vacanti CA, Bonassar LJ: Injection molding of chondrocyte/alginate constructs in the shape of facial implants. *J Biomed Mater Res* 55:503-11, 2001.

28. Chen AC, Masuda K, Nakagawa K, Wong VW, Pfister BE, Thonar EJ, Sah RL: Tissue engineered cartilage from adult human chondrocytes: biomechanical properties and function-composition relationships. *Trans Orthop Res Soc* 28:945, 2003.

29. Chen SS, Falcovitz YH, Schneiderman R, Maroudas A, Sah RL: Depth-dependent compressive properties of normal aged human femoral head articular cartilage: relationship to fixed charge density. *Osteoarthritis Cartilage* 9:561-9, 2001.

30. Cherubino P, Grassi FA, Bulgheroni P, Ronga M: Autologous chondrocyte implantation using a bilayer collagen membrane: a preliminary report. *J Orthop Surg (Hong Kong)* 11:10-5, 2003.

31. Curl WW, Krome J, Gordon ES, Rushing J, Smith BP, Poehling GG: Cartilage injuries: a review of 31,516 knee arthroscopies. *Arthroscopy* 13:456-60, 1997.

32. Davisson TH, Kunig S, Chen AC, Sah RL, Ratcliffe A: Static and dynamic compression modulate biosynthesis in tissue engineered cartilage. *J Orthop Res* 20:842-8, 2002.

33. Dieppe PA, Lohmander LS: Pathogenesis and management of pain in osteoarthritis. *Lancet* 365:965-73, 2005.

34. Dudhia J: Aggrecan, aging and assembly in articular cartilage. *Cell Mol Life Sci* 62:2241-56, 2005.

35. Flannery CR, Urbanek PJ, Sandy JD: The effect of maturation and aging on the structure and content of link proteins in rabbit articular cartilage. *J Orthop Res* 8:78-85, 1990.

36. Gribbon P, Hardingham TE: Macromolecular diffusion of biological polymers measured by confocal fluorescence recovery after photobleaching. *Biophys J* 75:1032-9, 1998.

37. Gribbon P, Heng BC, Hardingham TE: The molecular basis of the solution properties of hyaluronan investigated by confocal fluorescence recovery after photobleaching. *Biophys J* 77:2210-6, 1999.

38. Hardingham TE, Fitton-Jackson S, Muir H: Replacement of proteoglycans in embryonic chick cartilage in organ culture after treatment with testicular hyaluronidase. *Biochem J* 129:101-12, 1972.

39. Hardingham TE, Muir H, Kwan MK, Lai WM, Mow VC: Viscoelastic properties of proteoglycan solutions with varying proporations present as aggregates. *J Orthop Res* 5:36-46, 1987.

40. Hardingham TE, Perkins SJ, Muir H: Molecular conformations in proteoglycan aggregation. *Biochem Soc Trans* 11:128-30, 1983.

41. Heinegard D, Sommarin Y: Isolation and characterization of proteoglycans. *Methods Enzymol* 144:305-19, 1987.

42. Hjelle K, Solheim E, Strand T, Muri R, Brittberg M: Articular cartilage defects in 1,000 knee arthroscopies. *Arthroscopy* 18:730-4, 2002.

43. Hott ME, Megerian CA, Beane R, Bonassar LJ: Fabrication of tissue engineered tympanic membrane patches using computer-aided design and injection molding. *Laryngoscope* 114:1290-5, 2004.

44. Hung CT, Lima EG, Mauck RL, Taki E, LeRoux MA, Lu HH, Stark RG, Guo XE, Ateshian GA: Anatomically shaped osteochondral constructs for articular cartilage repair. *J Biomech* 36:1853-64, 2003.

45. Hunziker EB: Articular cartilage structure in humans and experimental animals. In: *Articular Cartilage and Osteoarthritis,* ed. by KE Kuettner, Schleyerbach R, Peyron JG, Hascall VC, Raven Press, New York, 1992, 183-99.

46. Isogai N, Landis W, Kim TH, Gerstenfeld LC, Upton J, Vacanti JP: Formation of phalanges and small joints by tissue-engineering. *J Bone Joint Surg Am* 81-A:306-16, 1999.

47. Kamil SH, Kojima K, Vacanti MP, Bonassar LJ, Vacanti CA, Eavey RD: In vitro tissue engineering to generate a human-sized auricle and nasal tip. *Laryngoscope* 113:90-4, 2003.

48. Kang SW, Son SM, Lee JS, Lee ES, Lee KY, Park SG, Park JH, Kim BS: Regeneration of whole meniscus using meniscal cells and polymer scaffolds in a rabbit total meniscectomy model. *J Biomed Mater Res A* 78:659-71, 2006.

49. Khouri RK, Koudsi B, Reddi H: Tissue transformation into bone in vivo. A potential practical application. *JAMA* 266:1953-5, 1991.

50. Klein TJ, Malda J, Sah RL, Hutmacher DW: Tissue Engineering of Articular Cartilage with Biomimetic Zones. *Tissue Eng Part B Rev* 15:143-57, 2009.

51. Klein TJ, Schumacher BL, Schmidt TA, Li KW, Voegtline MS, Masuda K, Thonar EJ-MA, Sah RL: Tissue engineering of stratified articular cartilage from chondrocyte subpopulations. *Osteoarthritis Cartilage* 11:595-602, 2003.

52. Koh JL, Wirsing K, Lautenschlager E, Zhang LO: The effect of graft height mismatch on contact pressure following osteochondral grafting. A biomechanical study. *Am J Sports Med* 32:317-20, 2004.

53. Li XQ, Stevenson S, Klein L, Davy DT, Shaffer JW, Goldberg VM: Differential patterns of incorporation and remodeling among various types of bone grafts. *Acta Anat* 140:236-44, 1991.

54. Lohmander S: Turnover of proteoglycans in guinea pig costal cartilage. *Arch Biochem Biophys* 180:93-101, 1977.

55. Maroudas A: Glycosaminoglycan turn-over in articular cartilage. *Philos Trans R Soc Lond B Biol Sci* 271:293-313, 1975.

56. Maroudas A: Balance between swelling pressure and collagen tension in normal and degenerate cartilage. *Nature* 260:808-9, 1976.

57. Maroudas A: Physico-chemical properties of articular cartilage. In: *Adult Articular Cartilage,* ed. by MAR Freeman, Pitman Medical, Tunbridge Wells, England, 1979, 215-90.

58. Maroudas A, Wachtel E, Grushko G, Katz EP, Weinberg P: The effect of osmotic and mechanical pressures on water partitioning in articular cartilage. *Biochim Biophys Acta* 1073:285-94, 1991.

59. Martin I, Miot S, Barbero A, Jakob M, Wendt D: Osteochondral tissue engineering. *J Biomech* 40:750-65, 2007.

60. Matsusue Y, Yamamuro T, Hama H: Arthroscopic multiple osteochondral transplantation to the chondral defect in the knee associated with anterior cruciate ligament disruption. *Arthroscopy* 9:318-21, 1993.

61. Mauck RL, Soltz MA, Wang CC, Wong DD, Chao PH, Valhmu WB, Hung CT, Ateshian GA: Functional tissue engineering of articular cartilage through dynamic loading of chondrocyte-seeded agarose gels. *J Biomech Eng* 122:252-60, 2000.

62. Melching LI, Roughley PJ: Studies on the interaction of newly secreted proteoglycan subunits with hyaluronate in human articular cartilage. *Biochim Biophys Acta* 1035:20-8, 1990.

63. Morgelin M, Heinegard D, Engel J, Paulsson M: The cartilage proteoglycan aggregate: assembly through combined protein-carbohydate and protein-protein interactions. *Biophys Chem* 50:113-28, 1994.

64. Mow VC, Zhu W, Ratcliffe A: Structure and function of articular cartilage and meniscus. In: *Basic Orthopaedic Biomechanics,* ed. by VC Mow, Hayes WC, Raven Press, New York, 1991, 143-98.

65. Natoli RM, Responte DJ, Lu BY, Athanasiou KA: Effects of multiple chondroitinase ABC applications on tissue engineered articular cartilage. *J Orthop Res* 27:949-56, 2009.

66. Ng KW, Kugler LE, Doty SB, Ateshian GA, Hung CT: Scaffold degradation elevates the collagen content and dynamic compressive modulus in engineered articular cartilage. *Osteoarthritis Cartilage* 17:220-7, 2009.

67. Ng KW, Saliman JD, Lin EY, Statman LY, Kugler LE, Lo SB, Ateshian GA, Hung CT: Culture Duration Modulates Collagen Hydrolysate-Induced Tissue Remodeling in Chondrocyte-Seeded Agarose Hydrogels. *Ann Biomed Eng* 35:1914-23, 2007.

68. Ohno H, Blackwell J, Jamieson AM, Carrino DA, Caplan AI: Calibration of the relative molecular mass of proteoglycan subunit by column chromatography on Sepharose CL-2B. *Biochem J* 235:553-7, 1986.

69. Poole AR, Pidoux I, Reiner A, Tang L-H, Choi H, Rosenberg L: Localization of proteoglycan monomer and link protein in the matrix of bovine articular cartilage: an immunohistochemical study. *J Histochem Cytochem* 28:621-35, 1980.

70. Rodriguez E, Roughley P: Link protein can retard the degradation of hyaluronan in proteoglycan aggregates. *Osteoarthritis Cartilage* 14:823-9, 2006.

71. Rosenberg L, Choi HU, Tang LH, Pal S, Johnson T, Lyons DA, Laue TM: Proteoglycans of bovine articular cartilage. The effects of divalent cations on the biochemical properties of link protein. *J Biol Chem* 266:7016-24, 1991.

72. Rosenberg L, Tang L-H, Pal S, Johnson TL, Choi HU: Proteoglcyans of bovine articular cartilage: studies of the direct interaction of link protein with hyaluronate in the absence of proteoglycan monomer. *J Biol Chem* 263:18071-7, 1988.

73. Roughley PJ: The structure and function of cartilage proteoglycans. *Eur Cell Mater* 12:92-101, 2006.

74. Roughley PJ, White RJ: Age-related changes in the structure of the proteoglycan subunits form human articular cartilage. *J Biol Chem* 255:217-24, 1980.

75. Sah RL, Grodzinsky AJ, Plaas AH, Sandy JD: Effects of tissue compression on the hyaluronate-binding properties of newly synthesized proteoglycans in cartilage explants. *Biochem J* 267:803-8, 1990.

76. Sajdera SW, Hascall VC: Proteinpolysaccharide complex from bovine nasal cartilage. A comparison of low and high shear extraction procedures. *J Biol Chem* 244:77-87, 1969.

77. Schinagl RM, Gurskis D, Chen AC, Sah RL: Depth-dependent confined compression modulus of full-thickness bovine articular cartilage. *J Orthop Res* 15:499-506, 1997.

78. Sedrakyan S, Zhou ZY, Perin L, Leach K, Mooney D, Kim TH: Tissue engineering of a small hand phalanx with a porously casted polylactic acid-polyglycolic acid copolymer. *Tissue Eng* 12:2675-83, 2006.

79. Sharma B, Williams CG, Kim TK, Sun D, Malik A, Khan M, Leong K, Elisseeff JH: Designing zonal organization into tissue-engineered cartilage. *Tissue Eng* 13:405-14, 2007.

80. Skalak R, Fox CF, eds. Tissue Engineering: Proceedings of a Workshop held at Granlibakken, Lake Tahoe, California, February 26-29, 1988. New York: Liss; 1988.

81. Tang L-H, Rosenberg L, Reeiner A, Poole AR: Proteoglycans from bovine nasal and articular cartilage: properties of a soluble form of link protein. *J Biol Chem* 254:10523-31, 1979.

82. Tang LH, Buckwalter JA, Rosenberg LC: Effect of link protein concentration on articular cartilage proteoglycan aggregation. *J Orthop Res* 14:334-9, 1996.

83. Temple MM, Bae WC, Chen MQ, Lotz M, Amiel D, Coutts RD, Sah RL: Age- and site-associated biomechanical weakening of human articular cartilage of the femoral condyle. *Osteoarthritis Cartilage* 15:1042-52, 2007.

84. Venn G, Billingham MEJ, Hardingham TE: Increased proteoglycan synthesis in cartilage in experimental canine osteoarthritis does not reflect a permanent change in chondrocyte phenotype. *Arthritis Rheum* 38:525-32, 1995.

85. Venn MF, Maroudas A: Chemical composition and swelling of normal and osteoarthritic femoral head cartilage. I. Chemical composition. *Ann Rheum Dis* 36:121-9, 1977.

86. Vinatier C, Mrugala D, Jorgensen C, Guicheux J, Noel D: Cartilage Engineering: A Crucial Combination of Cells, Biomaterials and Biofactors. *Trends Biotechnol* 27:307-14, 2009.

87. von den Hoff JW, van Kampen GPJ, van de Stadt RJ, van der Korst JK: Kinetics of proteoglycan turnover in bovine articular cartilage explants. *Matrix* 13:195-201, 1993.

88. Williamson AK, Chen AC, Sah RL: Compressive properties and function-composition relationships of developing bovine articular cartilage. *J Orthop Res* 19:1113-21, 2001.

89. Xu JW, Johnson TS, Motarjem PM, Peretti GM, Randolph MA, Yaremchuk MJ: Tissue-engineered flexible ear-shaped cartilage. *Plast Reconstr Surg* 115:1633-41, 2005.

CHAPTER 2

SHAPED, STRATIFIED, SCAFFOLD-FREE GRAFTS FOR ARTICULAR CARTILAGE DEFECTS

2.1 Abstract

One goal of treatment strategies for large articular cartilage defects is the restoration of the anatomical contour of the joint with tissue having a structure similar to native cartilage. Shaped and stratified cartilaginous tissue may be fabricated into a suitable graft to achieve such restoration. The objective of this study was to determine if scaffold-free cartilaginous constructs, anatomically shaped and targeting spherically-shaped hip joints, can be created using a molding technique and if biomimetic stratification of the shaped constructs can be achieved with appropriate superficial and middle/deep zone chondrocyte subpopulations. The shaped, scaffold-free constructs were formed from the alginate-released bovine calf chondrocytes with shaping on one (saucer), two (cup), or neither (disk) surfaces. The saucer and cup constructs had shapes distinguishable quantitatively (radius of curvature of 5.5 ± 0.1 mm for saucer and 2.8 ± 0.1 mm for cup) and had no adverse effects on the glycosaminoglycan and collagen contents and their distribution in the constructs as assessed by biochemical assays and histology, respectively. Biomimetic stratification of chondrocyte subpopulations in saucer- and cup-shaped constructs was confirmed

and quantified using fluorescence microscopy and image analysis. This shaping method, combined with biomimetic stratification, has the potential to create anatomically-contoured large cartilaginous constructs.

2.2 Introduction

One aim of repair strategies for large defects in articular cartilage is to restore the anatomical contour of the joint [4]. Focal defects in cartilage are commonly found during arthroscopy [12, 16], and have a limited capacity for self-repair [5]. Large defects and widespread joint degeneration, as found in osteoarthritis, impair normal joint function and are associated with pain [13]. Surface restoration is one of the goals of treatment with osteochondral allografts [6] and autografts or mosaicplasty [30], as well as with tissue engineering-based, chondral graft treatments, such as autologous cell implantation (ACI) [3] and matrix-guided ACI (MACI) [11]. However, these treatments are limited by availability of donor tissue sources, donor site morbidity, and prolonged rehabilitation times.

Grafts that match the complex surface geometries of larger articular cartilage defects may facilitate healing. Second-generation tissue-engineered cartilaginous constructs that are in development have flat surfaces that do not address the highly contoured surfaces in large articular cartilage defects. Surface incongruity of osteochondral grafts to the surrounding native cartilage surface has been shown to result in local mechanical stresses that may be unfavorable for the success of the graft treatment [27]. Previous studies have examined shaped, tissue-engineered constructs for articular cartilage restoration or replacement have been created for patella [19], middle and distal phalanx [20, 35], and mandibular condyle [1]. Fabrication approaches for these shaped cartilaginous constructs are grouped into two main areas. In the scaffold pre-fabrication approach, a scaffold is shaped into the desired geometry, subsequently seeded with cells (chondrocytes, stem cells, etc.), and cultured

ex vivo or subcutaneously [7, 22]. This approach is commonly used for osteochondral grafts, where most of the scaffold is used for the bony substance [35]. In the molding approach, a mixture of cell and scaffold is placed together into a mold where the scaffold is polymerized, and the shaped construct is cultured. Scaffolds for the molding method are commonly hydrogels, including agarose [19], alginate [8], and photopolymerizable polyethylene glycol derivative [1]. While the results of these studies are promising, the resultant constructs vary from the desired shape due to growth and remodeling, and the surface contours of these constructs have not been analyzed.

The hip joint has a high occurrence of osteoarthritis and fracture, is commonly treated by total joint replacement [15, 32], and is thus a potential site for biological resurfacing using shaped cartilaginous constructs. The articulating surfaces of the hip joint contain two nearly spherical cartilage surfaces, concave on the acetabulum and convex on the femoral head [34]. Thus, a hemi-spherical cup-shaped graft may be useful as a replacement “cap” for a degenerate femoral head cartilage while a saucer-shaped graft with a hemispherical concave impression may be analogously useful for a degenerate acetabulum.

Biomimetic zonal stratification, another important structural feature of the articular cartilage, has been achieved in tissue-engineered chondral grafts. Cartilaginous constructs have been created with stratification of superficial and middle/deep zone subpopulations [26, 36] and with deep zone layer and calcified cartilage layer [2]. Such constructs have been shown to maintain the zonal-specific characteristics, including the synthesis and secretion of proteoglycan 4 by the

chondrocytes derived from the superficial zone [26], relatively high levels of matrix production by deep zone chondrocytes [36], and mineralization in the calcified cartilage layer [2]. This structural organization may be important since various cellular products are correlated with inhomogeneous biochemical and mechanical properties of articular cartilage [28].

Thus, the objective of this study was to establish and validate a molding technique for fabrication of cartilaginous constructs that are anatomically shaped on one or two surfaces, targeting the spherically-shaped hip joint, and biomimetically stratified with superficial and middle/deep zone chondrocyte subpopulations.

2.3 Materials and Methods

Study I: Fabrication of scaffold-free, shaped cartilaginous constructs

The objective of this study was to determine if scaffold-free cartilaginous constructs that were either flat (disk) or shaped on one (saucer) or two sides (cup) could be created. The surface contours of these constructs were assessed qualitatively and quantitatively in addition to their biochemical content (Fig. 2.1A).

To prepare for construct formation, the isolated chondrocytes were cultured in alginate beads for 7 days as described previously [25, 29]. The chondrocytes from the distal femoral condyles of bovine calf knees (1-3 weeks old) were isolated by sequential digestion in 0.2% pronase for 1 hour and 0.019% collagenase P for 16 hours. Then, the chondrocytes in 1.2% alginate at $4x10^6$ cells/ml were expelled into 102 mM calcium chloride using a 22-gauge needle and were cultured in DMEM/F12 with additives (100 U/ml penicillin, 100 μg/ml streptomycin, 0.25 μg/ml fungizone, 0.1 mM MEM non-essential amino acids, 0.4 mM L-proline, 2 mM L-glutamine), 20% fetal bovine serum (FBS), and 25 μg/ml ascorbic acid at 1 ml/$1x10^6$ cells·day. After 7 days the chondrocytes with their cell-associated matrix were then released from alginate in 55 mM sodium citrate in 150 mM sodium chloride.

The shaped constructs were formed from the alginate recovered chondrocytes (ARC) with molds. The culture chambers for construct formation were machined from polysulfone and had a porous base of filter paper with 2% agarose to allow for nutrient transfer. The ARCs were seeded at $20x10^6$ cells/ml into one of three culture chamber types: disk, saucer, and cup. Traditional disk constructs, with a flat base and no molding at the free surface, served as the control. For shaping of one cartilaginous

surface, saucer-shaped constructs were created using polysulfone hemispherical molds (radius=4.1 mm) which were placed on top of the chamber for the first 2 days of culture. For shaping of two cartilaginous surfaces, cup constructs were formed by seeding cells on hemispherical, concave agarose supports (r=4.1 mm) inside the culture chamber, again with application of hemispherical molds (r=3.2 mm) on top for initial culture. The disk and saucer constructs contained approximately $6x10^6$ cells total, and the cup constructs contained about $1.6x10^6$ cells total. All constructs were cultured in DMEM with additives, 10% FBS, and 25 μg/ml ascorbic acid at 1 ml/$1x10^6$ cells·day for an additional 10 days, for a total of 17 days in culture. For the first two days of culture, medium was changed every day to prevent the medium from flooding over the top of culture chamber and disturbing the coalescence of the ARC into a cohesive construct. After two days the molds were removed, and medium was added to submerge the culture chamber for the rest of the culture period. Medium was changed every two days after the first two days of construct culture. Two days was chosen as the molding time as a pilot study demonstrated that this was sufficient time for molding.

After culture, the constructs were transferred to phosphate buffered saline (PBS), weighed wet, and photographed for qualitative assessment of the construct shape.

To quantify surface contour, constructs were raster-scanned (ΔX of 0.2 mm and ΔY of 0.5 mm) with a non-contact laser displacement sensor (25 μm resolution; Acuity AR200, Schmitt Industries, Portland, OR). The three-dimensional surface measurements contain over 1,000 individual points for each of the disk and saucer-

shaped constructs and over 600 points for each of the cup-shaped constructs. The measurements were processed with MATLAB (MathWorks, Natick, MA) to fit a flat plane on top of the disk constructs or spherical surface on top of the saucer and cup constructs. From the fits, the radii of curvature of the saucer and the inner surface of cup constructs were computed. In addition, for each type of construct, the roughness of fit was assessed by root mean square (RMS) of error calculated from the fitted planes and spheres in comparison to the measured data.

The constructs were cut in half using a cutting guide with half circle cut-outs. One half of each construct was fixed in 4% paraformaldehyde at 4°C for 2 days, dehydrated, embedded in paraffin, sectioned at 5 μm, and stained with Safranin O to qualitatively assess glycosaminoglycan (GAG) distribution [33].

To quantitatively assess the biochemical contents, the other half of each construct was solubilized with proteinase K and assayed for DNA using PicoGreen (Invitrogen, Carlsbad, CA) [31], GAG using dimethylmethylene blue [14], and collagen using dimethylaminobenzaldehyde assay for hydroxyproline [40].

Data are expressed as mean ± standard error of the mean (SEM). The measured radii of curvature for saucer and cup constructs were compared to the mold radii as the hypothesized means by one-sample t test. The effect of construct shaping on RMS roughness and biochemical content were assessed by one-way analysis of variance with Tukey post hoc test ($p < 0.05$). Power calculations were performed to determine the number of samples (n) sufficient for detecting the expected difference δ with α=0.05, and 1-β=0.8. With the expected ratio of treatment effect for radius of curvature at about 3.6, n=3 samples per group was appropriate. There was a total of 15

constructs (6 disks, 5 saucer-shaped, and 4 cup-shaped) that were cultured for a total of 17 days.

Study II: Fabrication of stratified, shaped, scaffold-free cartilaginous constructs

The objective of this study was to determine if shaped cartilaginous constructs in disk, saucer, and cup geometries could be fabricated with biomimetic stratification of superficial and middle/deep zone chondrocytes. The stratification was assessed using fluorescence microscopy (Fig. 2.1B).

Bovine calf chondrocytes from superficial zone (designated as S) (0 – 200 μm from the articular surface) and middle/deep zones (designated as M) (600 – 1600 μm) from patellofemoral grooves of multiple bovine calves were obtained using a microtome and isolated as described [25]. The S and M isolated chondrocytes were separately seeded in monolayer at 20,000 cells/cm^2, cultured with DMEM with additives, 10% FBS, and 25 μg/ml ascorbate, and expanded until about 80 – 90 % confluent (11 days). The chondrocytes were expanded in monolayer to obtain numbers required for construct formation. The S and M chondrocytes were then released into single cell suspensions using sequential digestion with 0.2% pronase for 5 minutes and 0.025% collagenase for 90 minutes. The S chondrocytes were labeled with 20 μM PKH26 (Sigma, St. Louis, MO) for 5 minutes at 25°C according to manufacturer's instructions [10]. S and M chondrocytes were then cultured for 9 and 7 days respectively in 1.2% alginate beads with DMEM/F12 with additives, 20% FBS, and 25 μg/ml ascorbate as described above. The chondrocytes were cultured for 29 days in total for expansion, pre-culture, and construct formation.

After 7 days in alginate bead culture the M chondrocytes were released from alginate beads and labeled with 20 μM carboxyfluorescein diacetate, succinimidyl ester (CFSE) (Invitrogen, Carlsbad, CA) for 15 minutes at 37°C according to manufacturer's instructions. These labeled M ARCs were then seeded into the three culture chamber types as described above. Two days after the initial seeding, the S chondrocytes were released from alginate beads and seeded on top of the M ARCs in the three culture chamber types at 25 $x10^6$ cells/ml with new molds with radii that are 0.8 mm smaller in the center (r=3.2 mm for saucer constructs and r=2.5mm for cup constructs). The disk (n=4) and saucer (n=5) constructs contained approximately 1.6 $x10^6$ S cells, and the cup (n=4) constructs contained about 1 $x10^6$ S cells. The molds were removed two days later, and the constructs were cultured for 7 more days, for a total of 11 days (11 days with middle zone chondrocytes and 9 days with superficial chondrocytes in culture chamber set up) in with DMEM with additives, 10% FBS, and 25 μg/ml ascorbate at 1 ml/$1x10^6$ cells·day. The chondrocytes were cultured for 29 days in total for expansion, pre-culture, and construct formation.

At the end of the culture period, these constructs were fixed for 2 days in 4% paraformaldehyde in the dark at 4°C and snap frozen with Tissue-Tek® optimal cutting temperature (OCT) compound (Sakura Finetek, Torrance, CA) in isopentane cooled with liquid nitrogen. These constructs were then cryosectioned vertically at 40 μm thickness and visualized using epifluorescence and phase contrast microscopy with a 4x objective (Eclipse TE300, Nikon, Melville, NY). Fluorescent images of PKH26-labeled S cells (red signal) and CFSE-labeled M cells (green signal) in the identical field were obtained separately and subsequently processed and merged.

The extent of stratification was quantified by two methods of analysis of images (field of view of 2.9 x 2.2 mm^2) visualizing vertical cross-sections of the constructs. First, the area fraction, relative to the overall construct area, occupied by PKH26-labeled S chondrocytes calculated from manual tracings. This area fraction occupied by the S chondrocytes was then compared to the theoretical percentage of S chondrocytes relative to all the cells seeded. Second, three selected areas of width of 0.362 mm (200 pixels) and construct full-thickness from each fluorescent image were analyzed to calculate red and green intensity profiles as a function of thickness-normalized distance from the construct surface. The profiles were averaged and plotted with respect to the distance from the surface of the constructs normalized to the construct thickness.

Data are expressed as mean ± SEM. One-sample t tests were performed after arcsine transformation to compare the measured S area fractions to the expected values based on S chondrocytes seeded compared to the total chondrocytes seeded (21% for disk and saucer constructs and 38% for cup constructs). Power calculations were performed to determine the number of samples (n) sufficient for detecting the expected difference δ with α=0.05, and 1-β=0.8. With the expected ratio of treatment effect for S area fraction approximately 2.8, n=4 samples per group was appropriate. There was a total of 13 constructs (4 disks, 5 saucers, and 4 cups) that were cultured for a total of 29 days.

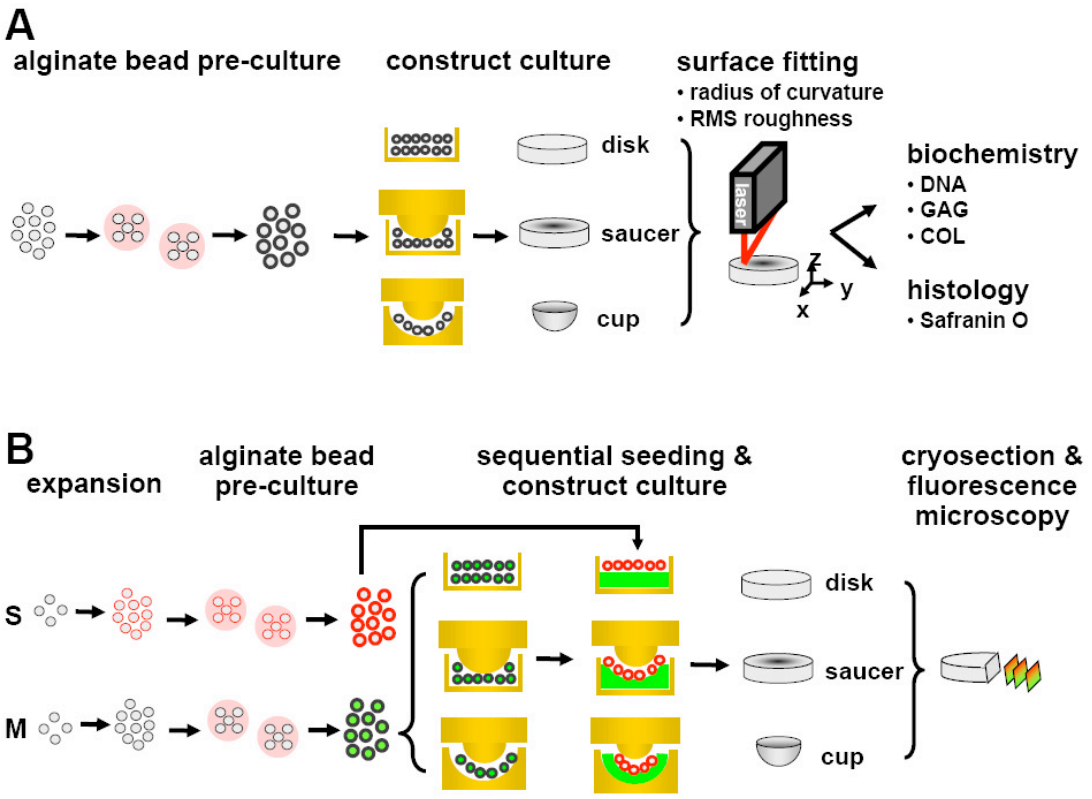

Figure 2.1: Schematic of methods for fabrication of shaped, scaffold-free cartilaginous constructs with (A) full-thickness chondrocytes and (B) zonal subpopulations with stratification. Freshly isolated or expanded chondrocytes were cultured in alginate beads, released, and seeded into construct chambers with or without molds. (A) The shaped constructs in disk, saucer, and cup geometries were analyzed for surface contour, biochemical content, and histology. (B) The stratified constructs were composed of chondrocytes from the superficial (S) and middle (M) layer sections of cartilage and were analyzed for stratification using fluorescence micrographs of cryosections.

2.4 Results

Cartilaginous constructs, in disk, saucer, and cup geometries, were fabricated consistently. These constructs were able to withstand manual handling and maintain their shapes. Qualitatively, such constructs had distinct surface contours, with top, both top and bottom, or neither surfaces molded and shaped for saucer, cup, and flat constructs respectively (Fig. 2.2).

Quantitative analysis of surface contour measurements (Fig. 2.3) showed that saucer and cup constructs had significantly different radii of curvature from each other (5.5±0.1 mm and 2.8±0.1mm), with the inner surface of cup constructs having smaller radius of curvature than the saucer constructs ($p<0.001$) (Table 2.1). The fitted planes and curves were relatively smooth, as evidenced by the RMS roughness values (<0.3mm) that were not significantly different between groups ($p=0.175$). The radius of curvature of the saucer-shaped contour was less than that of the corresponding mold ($p<0.001$), while that of the cup shaped contour was slightly less than that of its corresponding mold ($p<0.05$) (Table 2.1).

Constructs of all shapes had DNA, GAG, and collagen per wet weight that generally were similar (Fig. 2.4). The cup constructs had higher collagen content than the other construct types ($p<0.005$ vs disk and saucer). All three construct types contained GAG through the construct based on Safranin O staining (Fig. 2.5).

Stratification by sequential seeding of two distinct chondrocyte subpopulations was achieved for cartilaginous constructs of all shapes (Fig. 2.6). The superficial zone chondrocyte layer, fluorescing red, was qualitatively distinct from the middle zone chondrocyte layer, fluorescing green, in all constructs as evidenced by fluorescence

micrographs. A comparison of fluorescence micrographs and phase contrast micrographs indicated that majority of the chondrocytes were positively labeled with only one of the dyes. The percent area occupied by S chondrocytes (S area fraction) in the shaped constructs (saucer and cup) were similar to the expected values based on seeded cells ($p>0.7$) (Fig. 2.7A). The fluorescence intensity profiles indicated that all three constructs achieved stratification of S atop M chondrocytes (Fig. 2.7B, C, D). The transitions from S to M chondrocytes occurred further from the surface in the shaped constructs than for the flat disk constructs, supporting the data from area fraction occupied by S chondrocytes.

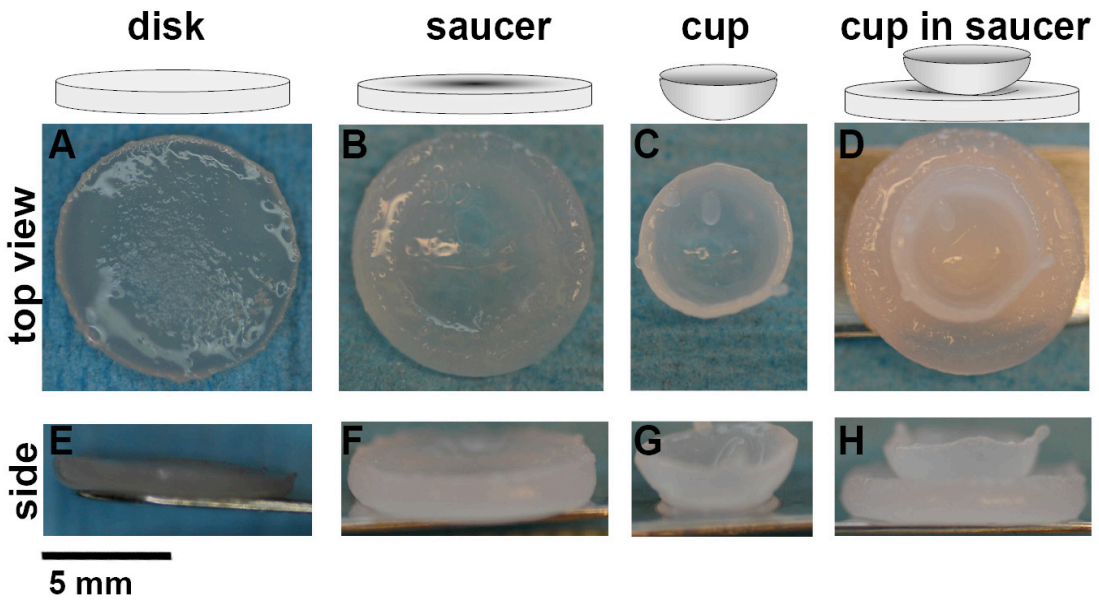

Figure 2.2: Macroscopic images of shaped cartilaginous constructs. (A, E) Disk construct with no molding. (B, F) Saucer constructs with molding on top. (C, G) Cup constructs with molding on two surfaces. (D, H) Cup construct on top of saucer construct.

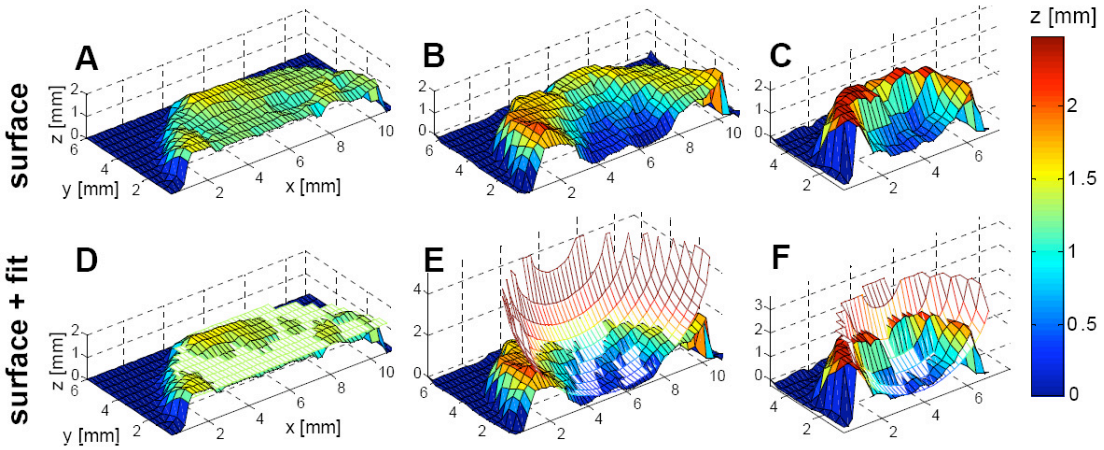

Figure 2.3: Representative 3D surface contours of half of (A) disk, (B) saucer, and (C) cup constructs. The surface contours were fit to plane and sphere for (D) disk, (E) saucer, and (F) cup constructs. The color scale indicates the heights in the z-axis in mm.

Table 2.1: Quantification of shape of constructs by analysis of fitted planes and spheres. (mean ± SEM, n=3-6, *p<0.001 vs mold, **p<0.05 vs mold, ^p<0.001 vs saucer)

	disk	saucer	cup
radius of mold [mm]		**4.1**	**3.2**
radius of curvature measured [mm]	**--**	**5.5 ± 0.1***	**2.8 ± 0.1 **,^**
RMS roughness [mm]	**0.20 ± 0.04**	**0.15 ± 0.01**	**0.26 ± 0.05**

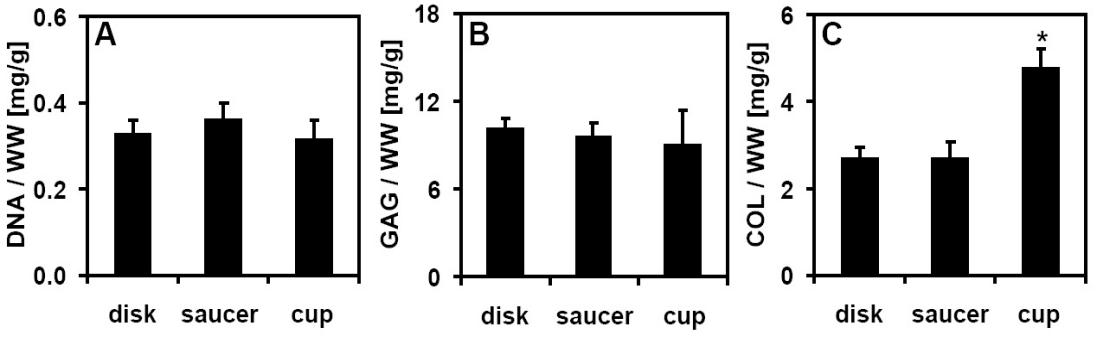

Figure 2.4: Biochemical content of constructs. (A) DNA, (B) GAG, and (C) collagen contents normalized by wet weight for disk, saucer, and cup constructs. (mean ± SEM, n=4-6, * $p<0.005$ vs disk and saucer)

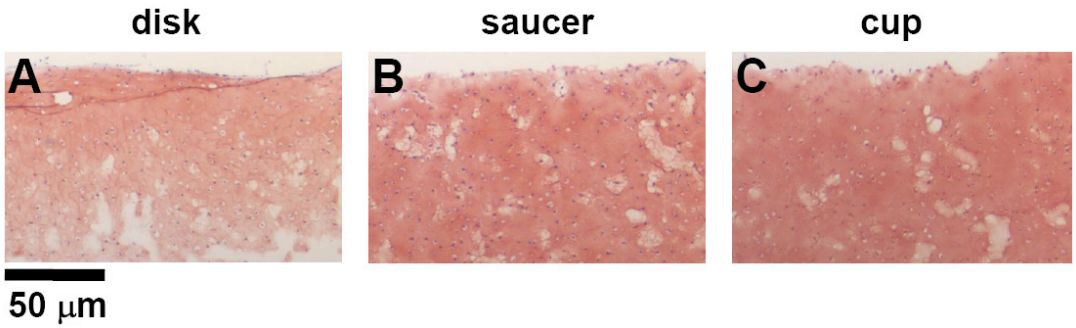

Figure 2.5: Safranin-O histochemical sections of (A) disk, (B) saucer, and (C) cup constructs.

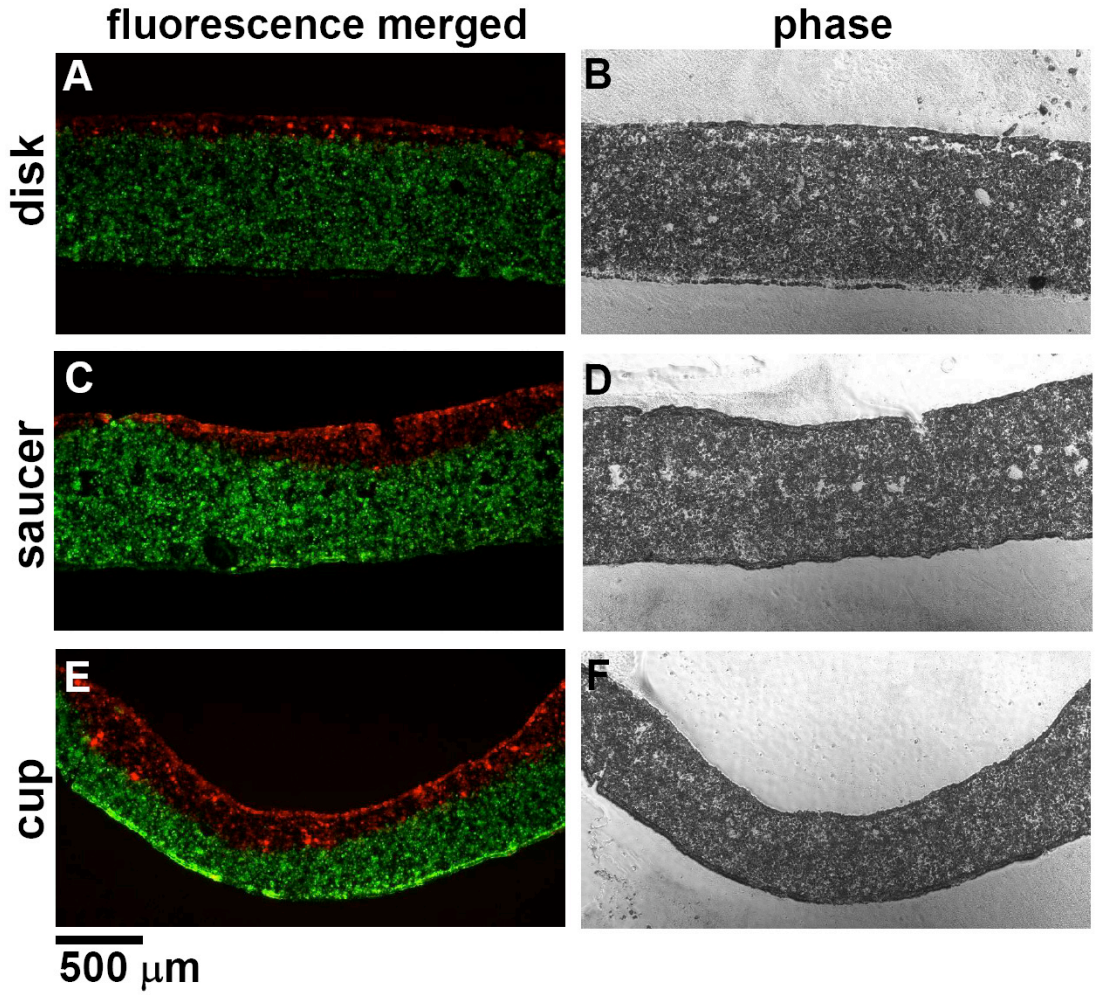

Figure 2.6: Merged fluorescence and phase micrographs of stratified constructs of (A, B) disk, (C, D) saucer, and (E, F) cup geometries. Superficial zone chondrocytes labeled with PKH26 dye, which fluoresces red, were seeded on top of middle zone chondrocytes labeled with CFSE dye, which fluoresces green.

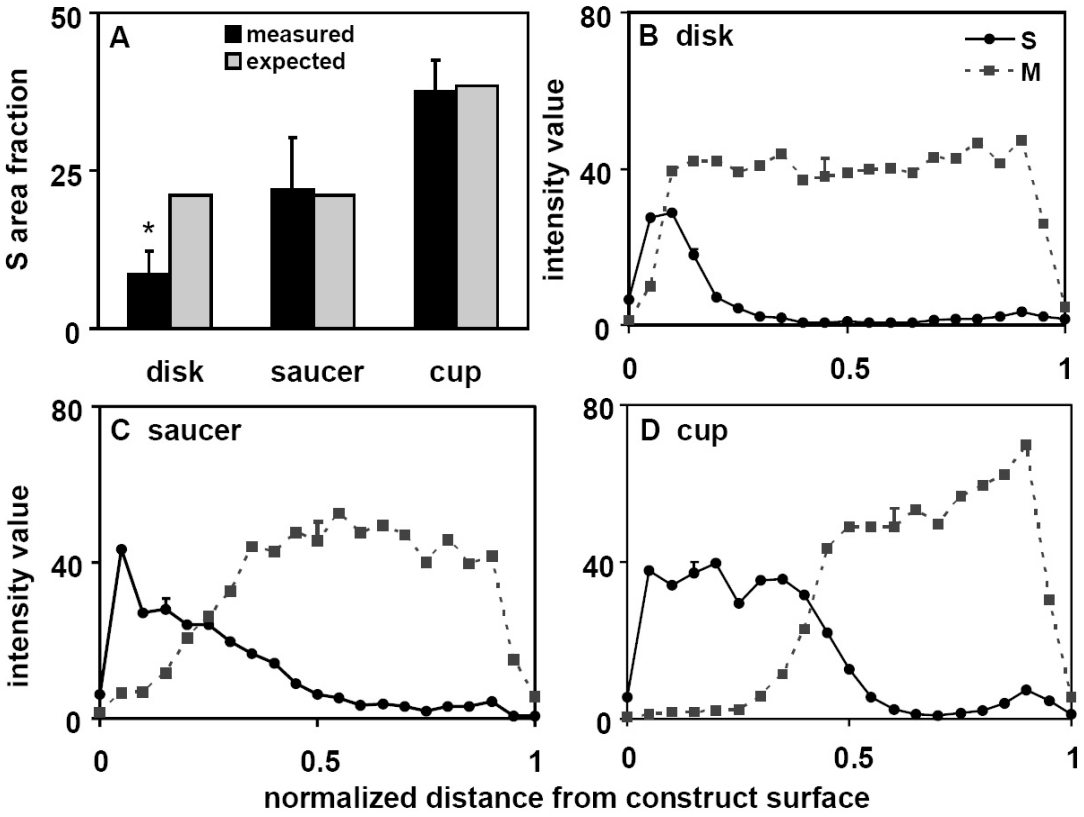

Figure 2.7: Quantification of stratification in (A, B) disk, (A, C) saucer, and (A, D) cup constructs. (A) Measure and expected areas covered by S chondrocytes. The fluorescence intensity profiles of the PKH26-labeled superficial (S) layer chondrocytes and CFSE-labeled middle (M) layer chondrocytes for (B) disk, (C) saucer, and (D) cup constructs with error bar indicating average SEM values. (n=4-5, *$p<0.05$ vs expected)

2.5 Discussion

One goal of treatments for large articular cartilage defects is the restoration of the anatomical contour of the joint with tissue having a structure similar to native cartilage. Since surface incongruities may limit graft success, shaped and stratified cartilaginous tissue may be a suitable graft to achieve such restoration. The objective of this study was to establish and validate a molding technique for fabrication of cartilaginous constructs that are anatomically shaped, targeting the spherically shaped hip, and biomimetically stratified with superficial and middle/deep zone chondrocyte subpopulations. We present a molding technique for fabrication of shaped cartilaginous constructs using ARCs in saucer and cup shapes with one and two surfaces molded, respectively (Fig. 2.2). Qualitatively, the shaped constructs had surface contours different from those of the control disk constructs. Quantitatively, the saucer and cup constructs were distinct in their radii of curvature (Table 2.1). These results demonstrate molding fabrication can generate constructs that are contoured and fabricated from only chondrocytes and their biosynthetic products. The matrix products accumulated fairly similarly regardless of the shape of the construct, demonstrating the shaping does not adversely affect chondrocyte functions (Figs. 2.4, 2.5). Additionally, this molding technique was adapted to create shaped cartilaginous constructs with biomimetic stratification (Fig. 2.6). Thus, in this study tissue-engineered cartilaginous constructs were designed to have, and analyzed for, anatomic three-dimensional contours and biomimetic stratification.

There were several limitations to this study. Cell source is an important consideration since these constructs were formed solely from the chondrocytes and the

pericellular matrix they produced. While this study was performed with immature calf chondrocytes, which are metabolically active, this shaping technology would likely be applicable to chondrocytes from mature articular cartilage since such chondrocytes can be used to form scaffold-free disk constructs [29]. Additionally, the cell source limitation may be circumvented by expansion of the cell source followed by three-dimensional alginate bead culture [9, 38].

Previous studies on shaped tissue engineering of cartilage have utilized molding or machining of the scaffold material to define the contour of the construct. These methods have been used for engineering of elastic and non-articular cartilage such as auricle [7, 21, 41], nose [8, 21], and tympanic membrane [17]. Several shaped osteochondral constructs containing articular cartilaginous sections, for phalanx [20, 35] and mandibular condyle [1] for example, have been fabricated. Bone grafts also have been constructed in various shapes, including femoral head and mandible [23]. Many of these previous works rely on scaffolds to provide mechanical stability to the constructs and aid in the maintenance of their shapes. Like some of these previous studies, molding was used to shape the constructs in this study. However, here we sought to develop three dimensionally-shaped cartilaginous constructs supported only by the cells and its biosynthetic products, using a molding technique.

In previous studies the shape of constructs changed qualitatively from the initial scaffold or mold shape due to growth and/or remodeling of the scaffold during culture [7, 22, 35]. Additionally, many of the previous work on shaped cartilaginous grafts do not contain quantification of the construct shapes or contours. In the present study, considerable effort went into the development of the analysis of the surface

contour of the shaped constructs, from the determining a method of accurate data acquisition and the development of the appropriate image processing protocol using MATLAB. Here, the measured radii of curvature of the shaped constructs differed from those of the hemi-spherical molds that were used (Table 1). However, contraction of scaffold-free constructs noted in a previous study with expanded chondrocytes cultured on agarose [18] was not observed here, possibly due to phenotype stabilization during alginate pre-culture. A longer shaping period with a permeable mold may allow for better retention of the initial shape and also adequate nutrient transfer. Also, reshaping by mechanical loading following the initial construct formation period may allow for finer control of construct shape [39], This molding technique for shaping of tissue-engineered construct may also be applied to joints with geometries and contours that are more complex than those of the hip.

A biomimetic approach to cartilage tissue engineering in terms of construct shape and structural organization may be advantageous for clinical applications. The use of tissue-engineered grafts with flat surfaces may be sufficient to approximate the normal cartilage surface for smaller defects but not larger defects. Surface incongruity between osteochondral grafts and the surrounding native cartilage results in local mechanical stresses that may be unfavorable for the graft survival and treatment efficacy [27].

The applicability of this shaping technology to constructs with a biomimetic cellular organization suggests the possible application to tissue with multiple layers. Previously, stratified cartilaginous constructs with superficial zone chondrocytes atop middle/deep zone chondrocytes have been shown to maintain the zonal characteristics

typical of their source, such as proteoglycan 4 and differential matrix production [26, 36]. Such differential spatial characteristics result in inhomogeneous biochemical and biomechanical properties of native cartilage with respect to depth and may be important in the maturation and, ultimately, function of tissue-engineered cartilaginous constructs as well [24]. The stratification can be customized with different types and arrangements of cells and materials for various target application and location.

The biochemical content of the shaped constructs in this current study is consistent with previously-described constructs [26, 29, 38]. Like many tissue-engineered cartilaginous constructs, the constructs here had lower extracellular matrix content, especially collagen, compared to that of native cartilage. The slightly elevated deposition of collagen in cup-shaped constructs may be due to enhanced nutrient transport provided by the thinner cup constructs as compared to thicker disk and saucer-shaped constructs. It is also possible that the thicker agarose support on the bottom of cup constructs helped to retain more of the matrix products.

The shaping technique presented here has the potential to facilitate treatment of larger articular cartilage defects where recreation of surface contour is important. Such shaping methods may be coupled with non-invasive 3-dimensional imaging to determine the surface contour of subchondral bone and/or of contralateral cartilage in order to appropriately tailor the shape of the construct [37]. Improved control over shaping and stratification would be useful in clinical translation of these shaped, stratified, scaffold-free grafts. Larger constructs that are needed for repair of large articular cartilage defects may become feasible with expansion and redifferentiation methods for the cells in conjunction with a bioreactor for improved construct growth

and maturation. To attach such constructs to the surrounding native tissue, such shaped grafts may either be fixed in the defect area with fibrin glue, as with current tissue-engineered grafts like MACI [11], or be fabricated *in vitro* atop a boney substance, which can integrate into the surrounding native bone after implantation as with current allo- or autograft techniques. *In vivo* implantation of these grafts is needed to better assess the functionality and durability of such biomimetic, tissue-engineered grafts with appropriate shape and stratification.

2.6 Acknowledgments

This chapter, in full, was published in *Clinical Orthopaedics and Related Research.* The dissertation author is the primary investigator and thanks co-authors, Drs. Won C. Bae and Nancy D. Hsieh-Bonassera, Mr. Van W. Wong, Mrs. Barbara L. Schumacher, and Drs. Simon Görtz, Koichi Masuda, William D. Bugbee, and Robert L. Sah for their contributions to this work. This work was supported by National Football League Charities, Musculoskeletal Transplant Foundation, and by a grant to University of California-San Diego, in support of Prof. Robert L. Sah, from the Howard Hughes Medical Institute through the HHMI Professors Program. Additional support was received from NIH, NSF, and an NSF Graduate Research Fellowship (EHH).

2.7 References

1. Alhadlaq A, Mao JJ: Tissue-engineered osteochondral constructs in the shape of an articular condyle. *J Bone Joint Surg Am* 87:936-44, 2005.

2. Allan KS, Pilliar RM, Wang J, Grynpas MD, Kandel RA: Formation of biphasic constructs containing cartilage with a calcified zone interface. *Tissue Eng* 13:167-77, 2007.

3. Brittberg M, Lindahl A, Nilsson A, Ohlsson C, Isaksson O, Peterson L: Treatment of deep cartilage defects in the knee with autologous chondrocyte transplantation. *N Engl J Med* 331:889-95, 1994.

4. Buckwalter JA: Evaluating methods of restoring cartilaginous articular surfaces. *Clin Orthop Rel Res* 367S:224-38, 1999.

5. Buckwalter JA, Mankin HJ: Articular cartilage. Part II: degeneration and osteoarthrosis, repair, regeneration, and transplantation. *J Bone Joint Surg Am* 79-A:612-32, 1997.

6. Bugbee WD, Convery FR: Osteochondral allograft transplantation. *Clin Sports Med* 18:67-75, 1999.

7. Cao Y, Vacanti JP, Paige KT, Upton J, Vacanti CA: Transplantation of chondrocytes utilizing a polymer-cell construct to produce tissue-engineered cartilage in the shape of a human ear. *Plast Reconstr Surg* 100:297-302; discussion 3-4, 1997.

8. Chang SC, Rowley JA, Tobias G, Genes NG, Roy AK, Mooney DJ, Vacanti CA, Bonassar LJ: Injection molding of chondrocyte/alginate constructs in the shape of facial implants. *J Biomed Mater Res* 55:503-11, 2001.

9. Chawla K, Klein TJ, Schumacher BL, Jadin KD, Shah BH, Nakagawa K, Wong VW, Chen AC, Masuda K, Sah RL: Short-term retention of labeled chondrocyte subpopulations in stratified tissue-engineered cartilaginous constructs implanted in vivo in mini-pigs. *Tissue Eng* 13:1525-37, 2007.

10. Chawla K, Klein TJ, Schumacher BL, Schmidt TA, Voegtline MS, Thonar EJ-MA, Masuda K, Sah RL: Tracking chondrocytes and assessing their proliferation with PKH26: effects on secretion of proteoglycan 4 (PRG4). *J Orthop Res* 24:1499-508, 2006.

11. Cherubino P, Grassi FA, Bulgheroni P, Ronga M: Autologous chondrocyte implantation using a bilayer collagen membrane: a preliminary report. *J Orthop Surg (Hong Kong)* 11:10-5, 2003.

12. Curl WW, Krome J, Gordon ES, Rushing J, Smith BP, Poehling GG: Cartilage injuries: a review of 31,516 knee arthroscopies. *Arthroscopy* 13:456-60, 1997.

13. Dieppe PA, Lohmander LS: Pathogenesis and management of pain in osteoarthritis. *Lancet* 365:965-73, 2005.

14. Farndale RW, Buttle DJ, Barrett AJ: Improved quantitation and discrimination of sulphated glycosaminoglycans by use of dimethylmethylene blue. *Biochim Biophys Acta* 883:173-7, 1986.

15. Felson DT: Epidemiology of hip and knee osteoarthritis. *Epidemiol Rev* 10:1-28, 1988.

16. Hjelle K, Solheim E, Strand T, Muri R, Brittberg M: Articular cartilage defects in 1,000 knee arthroscopies. *Arthroscopy* 18:730-4, 2002.

17. Hott ME, Megerian CA, Beane R, Bonassar LJ: Fabrication of tissue engineered tympanic membrane patches using computer-aided design and injection molding. *Laryngoscope* 114:1290-5, 2004.

18. Hu JC, Athanasiou KA: Chondrocytes from different zones exhibit characteristic differences in high density culture. *Connect Tissue Res* 47:133-40, 2006.

19. Hung CT, Lima EG, Mauck RL, Taki E, LeRoux MA, Lu HH, Stark RG, Guo XE, Ateshian GA: Anatomically shaped osteochondral constructs for articular cartilage repair. *J Biomech* 36:1853-64, 2003.

20. Isogai N, Landis W, Kim TH, Gerstenfeld LC, Upton J, Vacanti JP: Formation of phalanges and small joints by tissue-engineering. *J Bone Joint Surg Am* 81-A:306-16, 1999.

21. Kamil SH, Kojima K, Vacanti MP, Bonassar LJ, Vacanti CA, Eavey RD: In vitro tissue engineering to generate a human-sized auricle and nasal tip. *Laryngoscope* 113:90-4, 2003.

22. Kang SW, Son SM, Lee JS, Lee ES, Lee KY, Park SG, Park JH, Kim BS: Regeneration of whole meniscus using meniscal cells and polymer scaffolds in a rabbit total meniscectomy model. *J Biomed Mater Res A* 78:659-71, 2006.

23. Khouri RK, Koudsi B, Reddi H: Tissue transformation into bone in vivo. A potential practical application. *JAMA* 266:1953-5, 1991.

24. Klein TJ, Chaudhry M, Bae WC, Sah RL: Depth-dependent biomechanical and biochemical properties of fetal, newborn, and tissue-engineered articular cartilage. *J Biomech* 40:182-90, 2007.

25. Klein TJ, Schumacher BL, Blewis ME, Schmidt TA, Voegtline MS, Thonar EJ-MA, Masuda K, Sah RL: Tailoring secretion of proteoglycan 4 (PRG4) in tissue-engineered cartilage. *Tissue Eng* 12:1429-39, 2006.

26. Klein TJ, Schumacher BL, Schmidt TA, Li KW, Voegtline MS, Masuda K, Thonar EJ-MA, Sah RL: Tissue engineering of stratified articular cartilage from chondrocyte subpopulations. *Osteoarthritis Cartilage* 11:595-602, 2003.

27. Koh JL, Wirsing K, Lautenschlager E, Zhang LO: The effect of graft height mismatch on contact pressure following osteochondral grafting. A biomechanical study. *Am J Sports Med* 32:317-20, 2004.

28. Maroudas A: Physico-chemical properties of articular cartilage. In: *Adult Articular Cartilage,* ed. by MAR Freeman, Pitman Medical, Tunbridge Wells, England, 1979, 215-90.

29. Masuda K, Sah RL, Hejna MJ, Thonar EJ-MA: A novel two-step method for the formation of tissue-engineered cartilage by mature bovine chondrocytes: the alginate-recovered-chondrocyte (ARC) method. *J Orthop Res* 21:139-48, 2003.

30. Matsusue Y, Yamamuro T, Hama H: Arthroscopic multiple osteochondral transplantation to the chondral defect in the knee associated with anterior cruciate ligament disruption. *Arthroscopy* 9:318-21, 1993.

31. McGowan KB, Kurtis MS, Lottman LM, Watson D, Sah RL: Biochemical quantification of DNA in human articular and septal cartilage using PicoGreen and Hoechst 33258. *Osteoarthritis Cartilage* 10:580-7, 2002.

32. Melzer D, Guralnik JM, Brock D: Prevalence and distribution of hip and knee joint replacements and hip implants in older Americans by the end of life. *Aging Clin Exp Res* 15:60-6, 2003.

33. Rosenberg LC: Chemical basis for the histological use of safranin O in the study of articular cartilage. *J Bone Joint Surg Am* 53-A:69-82, 1971.

34. Rushfeldt PD, Mann RW, Harris WH: Improved techniques for measuring in vitro the geometry and pressure distribution in the human acetabulum--I. ultrasonic measurement of acetabular surfaces, sphericity and cartilage thickness. *J Biomech* 14:253-60, 1981.

35. Sedrakyan S, Zhou ZY, Perin L, Leach K, Mooney D, Kim TH: Tissue engineering of a small hand phalanx with a porously casted polylactic acid-polyglycolic acid copolymer. *Tissue Eng* 12:2675-83, 2006.

36. Sharma B, Williams CG, Kim TK, Sun D, Malik A, Khan M, Leong K, Elisseeff JH: Designing zonal organization into tissue-engineered cartilage. *Tissue Eng* 13:405-14, 2007.

37. Sidler R, Kostler W, Bardyn T, Styner MA, Sudkamp N, Nolte L, Gonzalez Ballester MA: Computer-assisted ankle joint arthroplasty using bio-engineered autografts. *Med Image Comput Comput Assist Interv Int Conf Med Image Comput Comput Assist Interv* 8:474-81, 2005.

38. Stoddart MJ, Ettinger L, Hauselmann HJ: Generation of a scaffold free cartilage-like implant from a small amount of starting material. *J Cell Mol Med* 10:480-92, 2006.

39. Williams GM, Lin JW, Sah RL: Cartilage reshaping via in vitro mechanical loading. *Tissue Eng* 13:2903-11, 2007.

40. Woessner JF: The determination of hydroxyproline in tissue and protein samples containing small proportions of this imino acid. *Arch Biochem Biophys* 93:440-7, 1961.

41. Xu JW, Johnson TS, Motarjem PM, Peretti GM, Randolph MA, Yaremchuk MJ: Tissue-engineered flexible ear-shaped cartilage. *Plast Reconstr Surg* 115:1633-41, 2005.

CHAPTER 3

PROTEOGLYCAN OSMOTIC SWELLING PRESSURE CONTRIBUTION TO COMPRESSIVE PROPERTIES OF ARTICULAR CARTILAGE

3.1 Abstract

The negatively-charged proteoglycans (PG) provide compressive resistance to articular cartilage by their fixed charge density (FCD) and high osmotic pressure (π_{PG}), while the collagen networks (CN) provide the restraining forces to counterbalance π_{PG}. The objectives were to (1) account for collagen intrafibrillar water in transforming biochemical measurements into a FCD–π_{PG} relationship, (2) compute π_{PG} and CN contributions to compressive behavior of full-thickness cartilage during bovine growth (fetal, calf, adult) and human adult aging (young, old), and (3) predict the effect of depth from the articular surface on π_{PG} in human aging. Extrafibrillar FCD (FCD_{EF}) and π_{PG} increased with bovine growth due to an increase in CN concentration while PG concentration was steady; this maturation-related increase was amplified by compression. With normal human aging, FCD_{EF} and π_{PG} decreased. The π_{PG} were close to σ_{EQ} in all bovine and Young human cartilage but was only ~half of σ_{EQ} in Old human cartilage. Depth-related variations in the strain, FCD_{EF}, π_{PG}, and

σ_{CN} profiles in human cartilage suggested the functional deterioration of the superficial layer with aging. These results suggest the utility of the FCD–π_{PG} relationship for elucidating the contribution of matrix macromolecules to the biomechanical properties of cartilage.

3.2 Introduction

The main extracellular matrix components of articular cartilage, proteoglycans (PG) and collagens (COL), provide unique biomechanical properties that vary with growth, aging, and depth from the articular surface. The negatively-charged PG contribute to compressive resistance and provide a high osmotic pressure (π_{PG}) within the tissue. In contrast, the collagen network (CN) provides the restraining force that counterbalance π_{PG} at rest or during loading, and the high resistance of cartilage to tension [25]. Nearly 90% of PG is aggrecan that complexes with hyaluronan (HA) and link protein to form large PG aggregates entrapped within the CN [29]. The aggrecan monomers contain many long chains of sulfated glycosaminoglycans (GAG), specifically chondroitin sulfate (CS) and keratan sulfate (KS). CS and KS, in turn, provide a fixed charged density (FCD) to the tissue due to the sulfate and carboxyl groups of CS and sulfate groups of KS. With the electrostatic repulsion of negatively charged GAG moieties, the FCD contributes to the compressive resistance of the tissue by providing π_{PG} and an associated elevation in mobile ion concentration within the tissue [26].

Native cartilage tissue exhibits variations in compressive properties, both with age and with depth from the articular surface, which is generally attributed to variations in biochemical content. Even with a steady GAG concentration during bovine growth from fetal to adult stages, the compressive modulus increases ~2–fold due an increase in COL concentration by 2-3–fold [42]. On the other hand, human aging has been associated with a trend of decreasing compressive modulus and PG

concentration while COL concentration remains steady [1, 34]. Cartilage also displays compressive properties and biochemical content and organization that vary with depth from the articular surface to the bone. The superficial layers have a relatively low FCD and exhibit larger displacements and strains during compression compared to the deeper layers [14, 31, 39]. The depth-dependent variations in water content, PG content, FCD, and π_{PG} seen in normal cartilage are altered significantly with osteoarthritic disease in association with aging [39]. Such alterations perturb the balance between π_{PG} swelling and CN restraining stress, and the normal mechanics of the tissue [25].

Several models exist to describe the relationship between π_{PG} and PG content and are usually expressed in the form of FCD or GAG concentrations [5, 6, 10, 12]. The π_{PG} contribution to overall cartilage mechanical properties, such as compressive modulus or aggregate modulus, has been estimated [4, 10, 12]. Using the concept of balance of forces with π_{PG}, the CN contribution to compressive resistance also has been estimated [5, 23, 26]. Such comparisons are affected by the accuracy of the FCD and π_{PG} calculations and the assumptions made in those calculations. Estimates of FCD imply but often do not account explicitly for CS and KS charge differences (z_{CS}=~2, z_{KS}=~1 per disaccharide) and for varying CS:KS ratios, which vary substantially with age and with depth from the articular surface [33, 39]. Additionally, π_{PG} models are typically developed from relationships with aggrecan or CS in solution and have not needed to consider the interaction between PG and COL. However, in articular cartilage, the water closely associated with COL fibrils (intrafibrillar, IF) are unavailable to interact with the PG, and this water content also varies with external

stress applied to the tissue [5, 27]. Thus, the effective FCD and associated π_{PG} in cartilage may be actually higher than apparent values and may need to be calculated based on extrafibrillar (EF) water. Such modulation of π_{PG} by the CN may affect the biomechanical properties of cartilage.

The FCD–π_{PG} models may provide a useful tool to elucidate the relationship between the composition and function of articular cartilage by providing estimates of π_{PG} from a known PG concentration or FCD. Combined with measurements of tissue mechanical properties, the models also can provide insights into the CN mechanical properties [35]. The effect of compression on FCD and π_{PG} has been considered previously for full-thickness cartilage [10] and layers of adult bovine cartilage [43] but has not been characterized with growth and aging. Thus, the objectives of this work were to (1) describe relationships to explicitly account for variations in CS:KS ratios and exclusion of IF water in a FCD–π_{PG} relationship, (2) to predict π_{PG} and COL contribution to compression using experimentally-obtained biochemical data and compressive equilibrium stress (σ_{EQ}) for full-thickness cartilage for various stages of bovine growth (fetal, calf, adult) and human aging (young, old), and (3) predict the effect of depth from the articular surface in human young and old cartilage on π_{PG} using experimentally-obtained biochemical data.

3.3 Materials and Methods

Bovine Cartilage Biochemical and Biomechanical Data

Data from a previous study were used [42]. Briefly, 1000 μm-thick cylindrical slices (d=4.8 mm) were taken from bovine fetal (2^{nd} and 3^{rd} trimester, n=6), calf (1-3 months old, n=8), and adult (1-2 years old, n=7) femoral condyle and patello-femoral groove cartilage, and wet weights (WW) of the samples were taken. The samples then underwent uniaxial confined compression in a radially confining ring in between two porous platens to compressive strain (ε) of 15% and 30%. After 400 s of ramp compression followed by relaxation to equilibrium (either 3600 s or <0.003 MPa change after 1800s), the equilibrium stress at each compression level was obtained. The samples were subsequently analyzed for dry weight (DW), solubilized by proteinase K digestion for analysis of sGAG content by dimethylmethylene blue assay [19], and COL content by hydroxyproline assay [44] (Fig. 3.1).

Human Cartilage Biochemical and Biomechanical Data

Data from a previous study were used [18]. Briefly, normal adult human articular cartilage from the femoral condyles of Young (30.4 ± 1.8 years old, n=7) and Old (69.1 ± 2.1 years old, n=7) cadaveric donors were analyzed. From one portion of samples, ~250 μm-thick slices of the tissue, spanning the majority of the thickness from the surface to the deep zone were each analyzed for wet weight, dry weight, sGAG content, and COL content (Fig. 3.1). Donor-matched hemi-cylindrical osteochondral samples with full-thickness articular cartilage (d=4.8 mm) underwent uniaxial confined compression to an overall compression of ~10%, ~20%, and ~30%

in a radially confining chamber with video microscopy to track labeled cells [15, 30]. At equilibrium, the stress was measured along with depth-dependent displacement and strain [18].

Incorporation of CS:KS Ratio and Exclusion of IF Water into FCD-π_{PG} Relationship

To compute FCD accounting for variation in the CS:KS ratio, a relationship (Eq. 1) was described using molecular weights per disaccharide of CS (MW_{CS} = 457 g/mol) and KS (MW_{KS} = 444 g/mol), weights of CS (m_{CS}) and KS (m_{KS}), mol-charges of CS (z_{CS} = 2 charge/disaccharide) and KS (z_{KS} = 1 charge/disaccharide), and weight of EF water ($m_{EF,H2O}$). The MW of CS and KS were calculated from the molecular structures of each disaccharide found in the repeating portion of a chain (MW_{CS} = 457 g/mol and MW_{KS} = 444 g/mol). CS and KS content can be determined by several methods, including ELISA, selective enzymatic digestion, and assays that take advantage of different hexose composition of CS and KS [7-9, 36]. Details of FCD_{EF} calculation from commonly used assays to determine GAG content are provided in Appendix A.

$$FCD_{EF} = \frac{\left(m_{CS} * \frac{z_{CS}}{MW_{CS}}\right) + \left(m_{KS} * \frac{z_{KS}}{MW_{KS}}\right)}{m_{EF,H2O}} * \frac{1000\text{mEq}}{1\text{mol} - \text{charge}} \quad (1)$$

To predict π_{PG} based on FCD_{EF}, a piecewise continuous function of 4 segments with monotonically increasing, quadratic equations and continuous first derivatives were fit to the FCD–π_{PG} data by weighted least squared error fit (Fig. 3.2). The PG–π_{PG} data from Figure 2 of Buschmann, et al [10], originally from Williams and Comper [41], and the FCD–π_{PG} data from Figure 3 of Basser, et al [5], originally from

Urban, et al [37] were used for the fit which was made to be continuous to FCD–π_{PG} points from the Donnan equations at FCD > 0.5 mEq/ml [10]. The Donnan model provides a good model at higher FCD or under macro-continuum conditions since the Donnan model and the Poisson-Boltzmann-cell model converge under those conditions [3], and the models appear to fit the high FCD–π_{PG} experimental data from Basser, et al. The PG concentrations from [10] were converted to FCD using the aggrecan dry weight/uronic acid ratio (DW/UA) of 3.29 and the molecular weight of glucurunolactone ($MW_{glucurunolactone}$ = 176.124 g/mol) [41] as described in Appendix A.

The 4-segment piecewise continuous equations to describe the FCD–π_{PG} relationship were of the form:

$$\pi_{PG,i} = a_i (FCD_{EF} - x_i)^2 + b_i (FCD_{EF} - x_i) + c_i \text{ for } x_i < FCD_{EF} \leq x_{i+1} \quad (2)$$

with the constants in Table 1. This FCD_{EF}–π_{PG} relationship provided a good fit, including at low FCD values, which are typical of cartilage in the superficial zone and at low compression (Fig. 3.2).

The extrafibrillar FCD (FCD_{EF}) was calculated using EF water content ($m_{EF,H2O}$), given by the difference between total water content (m_{H2O}) and IF water content ($m_{IF,H2O}$). EF water content was iteratively calculated using COL hydration relationship from π_{PG} set as the extrafibrillar stress (π_{EF}) and COL mass (m_{COL}) (Eq. 4) [5].

$$m_{H2O} = \text{wet weight} - \text{dry weight} \quad (3)$$

$$m_{IF,H2O} = (0.726\ 0 + 0.538 * \exp(-0.258 * \pi_{EF})) * m_{COL} \text{ where } \pi_{EF} = \pi_{PG} \quad (4)$$

$$m_{EF,H2O} = m_{H2O} - m_{IF,H2O} \quad (5)$$

The effect of IF water exclusion was studied by calculating FCD normalized by total water content or by EF water content and the resulting π_{PG} for bovine Fetal, Calf, and Adult femoral condyle cartilage under compression of 0–30%.

π_{PG} and σ_{COL} for Various Stages of Growth and Aging under Compression

Using the FCD–π_{PG} relationship described above, π_{PG} values during compression were estimated for full-thickness cartilage using the experimentally obtained biochemical data for various stages of bovine growth (Fetal, Calf, Adult) [42] and human aging (Young, Old) (Fig. 3.1) [18].

For human cartilage, thickness-weighted averages of the biochemical data were computed to obtain biochemical values for the full-thickness tissue. Then, for both bovine and human cartilage, FCD_{EF} was determined from the sulfated GAG content measured using DMMB assay (m_{DMMB}) with standards containing CS sodium salt (Sigma, St. Louis, MO), accounting for the impurities present in the CS sodium salt (~14-15%) such as water and extra sodium salts. Details can be found in Appendix A.

To estimate the π_{PG} for each sample under compression, the FCD_{EF} at each compression level was first calculated. With compression, it was assumed that all the matrix content, including m_{GAG} and m_{COL}, in the tissue was maintained while only fluid was expelled from the displaced volume (ΔV). The relationship for EF water with compression becomes

$$m_{EF,H2O} = m_{H2O} - m_{IF,H2O} - \rho_{water}*\Delta V \quad (6)$$

where $\rho_{water} = 1.0$ and $\Delta V = \varepsilon*\pi*r^2$ for a cylindrical sample or $\Delta V = ½*\varepsilon*\pi*r^2$ for a hemi-cylindrical sample under uniaxial confined compression of ε. Then, the FCD_{EF}

was used to calculate π_{PG} using the FCD_{EF}–π_{PG} model. Since π_{PG} is a function of $m_{IF,H2O}$ through FCD_{EF} the equations for π_{PG} and $m_{IF,H2O}$ were iteratively re-calculated until π_{EF} and π_{PG} converged.

The CN contribution to compression, CN stress (σ_{CN}), at each compression level, was estimated from the calculated π_{PG} and experimentally obtained compressive equilibrium stress (σ_{EQ}) using balance of forces [5, 26] (Eq. 7).

$$\sigma_{EQ} = \pi_{PG} + \sigma_{CN} \quad (7)$$

Then, the CN pre-stress at 0% compression level and the compression level at σ_{CN} = 0 kPa for both bovine and human cartilage were calculated. For the compression level at σ_{CN} = 0 kPa, only the samples where the σ_{CN} transitioned from tension (negative value) to compression (positive value) were considered (bovine: n=4-6; human n=6).

π_{PG} with Depth and Age in Human Cartilage under Compression

The ε, FCD_{EF}, π_{PG}, and σ_{CN} were calculated in 10 normalized layers through the thickness of Young and Old human cartilage. To estimate the $\pi_{PG,i}$ for the ~250 μm–thick layer i, free EF water ($m_{EF,H2O,i,\varepsilon}$) first was calculated from Eq. 4 using experimentally obtained strains (ε_i) for each layer at each overall compression levels of ~10%, ~20%, and ~30% [18]. The $FCD_{EF,\iota}$ then was calculated based on the biochemical data for each layer, and the $\pi_{PG,i}$ was calculated for each layer throughout the whole thickness of cartilage using the FCD–π_{PG} fit (Eq. 2). The $\sigma_{CN,i}$ in each layer at each strain was estimated from the calculated $\pi_{PG,i}$ and σ_{EQ} using Eq. 7. Then,

weighted averages of ε_i, $FCD_{EF,\iota}$, $\pi_{PG,i}$, and $\sigma_{CN,i}$ along with percent of total water/WW and EF water/WW were calculated for each of the 10 layers normalized through the depth of human cartilage. For the normalized layers, layer 1 was the most superficial layer at the articular surface and layer 10 the deepest layer next to the subchondral bone.

Statistical Analysis

Data are presented as mean ± standard error of the mean (SEM). The effect of bovine growth on cartilage biochemical data, and FCD_{EF} and π_{PG} at each compression level was assessed by one-way analysis of variance (ANOVA). Tukey post-hoc test was performed when significance was detected ($p<0.05$). Student's t-tests were performed to determine the effect of aging in human cartilage. For human cartilage, the effect of aging was assessed using repeated measures ANOVA with the depth as a repeated factor at each compression level. When the age was found to have a significant effect ($p<0.05$) or an interactive effect with layer ($p<0.05$), each layer was analyzed separately. When the depth had a significant effect ($p<0.05$), the pairwise comparisons of the layers for either Young or Old cartilage were performed with a Sidak correction of the p-value.

Table 3.1: Constants for the 4-segment quadratic equation fit to FCD–π_{PG} data.

i	**x_i**	**a_i**	**b_i**	**c_i**
1	0	587.12	38.79	0
2	0.1035	9255.44	160.38	10.31
3	0.1726	1198.7	1438.21	65.49
4	0.489	276.30	2196.78	640.58

3.4 Results

Variation of CS:KS ratios and IF water exclusion were incorporated into the calculation of FCD (Eq. 1-6). Approximately twice the amount (mass) of KS relative to CS was equivalent to the same FCD (Fig. 3.2C). Also, π_{PG} increased with an increasing CS:KS ratio, reflecting the charge difference between KS and CS. Considering IF water and using only EF water for calculation of PG-associated properties in (Eq. 4-6), FCD and, as a result, π_{PG} were substantially higher than values calculated using total water content for cartilage. With compression, the differences in FCD and π_{PG} calculated with EF water instead of total water content became even more pronounced (Fig. 3.3).

Applying the FCD_{EF}–π_{PG} relationship to data from full-thickness bovine femoral condyle cartilage revealed that FCD_{EF} and π_{PG} changed with growth (Fig. 3.4A and 3.5; ANOVA $p<0.05$ for FCD_{EF} at 0, 15 and 30% and π_{PG} at 30% compression). The Calf and Adult femoral condyle cartilage generally had higher FCD_{EF} and π_{PG} than Fetal cartilage at each compression level ($p<0.05$ for Calf vs Fetal for FCD_{EF} at 0-30% and π_{PG} at 30% compression). Even with similar GAG/WW at zero strain, the higher FCD_{EF} in Calf and Adult cartilage was due to the higher COL content (Fig. 3.1) and increased IF water (Fig. 3.2). For bovine cartilage, π_{PG} closely approximated σ_{EQ} for all growth stages at all compression levels (Fig. 3.5). The σ_{CN} were generally low and moved from tension (negative in this convention) at reference state to compression (positive stress) with increasing applied compression. The patello-femoral groove cartilage had similar trends as the condyle cartilage, with the

Calf and Adult cartilage generally having higher FCD_{EF} and π_{PG} than Fetal cartilage (ANOVA $p<0.05$ for FCD_{EF} and π_{PG} at all compressions, Fig. B.2 in Appendix B).

For full-thickness adult human cartilage, the Young cartilage had higher FCD_{EF} and π_{PG} than Old cartilage at all compressive strains (Fig. 3.4B and 6; $p<0.01$ at all compression levels). The π_{PG} for Young cartilage closely approximated σ_{EQ} at all strains levels while π_{PG} for Old cartilage accounted for only approximately half of σ_{EQ} (Fig. 3.6). The low π_{PG} for Old cartilage suggested that a larger proportion of σ_{CN} contribution to σ_{EQ} than found in Young human cartilage. The σ_{CN} for both Young and Old cartilage generally increased with compressive strain, moving from tension toward compression.

The properties of CN under compression were altered with growth and aging of cartilage. The CN pre-stress for bovine Calf and Adult cartilage tended to be higher than for Fetal cartilage (Fig. 3.7A; ANOVA $p=0.19$; $p=0.20$ for adult and $p=0.28$ for calf vs fetal). In human cartilage, the Young cartilage had higher CN pre-stress than the Old cartilage (Fig. 3.7B; $p<0.01$). The compression level at $\sigma_{CN}=0$, changing from pre-stressed tension to compression, tended to be higher for bovine Calf and Adult cartilage than for Fetal cartilage (Fig. 3.7C; ANOVA $p=0.24$; $p=0.38$ for adult and $p=0.28$ for calf vs fetal) and for human Young cartilage than for Old cartilage (Fig. 3.7D; $p=0.20$).

Under compression, the profiles of strain, FCD_{EF}, π_{PG}, σ_{CN}, total water content, and EF water content for human cartilage varied with depth from the articular surface (Fig. 3.8, Fig. C.1 in Appendix C; ANOVA $p<0.001$ for strain and EF water at all

compression and for FCD_{EF}, π_{PG}, σ_{CN}, and total water content at 0, 20, 30% compression). These profiles also were significantly different with the age of the tissue alone ($p<0.01$ for FCD_{EF} and π_{PG} at all compression and for σ_{CN} at 0% compression) and interactively with depth ($p<0.01$ for FCD_{EF}, π_{PG}, and σ_{CN} at 0% compression and for strain at 10% compression).

The strain profiles in Young and Old cartilage were distinct from each other. The highest strains in the Young cartilage were found only in the most superficial layer and linearly decreased with depth in all compression levels (Fig. 3.8A, C-E; $p<0.05$ for layer 1 vs 5-10 at 20% compression). However, in the Old cartilage, the highest strains were more evenly distributed into the middle layer, and the strain then decreased through the depth of the cartilage (Fig. 3.8B-E; $p=0.054$ for layer 1 vs 9 and 10; $p<0.05$ for layer 2 vs 8-10 at 20% compression).

The FCD_{EF} and π_{PG} profiles were different with depth ($p<0.001$ at 0, 20, 30% compression) and between the Old and Young cartilage ($p<0.005$) (Fig. 3.8F-Q). At zero strain, the local FCD_{EF} and π_{PG} varied with depth ($p<0.001$) and aging ($p<0.001$) (Fig. 3.8F-Q). The superficial layers had lower FCD_{EF} and π_{PG} than the deeper layers in both Young and Old cartilage (e.g. $p\leq0.05$ for layer 1 vs 6), with the Young cartilage having higher FCD_{EF} and π_{PG} in deeper layers than Old cartilage ($p<0.05$ for layers 5-10). With compression, the FCD_{EF} and π_{PG} profiles for Young cartilage increased in the superficial layers and evened out through the depth of the cartilage for 10% and 20% compression ($p>0.2$) and peaked in the superficial layers and the upper deep layers at 30% compression ($p<0.05$ for layer 5 vs layers 9, 10). However, the

FCD_{EF} and π_{PG} profiles for Old cartilage tended to peak in the middle layer (layer 4) at all compression levels, which increasing amplitude with increasing compression.

For both Young and Old cartilage, the σ_{CN} profiles at zero compression were generally in tension more in the deep layer than the superficial layer (Fig. 3.8R-T; $p<0.05$ in Young and $p=0.056$ in Old for layer 1 vs 6). The σ_{CN} profiles shifted toward compression at 10% and 20% compression, with the Old cartilage tending to shift to slightly higher stresses than Young cartilage at corresponding depth layers (Fig. 3.8U, V). At the 30% compression for young cartilage, the superficial and middle layer CN were back in tension while that for the deep layer CN was in compression (Fig. 3.8W). For Old cartilage, most of the CN were in compression with just the middle layers in tension.

The FCD_{EF}, π_{PG}, and σ_{CN} profiles for the Old cartilage generally were similar to the trends in the profiles for the Young cartilage at normalized depth 0.2 and deeper. These variations in FCD_{EF}, π_{PG}, and σ_{CN} with depth of cartilage and aging may play a role in the changes observed with the overall mechanical properties of the tissue.

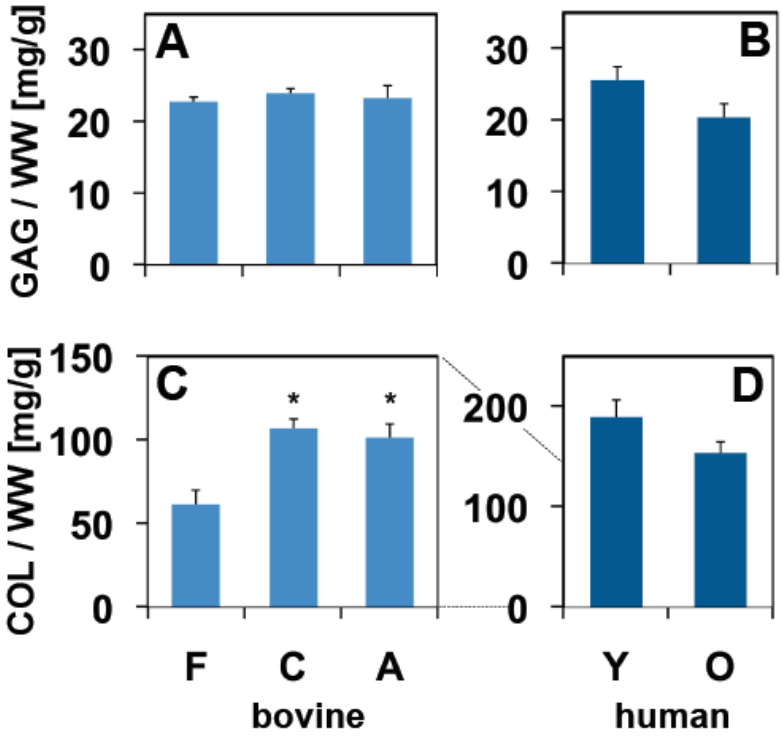

Figure 3.1: GAG/wet weight (A, B) and collagen/wet weight (C, D) of bovine femoral condyle cartilage (Fetal, Calf, Adult) (A, C) and human femoral condyle cartilage (Young, Old) (B, D). (* $p<0.005$ vs fetal)

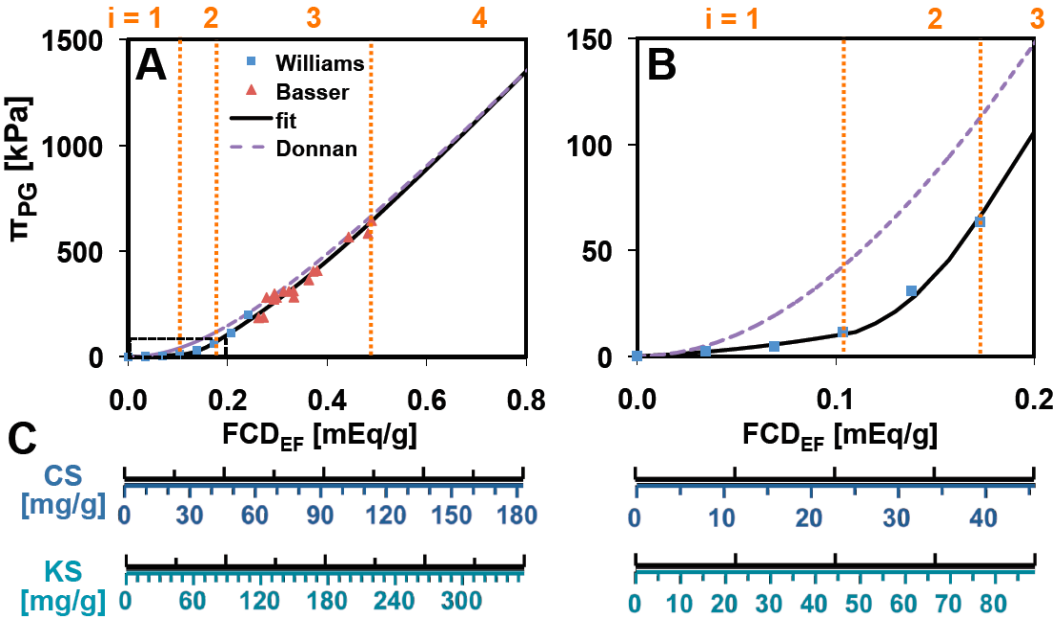

Figure 3.2: Four-segment piecewise curve fitting (A, B) to the data from Williams and Compers, and Basser, et al. with the nomogram of CS and KS content, indicated by downward tic marks, for corresponding FCD, indicated by upward tic marks (C). An inset of (A) at lower FCD values is shown in (B).

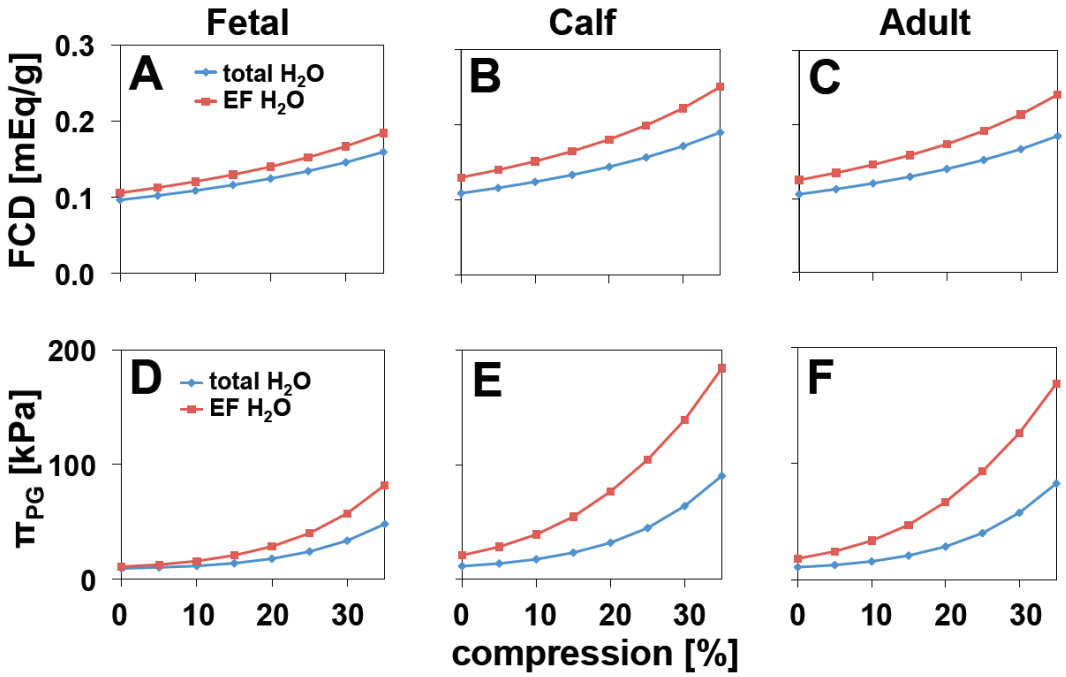

Figure 3.3: FCD (A-C) and π_{PG} (D-F) for bovine fetal (A, D), calf (B, E), and adult (C, F) femoral condyle cartilage calculated using total water or extrafibrillar (EF) water content.

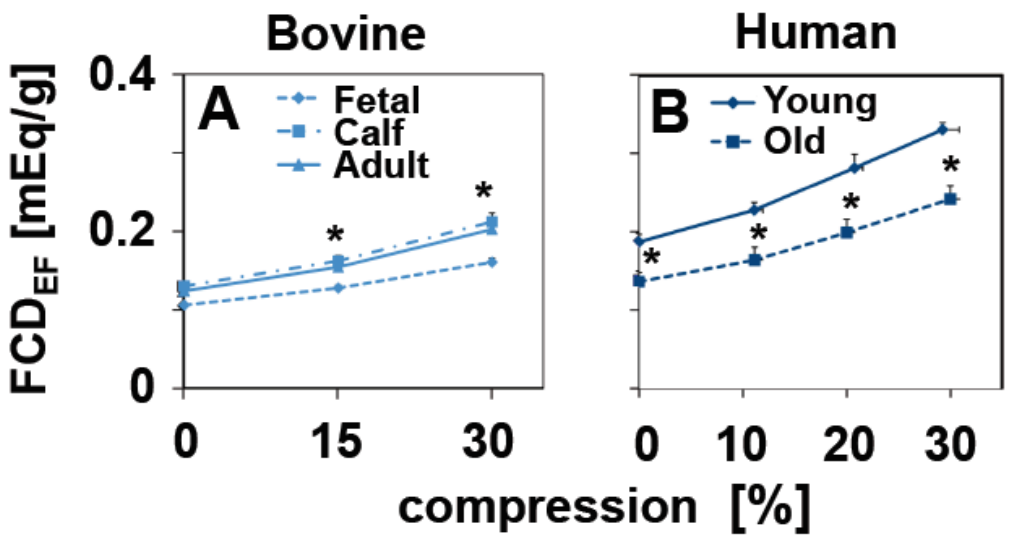

Figure 3.4: FCD_{EF} for bovine (A) and human (B) femoral condyle cartilage. (*$p<0.05$ vs Fetal or $p<0.01$ vs Young).

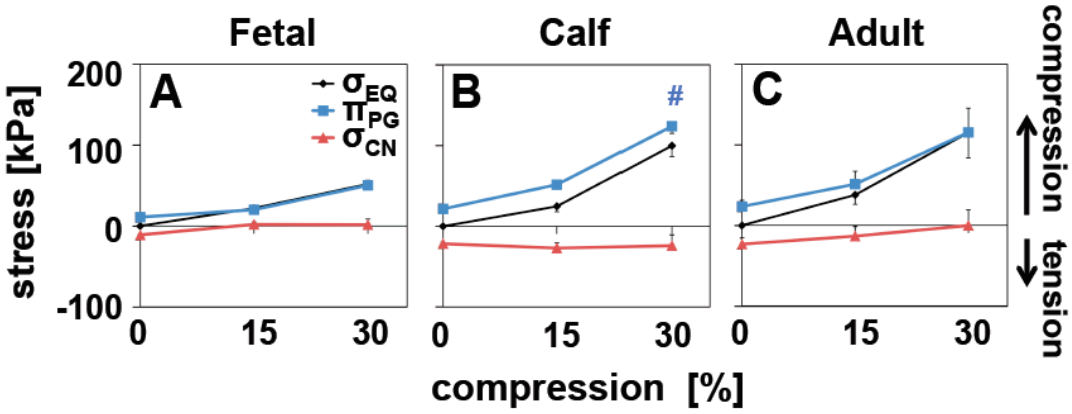

Figure 3.5: π_{PG} along with σ_{EQ} and σ_{CN} for bovine Fetal (A), Calf (B), and Adult (C) femoral condyle cartilage. (# $p<0.05$ vs Fetal).

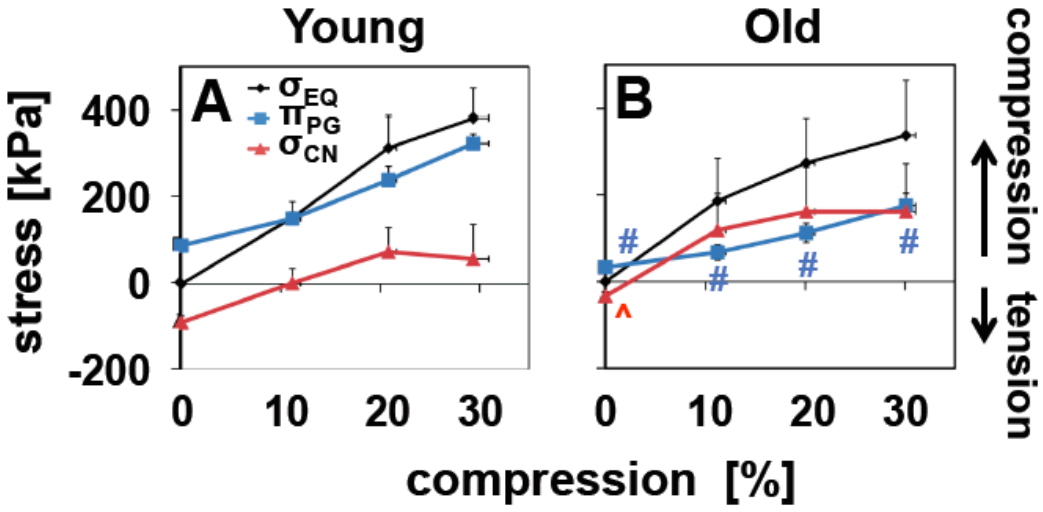

Figure 3.6: π_{PG} along with σ_{EQ} and σ_{CN} for human Young (A) and Old (B) femoral condyle cartilage. (# for π_{PG} and ^ for σ_{CN}, $p<0.01$ vs Young)

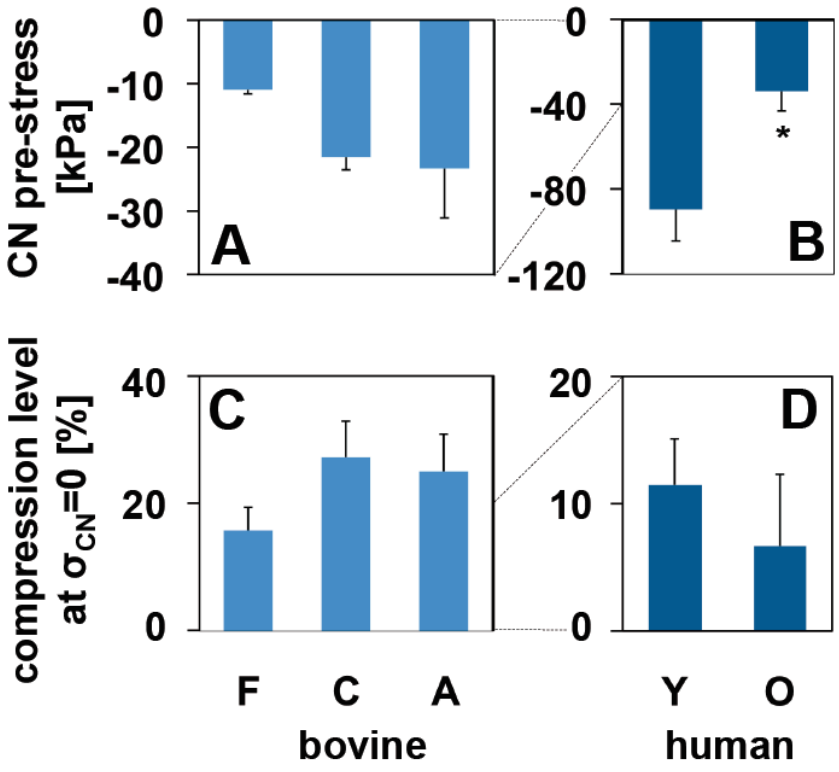

Figure 3.7: CN pre-stress (A, B) and compression level at σ_{CN}=0 (C, D) for bovine (A, C) and human (B, D) cartilage. (* $p<0.01$ vs Young)

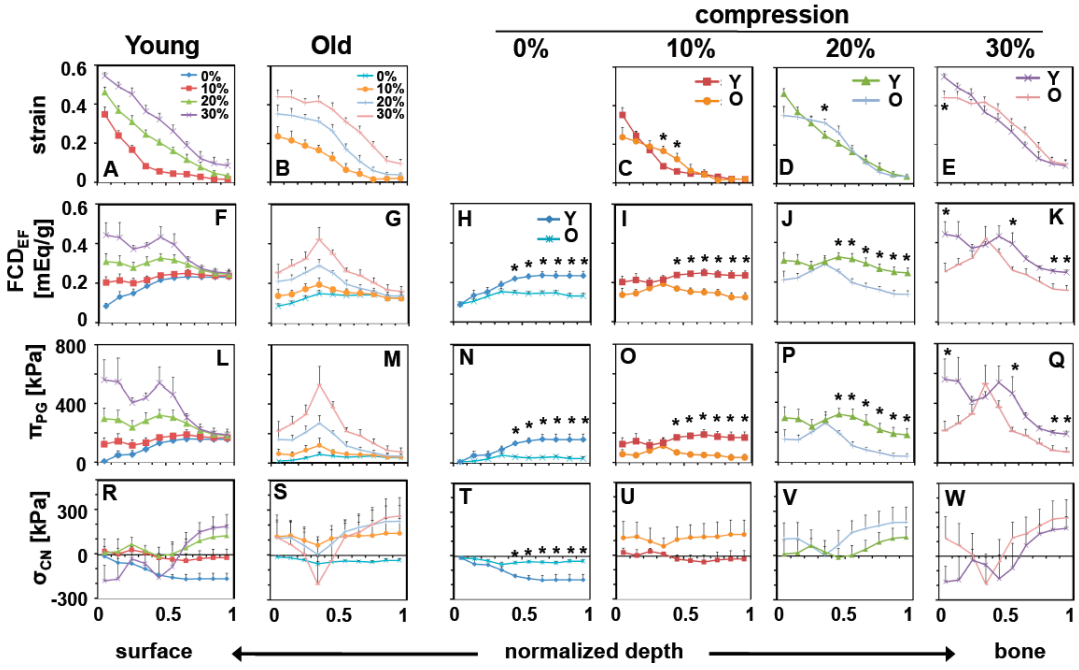

Figure 3.8: Strain (A-E), FCD_{EF} (F-K), π_{PG} (L-Q), and σ_{CN} (R-W) for human Young (A, F, L, R) and Old (B, G, M, S) cartilage with initial normalized depth of the tissue at each compression level (0%, 10%, 20%, 30%). (* $p<0.05$ vs Young)

3.5 Discussion

Presented here is the application of the FCD_{EF}–π_{PG} relationship to predict PG contribution to the compressive properties of articular cartilage. With accounting for CS:KS variation and for exclusion of IF water, π_{PG} appeared to be predicted reasonably for both bovine and human cartilage of various stages of growth and aging, and with depth from the articular surface during compression. Even with similar GAG/WW, more mature cartilage (bovine Calf and Adult) had higher FCD_{EF} and π_{PG} than less mature tissue (bovine Fetal), and this effect was amplified with compression. With aging, the overall FCD_{EF} and π_{PG} was lower in Old human cartilage as compared with the Young cartilage. The π_{PG} were close to σ_{EQ} in bovine cartilage with growth and human Young cartilage but only approximated half of σ_{EQ} in the human Old cartilage. The strain, FCD_{EF}, π_{PG}, and σ_{CN} profiles revealed depth-related variations in human cartilage that were altered substantially with normal aging, suggesting deterioration of a functional superficial layer. These results demonstrate that the FCD_{EF}–π_{PG} relationship, elucidated here, can provide a useful tool for assessing the contribution of PG and its interaction with the CN to the biomechanical properties of cartilage as they vary with growth, aging, and depth from the articular surface.

The accurate estimation of FCD_{EF} from CS and KS contents is important for a precise calculation of π_{PG}. The CS:KS ratio varies with depth, growth, and degeneration of articular cartilage [33, 40], and the charge difference between CS and KS can affect FCD_{EF} determined from GAG mass by as much as 50%. The non-sulfation or double sulfation of the GAG were not taken into account in the FCD

equation here; previous studies indicated that the assumption of normal sulfation gave excellent agreement between calculated and experimentally measured FCD [40]. The accurate accounting of the molecular weight in converting the mass of CS and KS into FCD is important as values in literature have varied by as much as ~10% (457 g/mol vs 503 g/mol for CS disaccharide [40]). Here, 457 g/mol disaccharide was chosen with the assumption of CS in a long chain, with loss of a water molecule between 2 disaccharides due to a glycosidic linkage (see Appendix A for details).

The curve fit of the FCD–π_{PG} relationship appeared to provide good estimations of π_{PG}, especially at low FCD_{EF} as found in cartilage in the superficial zone and at low compression. Previous FCD–π_{PG} fits, such as the quadratic relationships presented in works by Basser and Chahine [5, 12], provide excellent fits for FCD > 0.16 mEq/ml. To extend the FCD–π_{PG} relationship to the lower FCD range that is important for bovine cartilage and the upper layers of human articular cartilage, a piecewise quadratic relationship was fit to experimental data, including the low FCD data from Williams and Compers [5, 10, 41]. While the experimental data were from an extracted aggrecan solution, the measured FCD_{EF}–π_{PG} relationships were similar for extracted aggrecan in solution or for an intact tissue from the intervertebral disc [16]. The FCD–π_{PG} data points and the experimental data used here were for samples in a bath solution with isotonic buffer or equivalent to 0.15M NaCl, typical of the environment within a joint. The curve-fitting approach used here may also be useful to describe FCD–π_{PG} relationships at other salt concentrations from experimental data.

Accounting for exclusion of IF water to PG is also an important consideration that affects FCD_{EF} and π_{PG} values. The presence of COL hydration (IF water) and the

unavailability of this IF water to PG or other surrounding larger molecules have been studied previously [22, 27, 32]. The use of total water content instead of EF water leads to an underestimation of local FCD by as much as 30% in the samples analyzed here. This, subsequently, leads to an underestimation of π_{PG} by a larger percentage due to the nonlinear nature of the FCD–π_{PG} relationship. This may explain differences in the role of π_{PG} in the compressive aggregate modulus; results from previous studies accounted for ~1/3 of the compressive modulus [11, 12], while the present study accounted for nearly all of σ_{EQ} by π_{PG} in bovine cartilage and young human cartilage, and nearly half of σ_{EQ} in old human cartilage at physiological salt concentrations. With changes in COL content during growth, aging, and depth, the proportion of EF water available to interact with PG varies, resulting in changes in FCD_{EF} and π_{PG}. This highlights the importance of interaction between the ECM components, PG and CN, and the contribution from both components in the FCD_{EF} and π_{PG}.

The non-electrostatic contributions to the π_{PG}, such as configurational entropy and mixing entropy, are likely to be small at the physiological salt concentrations considered here. The mixing entropy is generally considered to be very low at physiological PG concentrations [24] and the configurational entropy has been suggested to be negligible at physiological salt concentration using the Debye-Huckel model with repulsive Lennard-Jones potential [6]. However, at high salt concentrations that shield the electrostatic contribution, the configurational entropy likely increases [6, 12, 24] and contributes to a larger proportion of the π_{PG} and the compressive properties with estimates of ~40-60% of compressive modulus values

from experimental studies [11, 12, 17]. For the case presented here using physiological salt concentrations with physiological concentrations of PG, it appears that the electrostatic contribution from the charged GAGs is the major source of the π_{PG}.

There may be other contributions to the overall tissue equilibrium compressive properties of the articular cartilage besides the π_{PG} and σ_{CN}, especially as observed for the human Old cartilage. While HA may provide a small π_{PG} as it contains a carboxyl group per disaccharide, the amount of HA in cartilage is very low (~0.7 mg/g WW in human young cartilage) [2], and the π_{HA} at these concentrations is very small compared to the π_{PG} [21]. Using the balance of forces concept, the calculations here indicate that the CN provide compressive resistance under certain circumstances, such as in human Old cartilage. This may indicate an unfavorable loading of the CN and other matrix structures, as wells the chondrocytes, in aged cartilage. The orientation of the collagen fibrils also may contribute to the compressive properties as observed in finite element modeling [38], which was not accounted for in this study.

The level of pre-stress exerted on the CN by π_{PG} at zero strain appears to have an important impact on the compressive properties of the tissue, as suggested previously [13]. The shift of the CN stress-strain curve from zero stress-strain state (i.e. 0, 0) into a pre-stress in tension at overall tissue zero strain indicates that CN participate in compression, where the pre-stress is relieved. The compressive strain where the combined effect from high-sloped tension from CN and low π_{PG} from lower FCD_{EF} likely contributes to the compressive softening that has been previously observed at low strains [13, 20, 30]. In addition, the degree of compression needed to relieve the CN pre-stress varies with growth, aging, and depth of the tissue. This

appears to be related to the maturity of the CN (e.g. presence of crosslinks and collagen orientation) since the CN in immature cartilage provide much less restraining force than more mature tissues, resulting in lower FCD_{EF} with compression and weaker compressive properties. The contribution to compressive properties from both PG and CN, especially at low strains, provides the unique biomechanical properties of articular cartilage.

The variations in FCD_{EF} and π_{PG} with depth of cartilage and with age appear to affect the overall functional properties of the tissue. The evening out of FCD_{EF}, π_{PG}, and σ_{CN} profiles through the depth in Young cartilage at 10% and 20% compression may represent the state of articular cartilage during steady-state loading. The changes in σ_{CN} of normal Young human cartilage from tension at zero strain to compression at lower applied compression (10%, 20%) and to tension in superficial CN while in compression in the deep layer CN at high applied compression level (30%) is supported by previous studies of the CN under compression. The collagen fibrils in the superficial and middle layer may dissipate the strain under lower load while the collagen fibrils in the deep layers initially buckle or crimp and then distribute the load to superficial layer under high load, leading to tension of the superficial collagen fibrils and compression of deeper zone collagen fibrils [28]. The FCD_{EF}, π_{PG}, and σ_{CN} profiles for the Old cartilage generally were similar to the trends observed for the Young cartilage at normalized depth 0.2 and deeper, consistent with a dysfunction of the superficial layer with normal aging [34]. With aging in the Old human cartilage, the highest levels of strains were observed into the middle layers and not just localized to the superficial layers as in Young cartilage, resulting in high local FCD_{EF} and π_{PG} in

the middle layers of the tissues. The FCD_{EF} and π_{PG} peak in aged cartilage may indicate an abnormal distribution of stress through the depth of the tissue that may be unfavorable to the health of the matrix and chondrocytes in those regions. While it is unclear if this peak in π_{PG} in the deeper layers is a result of matrix degradation or a cause of the matrix degradation, these depth-varying compressive properties likely have important implications for the mechanobiology of the tissues and provide a possible insight into the age-related changes that may lead to degeneration of the tissue.

The application of the FCD_{EF}–π_{PG} relationship to experimental biochemical data has the potential to predict π_{PG} for native cartilage of various sources (including human), depths, and state of growth, aging, and degeneration, as well as for engineered cartilaginous tissues with varying PG and COL contents. Since only biochemical and strain data are needed to estimate π_{PG}, the calculations described above may provide a useful tool in better understanding, predicting, and targeting biomechanical properties of native and engineered cartilaginous tissues, relating the composition of a tissue to its function.

3.6 Acknowledgments

The dissertation author is the primary investigator and thanks co-authors, Drs. Silvia S. Chen, Stephen M. Klisch, and Robert L. Sah for their contribution to this work. The authors gratefully acknowledge Dr. Amanda K. Williamson and Yehudit Falcovitz-Gerasso for the data used in this study and Barbara L. Schumacher for helpful discussions. This work was supported by National Institutes of Health, National Science Foundation, and a grant to University of California-San Diego, in support of Prof. Robert Sah, from the Howard Hughes Medical Institute through the HHMI Professors Program. Additional support was received from a NSF Graduate Research Fellowship (EHH).

3.7 References

1. Armstrong CG, Mow VC: Variations in the intrinsic mechanical properties of human articular cartilage with age, degeneration, and water content. *J Bone Joint Surg Am* 64-A:88-94, 1982.

2. Asanbaeva A, Tam J, Schumacher BL, Klisch SM, Masuda K, Sah RL: Articular cartilage tensile integrity: Modulation by matrix depletion is maturation-dependent. *Arch Biochem Biophys* 474:175-82, 2008.

3. Basser PJ, Grodzinsky AJ: The Donnan model derived from microstructure. *Biophys Chem* 46:57-68, 1993.

4. Basser PJ, Horkay F: Toward a Constitutive Law of Cartilage: A Polymer Physics Perspective. *Macromol Symp* 227:53-64, 2005.

5. Basser PJ, Schneiderman R, Bank RA, Wachtel E, Maroudas A: Mechanical properties of the collagen network in human articular cartilage as measured by osmotic stress technique. *Arch Biochem Biophys* 351:207-19, 1998.

6. Bathe M, Rutledge GC, Grodzinsky AJ, Tidor B: Osmotic pressure of aqueous chondroitin sulfate solution: a molecular modeling investigation. *Biophys J* 89:2357-71, 2005.

7. Belcher C, Yaqub R, Fawthrop F, Bayliss M, Doherty M: Synovial fluid chondroitin and keratan sulphate epitopes, glycosaminoglycans, and hyaluronan in arthritic and normal knees. *Ann Rheum Dis* 56:299-307, 1997.

8. Bitter T, Muir HM: A modified uronic acid carbazole reaction. *Anal Biochem* 4:330-4, 1962.

9. Brown GM, Huckerby TN, Bayliss MT, Nieduszynski IA: Human aggrecan keratan sulfate undergoes structural changes during adolescent development. *J Biol Chem* 273:26408-14, 1998.

10. Buschmann MD, Grodzinsky AJ: A molecular model of proteoglycan-associated electrostatic forces in cartilage mechanics. *J Biomech Eng* 117:179-92, 1995.

11. Canal Guterl C, Hung CT, Ateshian GA: Electrostatic and non-electrostatic contributions of proteoglycans to the compressive equilibrium modulus of bovine articular cartilage. *J Biomech* 43:1343-50, 2010.

12. Chahine NO, Chen FH, Hung CT, Ateshian GA: Direct measurement of osmotic pressure of glycosaminoglycan solutions by membrane osmometry at room temperature. *Biophys J* 89:1543-50, 2005.

13. Chahine NO, Wang CC, Hung CT, Ateshian GA: Anisotropic strain-dependent material properties of bovine articular cartilage in the transitional range from tension to compression. *J Biomech* 37:1251-61, 2004.

14. Chen AC, Bae WC, Schinagl RM, Sah RL: Depth- and strain-dependent mechanical and electromechanical properties of full-thickness bovine articular cartilage in confined compression. *J Biomech* 34:1-12, 2001.

15. Chen SS, Falcovitz YH, Schneiderman R, Maroudas A, Sah RL: Depth-dependent compressive properties of normal aged human femoral head articular cartilage: relationship to fixed charge density. *Osteoarthritis Cartilage* 9:561-9, 2001.

16. Ehrlich S, Wolff N, Schneiderman R, Maroudas A, Parker KH, Winlove CP: The osmotic pressure of chondroitin sulphate solutions: experimental measurements and theoretical analysis. *Biorheology* 35:383-97, 1998.

17. Eisenberg SR, Grodzinsky AJ: The kinetics of chemically induced nonequilibrium swelling of articular cartilage and corneal stroma. *J Biomech Eng* 109:79-89, 1987.

18. Falcovitz YH, Chen SS, Maroudas A, Sah RL: Compressive properties of normal human articular cartilage: age, depth and compositional dependencies. *Trans Orthop Res Soc* 26:58, 2001.

19. Farndale RW, Buttle DJ, Barrett AJ: Improved quantitation and discrimination of sulphated glycosaminoglycans by use of dimethylmethylene blue. *Biochim Biophys Acta* 883:173-7, 1986.

20. Ficklin T, Thomas G, Barthel JC, Asanbaeva A, Thonar EJ-MA, Masuda K, Chen AC, Sah RL, Davol A, Klisch SM: Articular cartilage mechanical and biochemical property relations before and after in vivo growth. *J Biomech* 40:3607-14, 2007.

21. Horkay F, Basser PJ, Londono DJ, Hecht AM, Geissler E: Ions in hyaluronic acid solutions. *J Chem Phys* 131:184902, 2009.

22. Katz EP, Wachtel EJ, Maroudas A: Extrafibrillar proteoglycans osmotically regulate the molecular packing of collagen in cartilage. *Biochim Biophys Acta* 882:136-9, 1986.

23. Klisch SM, Chen SS, Sah RL, Hoger A: A growth mixture theory for cartilage with applications to growth-related experiments on cartilage explants. *J Biomech Eng* 125:169-79, 2003.

24. Kovach IS: The importance of polysaccharide configurational entropy in determining the osmotic swelling pressure of concentrated proteoglycan

solution and the bulk compressive modulus of articular cartilage. *Biophys Chem* 53:181-7, 1995.

25. Maroudas A: Balance between swelling pressure and collagen tension in normal and degenerate cartilage. *Nature* 260:808-9, 1976.

26. Maroudas A: Physico-chemical properties of articular cartilage. In: *Adult Articular Cartilage,* ed. by MAR Freeman, Pitman Medical, Tunbridge Wells, England, 1979, 215-90.

27. Maroudas A, Wachtel E, Grushko G, Katz EP, Weinberg P: The effect of osmotic and mechanical pressures on water partitioning in articular cartilage. *Biochim Biophys Acta* 1073:285-94, 1991.

28. Moger CJ, Arkill KP, Barrett R, Bleuet P, Ellis RE, Green EM, Winlove CP: Cartilage collagen matrix reorientation and displacement in response to surface loading. *J Biomech Eng* 131:031008, 2009.

29. Morgelin M, Heinegard D, Engel J, Paulsson M: The cartilage proteoglycan aggregate: assembly through combined protein-carbohydate and protein-protein interactions. *Biophys Chem* 50:113-28, 1994.

30. Schinagl RM, Gurskis D, Chen AC, Sah RL: Depth-dependent confined compression modulus of full-thickness bovine articular cartilage. *J Orthop Res* 15:499-506, 1997.

31. Schinagl RM, Ting MK, Price JH, Gough DA, Sah RL: Video microscopy to quantitate the inhomogeneous strain within articular cartilage during confined compression. *ASME Advances in Bioengineering* BED-26:303-6, 1993.

32. Simha NK, Fedewa M, Leo PH, Lewis JL, Oegema T: A composite theory predicts the dependence of stiffness of cartilage culture tissues on collagen volume fraction. *J Biomech* 32:503-9, 1999.

33. Sweet MBE, Thonar EJMA, Immelman AR: Regional distribution of water and glycosaminoglycan in immature articular cartilage. *Biochim Biophys Acta* 500:173-86, 1977.

34. Temple MM, Bae WC, Chen MQ, Lotz M, Amiel D, Coutts RD, Sah RL: Age- and site-associated biomechanical weakening of human articular cartilage of the femoral condyle. *Osteoarthritis Cartilage* 15:1042-52, 2007.

35. Thomas GC, Asanbaeva A, Vena P, Sah RL, Klisch SM: A nonlinear constituent based viscoelastic model for articular cartilage and analysis of tissue remodeling due to altered glycosaminoglycan-collagen interactions. *J Biomech Eng* 131:101002, 2009.

36. Thonar EJ-M, Sweet MBE: Maturation-related changes in proteoglycans of fetal articular cartilage. *Arch Biochem Biophys* 208:535-47, 1981.

37. Urban JP, Maroudas A, Bayliss MT, Dillon J: Swelling of proteoglycans at the concentrations found in cartilaginous tissues. *Biorheology* 16:447-64, 1979.

38. van Turnhout MC, Kranenbarg S, van Leeuwen JL: Contribution of postnatal collagen reorientation to depth-dependent mechanical properties of articular cartilage. *Biomech Model Mechanobiol*.

39. Venn G, Billingham MEJ, Hardingham TE: Increased proteoglycan synthesis in cartilage in experimental canine osteoarthritis does not reflect a permanent change in chondrocyte phenotype. *Arthritis Rheum* 38:525-32, 1995.

40. Venn MF, Maroudas A: Chemical composition and swelling of normal and osteoarthritic femoral head cartilage. I. Chemical composition. *Ann Rheum Dis* 36:121-9, 1977.

41. Williams RP, Comper WD: Osmotic flow caused by polyelectrolytes. *Biophys Chem* 36:223-34, 1990.

42. Williamson AK, Chen AC, Sah RL: Compressive properties and function-composition relationships of developing bovine articular cartilage. *J Orthop Res* 19:1113-21, 2001.

43. Wilson W, Huyghe JM, van Donkelaar CC: Depth-dependent compressive equilibrium properties of articular cartilage explained by its composition. *Biomech Model Mechanobiol* 6:43-53, 2007.

44. Woessner JF: The determination of hydroxyproline in tissue and protein samples containing small proportions of this imino acid. *Arch Biochem Biophys* 93:440-7, 1961.

CHAPTER 4

TISSUE ENGINEERING BY MOLECULAR DISASSEMBLY AND REASSEMBLY: BIOMIMETIC RETENTION OF MECHANICALLY FUNCTIONAL AGGRECAN IN HYDROGEL

4.1 Abstract

In vitro assembly of key functional extracellular matrix constituents for tissue-engineered constructs may provide a tool to modulate the retention of proteoglycan (PG) aggregates, which are crucial to compressive biomechanical properties of connective tissues. This study tested the hypotheses that (1) biomimetic molecular reassembly of PG aggregates (native aggrecan (AGC) with hyaluronan (HA) ± link proteins (LP)) affects AGC retention kinetics in hydrogel constructs, (2) the compressive properties of such hydrogel constructs are related to the content of retained AGC, and (3) the reassembly method is compatible with chondrocytes. Addition of HA to AGC in hydrogel constructs increased AGC retention in a dose-dependent manner, and the addition of LP to AGC+HA further enhanced AGC retention. The level of AGC retention, in turn, was associated with increased equilibrium compressive stress of the constructs. Chondrocytes could be included in

the process, and maintained expression of the chondrogenic phenotype, secreting type II collagen but little type I collagen. Thus, by altering the assembly of PG aggregates with HA ± LP, which affects AGC retention, it may be possible to achieve the targeted levels of PG components in order to modulate the mechanical properties of the engineered construct for cartilage as well as other tissues containing PG and PG aggregates.

4.2 Introduction

The content and turnover of aggrecan (AGC) is central to the functional properties of a variety of connective tissues, including articular cartilage, intervertebral disc, meniscus, ligament, and tendon. The poly-anionic sulfated glycosaminoglycan (sGAG) moieties of AGC contribute to the compressive biomechanical properties of these tissues [3, 40, 51, 52]. This provides the tissue with a high osmotic pressure to retain water, a high resistance to fluid flow, and thereby resistance to compression, and pre-stress to the collagen network [8].

Normally, AGC retention in cartilage is governed by the non-covalent aggregation of AGC monomers with hyaluronan (HA) as stabilized by link protein (LP). *In vivo*, up to ~100 AGC monomers, each with large numbers of sGAG chains of chondroitin sulfate (CS) and keratan sulfate, non-covalently associate with a HA molecule to form a proteoglycan (PG) aggregate [34, 41]. LP binds to both AGC and HA to further stabilize their interaction and aids in the formation of more uniformly packed aggregates [8]. This helps to retain the functionally important poly-anionic AGC within the tissue due to the large size of aggregates and their entrapment within collagen network, especially under dynamic joint loading conditions.

In traditional approaches to cartilage tissue engineering, AGC accumulates in constructs over months as rates of biosynthesis by residing cells are gradually balanced by rates of loss [32]. Various chemical and mechanical factors have been used in order to accelerate the accumulation and organization of PG within engineered cartilaginous constructs [9, 10]. To augment the AGC content and to enhance the AGC synthesis and retention by the residing cells, various hydrogels and scaffolds

containing one or more PG components have been fabricated and studied, usually containing HA and/or CS and/or their derivatives [4, 11, 13, 47]. Less common are biomaterials containing LP or AGC, either in whole or peptide/truncated forms [13, 37], and those containing whole AGC have not been targeted for cartilage applications.

In vitro, AGC can be extracted from cartilage and then biomimetically reassembled into aggregates with HA±LP [21]. The AGC-HA interaction has been shown to be highest at 0.8% HA (w/w AGC) [5]. Addition of LP to the AGC-HA mixture increased aggregate stability and AGC per aggregate, with 6-8% (w/w AGC) LP (or 3-4:1 LP:AGC molar ratio) resulting in maximum aggregation of ~80% of initial AGC content [49]. Various measures of viscoelastic properties in solutions have been shown to be significantly altered by the formation of PG aggregates with AGC and HA as compared to AGC alone, and further increased in the presence of LP, indicating one functional implication of the formation of PG aggregates [20, 50].

By modulating the assembly of aggregated PG, it may be possible to achieve the desired levels of PG components, which may modulate the mechanical properties of the engineered construct [1, 36]. Additionally, the ability to accelerate the formation of PG aggregates in the engineered tissue has the potential to save a significant amount of time compared to the biological replenishment and redistribution of AGC. Thus, AGC may be a useful component to include during the assembly of cartilaginous constructs, either alone, +HA, or +HA+LP. Therefore, this study tested the hypotheses that (1) biomimetic molecular reassembly of AGC with HA ± LP affects AGC retention kinetics in hydrogel constructs, (2) the compressive properties

of such hydrogel constructs are related to the content of retained AGC, and (3) the reassembly method is compatible with chondrocytes and formation of cartilaginous tissue with type II collagen deposition.

4.3 Materials and Methods

Preparation of Proteoglycan Components

AGC and LP were purified from bovine calf knee articular cartilage as described previously [22, 43, 48]. Pharmaceutical grade HA was obtained as Healon® (4 MDa) (Advanced Medical Optics, Inc.). A1D6, containing LP, represents the least dense of the 6 fractions from the dissociative isopycnic centrifugation (D6) performed on the densest of the 3 fractions from the associative isopycnic centrifugation (A1). A1D6 fractions were subjected to size exclusion chromatography on a Sephacryl 300 column eluted with 4M guanidine-HCl. The protein-containing fractions were pooled and verified by SDS PAGE to contain LP by molecular size estimation (~44 and 48 kDa). A1D1, containing AGC monomers, represents the densest of 6 fractions from the dissociative isopycnic centrifugation (D1) performed on the densest of the 3 fractions from the associative isopycnic centrifugation (A1). A1D1 fractions were verified to contain high concentrations of sGAG that appeared as one sharp band on native agarose gel electrophoresis and had the ability to form large aggregates with HA as verified by native agarose gel electrophoresis and Sephacryl 1000 (S-1000) column chromatography [42].

Formation of Proteoglycan-Hydrogel Constructs

Disk constructs (d=4.8mm, h=1.5mm; n=10-20/group) were composed of 2% low-melting temperature agarose (SeaPlaque, Lonza) with variable amounts of AGC, HA, and LP (Table 4.1): (Group I) no aggrecan, (Group II) 2 mg/ml AGC, (Group III) AGC + 0.2% HA (by weight of AGC or 0.004 mg/ml), (Group IV) AGC + 1% HA (0.02 mg/ml), (Group V) AGC + 1% HA (0.02 mg/ml) + 5% LP (0.1 mg/ml), or

(Group VI) AGC + 5% HA (0.1 mg/ml). The concentrated PG solutions for each experimental group were dialyzed (MWCO 8-10kDa) against PBS, pH 7.0 at 4°C for 18 hours to remove the guanidine-HCl in order to allow for aggregation, which was verified by S-1000 column chromatography [42]. The percentage of sGAG contained in each fraction from the S-1000 column chromatography was plotted against K_{av}, the distribution coefficient; K_{av} is inversely related with the molecular size. The dialyzed PG solutions were warmed to 50°C and mixed well with a concentrated solubilized agarose solution, for a final agarose concentration of 2%. The PG-agarose solutions were gelled into 1.5 mm thick sheets at 4°C for at least one hour. Disk constructs were punched from the PG-agarose sheets and were placed into 300 μl (~10 disk volumes) of PBS, pH 7.0 containing protease inhibitors (PIs) (0.5 mM EDTA, 1 mM 4-(2-aminoethyl) benzenesulfonyl fluoride hydrochloride (AEBSF), 5 mM benzamidine-HCl, 5 mM N-ethylmaleimide (NEM)) in a U-shaped bottom, 96 well plate with gentle nutation. PBS with PIs was changed and collected daily for subsequent analysis of released PG components. The hydrogel constructs at the end of day 3 were solubilized with 300 μl of PBS at 80°C for 2 minutes and analyzed for retained PG components.

Biochemical Analysis of Released and Retained PG Components

To determine the sGAG retained and released from the constructs, the dimethylmethylene blue (DMMB) assay was performed on portions of solubilized constructs and PBS from days 1-3 [14].

To quantify the released and retained HA content, portions of solubilized constructs and pooled PBS from days 1-3 were digested overnight at 60°C with 0.5

mg/ml proteinase K to remove possible interference from HA binding regions of aggrecan in the HA assay. The samples were incubated with 1 mM AEBSF for 2 hours at 37°C to inhibit proteinase K and assayed using HA test kit (Corgenix, Broomfield, CO) [1]. HA was analyzed in PBS pooled from days 1-3, because the amount released was small in comparison to sGAG release as determined from a pilot study (Appendx D).

To determine the release and retention of LP in Group V, SDS PAGE was performed on portions of solubilized constructs and PBS pooled from days 1-3. The samples for SDS-PAGE were reduced with 10 mM dithiothreitol for 30 minutes at 37°C, alkylated with 55 mM iodoacetamide for 30 minutes at 37°C, and separated in 4-20% gradient Tris-glycine gels. A constant voltage of 125V (15.6V/cm) was applied for 105 minutes in Tris-glycine SDS running buffer (25 mM Tris base, 192 mM glycine, 0.1% SDS, pH 8.3). The gels were subsequently stained overnight for proteins with SYPRO Ruby® (Invitrogen, Carlsbad, CA) and imaged using Storm imaging system (GE Healthcare, Piscataway, NJ). The densities of the stained bands of approximately 40-50 kDa were quantified using ImageQuant software (GE Healthcare, Piscataway, NJ) to determine the percentage of LP retained in and released from the constructs.

Histology

To assess the spatial distribution of the sGAG and HA within the agarose constructs, the constructs from Groups I, II, IV-VI were fixed in 4% paraformaldehyde for 3 hours, snap frozen with optimal cutting temperature compound (Sakura Finetek, Torrance, CA) in isopentane cooled with liquid nitrogen, and cryosectioned across the

height of the constructs at 30 μm thickness. The sections were assessed for retained sGAG with Alcian blue [44], and for retained HA with hydrogen peroxide-conjugated HA binding protein (Corgenix, Broomfield, CO) and reaction with Vectastain VIP substrate. The sections were imaged using brightfield microscopy (Eclipse TE300, Nikon, Melville, NY).

Biomechanical Analysis of PG-Hydrogel Constructs

For compression testing, larger disk constructs (d=9.6 mm; n=6-8) for Groups I, II, IV-VI were punched from the PG-agarose sheets described above. The constructs were placed in 1.2 ml (~10 disk volumes) of PBS, pH 7.0 containing PIs with gentle nutation for 3 days with daily change of PBS with PIs. At the end of day 3, a stack of 2 hydrogel constructs was placed in a radially confining chamber between two porous platens filled with PBS + PIs and tested at 30%, 60%, 75%, and 90% compressive strains of initial thickness to equilibrium relaxation times using a mechanical spectrometer as previously described [52]. The relaxation times were sufficient for samples to reach equilibrium, based on stresses that were within 1.4 ± 0.6% of the equilibrium values predicted by fits of the load data to a logistic model $y=A-C/(1+e^{-b(x-M)})$. The testing protocol was validated to achieve similar results for an individual sample and a stack of 2 samples of the same total height, and also to maintain integrity of the constructs during and after the test (Appendix E). The high strains were applied in order to reach higher GAG concentrations, after volume adjustment at each strain, to allow for electrostatic repulsion. At each strain, the peak stress and equilibrium stress, calculated from the measured load at end of ramp compression and at end of relaxation divided by the circular confining chamber area, were analyzed. In order to

assess the contribution to the compressive stress from the retained PGs apart from the contribution from the agarose, assuming the equilibrium stress contributions were additive, the equilibrium compressive stress ascribed to PG at each strain was calculated by subtracting the equilibrium stress of the agarose only constructs. The secant modulus at equilibrium at each strain was also calculated by taking the slope of the stress-strain data with respect to the origin. The constructs and the PBS bath solution from the compression tests were analyzed for sGAG content after mechanical testing.

Short-term Culture of PG-Hydrogel Constructs with Chondrocytes

To determine the effect of the assembled PG on chondrogenic activity, disk constructs (d=3 mm, h=1.5 mm) containing sterilized PG solutions (Groups I, II, V) in 2% SeaPlaque agarose were prepared at 40ºC with the addition of isolated bovine calf chondrocytes at $4x10^6$ cells/ml [6, 18] The AGC and LP were sterilized by 0.45μm filtration prior to PG assembly. After 2 days of culture in DMEM with additives (100 U/ml penicillin, 100 μg/ml streptomycin, 0.25 μg/ml fungizone, 0.1 mM MEM non-essential amino acids, 0.4 mM L-proline, 2 mM L-glutamine), 10% FBS and 25 μg/ml ascorbate, the constructs were analyzed. Portions of constructs were assessed qualitatively by live/dead staining (Invitrogen, Carlsbad, CA) for chondrocyte viability, and after cryosectioning by immunohistochemistry for expression of collagen type I and II [24], and by Alcian blue staining for sGAG distribution.

Statistical Analysis

Data are presented as mean ± standard error of the mean (SEM). The data expressed in percentages (% sGAG released and retained and % HA retained in

constructs) were arcsine transformed to improve normality prior to subsequent analysis. The effects of construct type, along with time for released sGAG, were analyzed by analysis of variance (ANOVA) with post-hoc Tukey test when significant variation ($p<0.05$) was detected.

Table 4.1: Experimental groups.

		final concentration [mg/ml]		
Group	**in 2% agarose gel**	**sGAG**	**HA**	**LP**
I	**control**	0	0	0
II	**AGC**	2	0	0
III	**AGC + 0.2% HA**	2	0.004	0
IV	**AGC + 1% HA**	2	0.02	0
V	**AGC + 1% HA + 5% LP**	2	0.02	0.1
VI	**AGC + 5% HA**	2	0.1	0

4.4 Results

The addition of HA ± LP to AGC in the dialyzed PG solutions for each experimental group resulted in increased amounts of PG aggregates, as indicated by the increased size of the peaks of sGAG-containing molecules at the lower K_{av} values (Fig. 4.1). Column chromatography on S-1000 demonstrated that the percentage of sGAG in PG aggregates increased in a dose-dependent manner with HA (2% for Group II vs 31% for Group III vs 34% for Group IV vs 64% for Group VI) and increased further with the addition of 5% LP to AGC + 1% HA (81% for Group V).

The retention of sGAG in the construct was markedly affected by the presence of HA or HA with LP (Fig. 4.2A, C). In constructs with AGC only (Group II), sGAG was released extensively and rapidly, with 61% or 31 μg of the sGAG released on day 1 ($p<0.001$ vs day 1 PBS for Groups III-VI; $p<0.001$ vs day 2, 3 PBS for Group II), and 82% total over 3 days, with retention of only 18% or 9 μg by end of day 3. The addition of aggregating components (HA) stabilized AGC in the constructs, increasing 3-day retention in a dose-dependent manner to 31% for 0.2% HA (Group III), 61% for 1% HA (Group IV), 84% for 5% HA (Group VI) (all $p<0.001$ vs Groups II, III, IV). Retention was increased further with addition of 5% LP to 87% (Group V) ($p<0.001$ vs Group IV). The other PG components were mostly retained within the constructs at the end of day 3 when present initially. Most of the added HA was retained in constructs (>90% for Groups III-VI, $p=0.11$, Fig. 4.2B, D). Most of the added LP was also retained in the constructs when present initially (90 ± 2% for Group V, Fig. 4.3).

Histological stains for sGAG and HA on cryosections of the constructs at day 3 showed similar trends to the biochemical analysis, with more intense sGAG staining in the presence of HA and LP. Alcian blue staining for sGAG (Fig. 4.4A) on the cryosections of the constructs was lighter at the edges of AGC-containing constructs without LP (Groups II, IV, VI) and more uniform and intense when PG aggregate components were present (Groups IV-VI). HA staining (Fig. 4.4B) was uniform and intense throughout the constructs containing HA (Groups IV-VI).

Compressive properties of the constructs generally increased with the content of sGAG retained in the constructs, which was affected by presence of HA and LP. The peak and equilibrium stresses increased with the application of increasing strains for all constructs. The constructs with enhanced retention of AGC (groups IV, V, VI) exhibited higher peak stresses and higher equilibrium stresses than did constructs with less retained AGC (groups I and II), which was most evident at higher strains of 75% and 90% (Fig. 4.5A, B). The sGAG-dependence on the equilibrium compressive stress was evident after adjustment for stress contribution from agarose and adjustment in sGAG concentration for the volume changes at each strain (Fig. 4.5C). The secant modulus was generally higher for constructs with higher AGC retention (group IV, V, VI) and also increased with increasing strain-adjusted sGAG concentration (Fig. 4.5D).

Chondrocytes were compatible with varying degrees of assembled PG within agarose constructs as indicated by various cell metabolic markers. Chondrocyte viability was qualitatively high in the absence or presence of AGC alone or AGC + 1% HA + 5% LP (Fig. 4.6A). In addition, the cells expressed the chondrogenic

phenotype as indicated by positive type II collagen immunostaining (Fig. 4.6B), which was enhanced in the presence of PG aggregates (group V), lack of type I collagen staining (Fig. 4.6C), and pericellular Alcian blue staining indicative of sGAG (Fig. 4.6D).

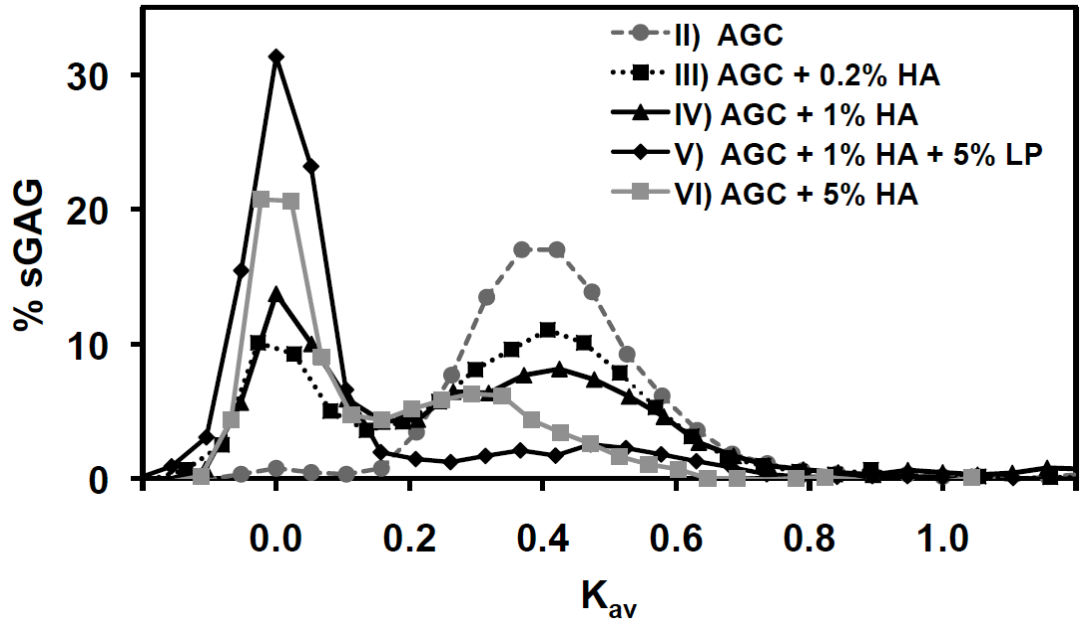

Figure 4.1: Representative S-1000 chromatograms of % sGAG content from concentrated PG solution of Groups II-VI at day 0 to determine the levels of AGC in PG aggregates and in monomeric forms.

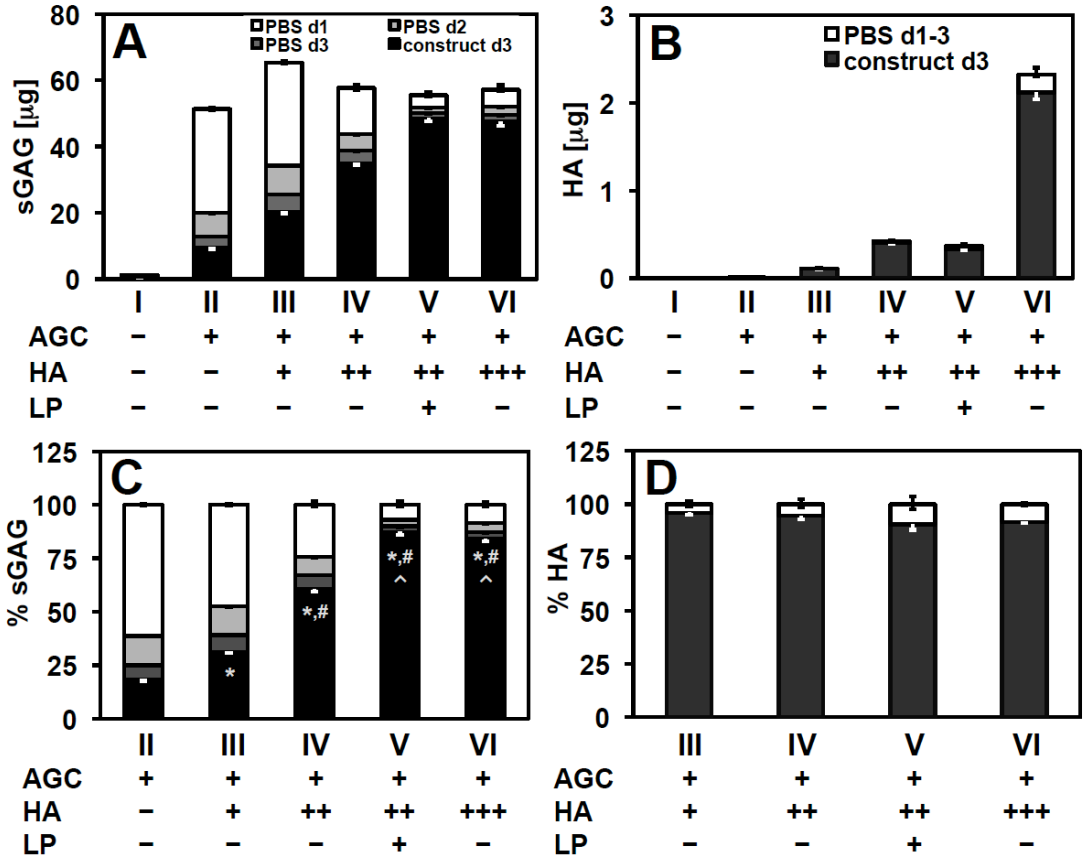

Figure 4.2: Biochemical analysis on the effect of PG aggregation with HA and LP on the release (PBS days 1-3) and retention (construct day 3) of PG components. Released and retained sGAG (A, C) and HA (B, D) from groups I – VI expressed as content (A, B) and percentage (C, D). + and – signs indicate the relative amounts of PG components present as compared to other experimental groups. (* $p<0.001$ vs II, # $p<0.001$ vs III, ^ $p<0.001$ vs IV)

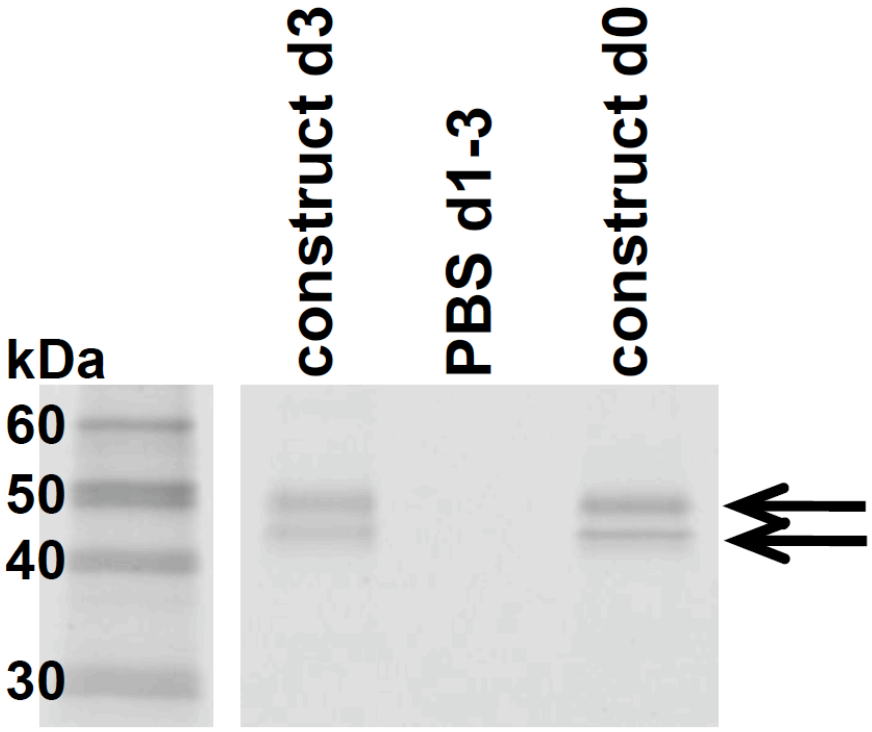

Figure 4.3: Visualization of SDS PAGE for LP (~44 and 48 kDa) of construct at day 3, PBS from days 1-3, construct at day 0 for typical group V sample (AGC + 1% HA + 5% LP).

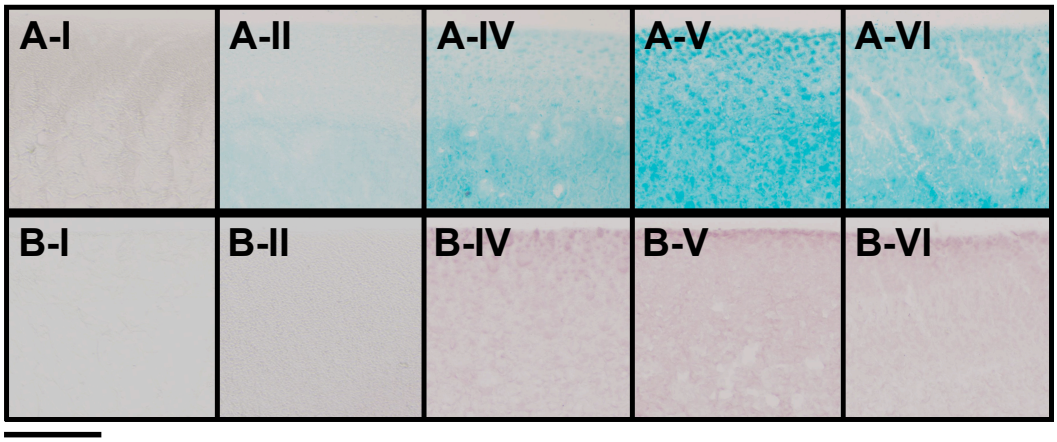

Figure 4.4: Histological staining on constructs at day 3 to assess distribution of PG components. Alcian blue staining for sGAG distribution (A) and purple staining for HA distribution (B) on sections of constructs from groups I (control), II (AGC), IV (AGC + 1% HA), V (AGC + 1% HA + 5% LP), and VI (AGC + 5% HA). (bar=250 μm)

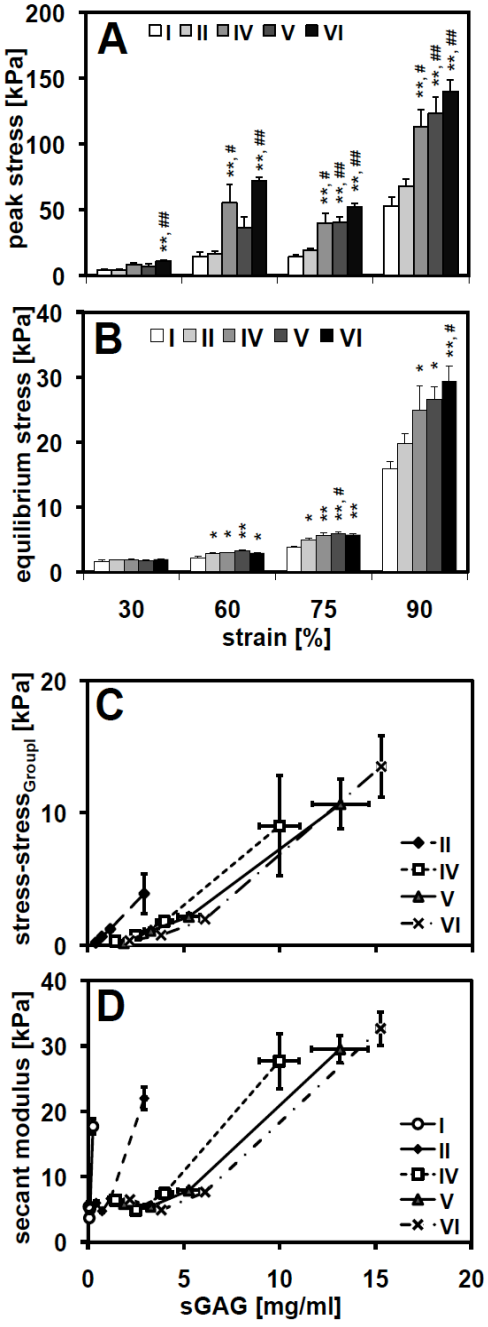

Figure 4.5: Compression properties of day 3 constructs from groups I (control), II (AGC), IV (AGC + 1% HA), V (AGC + 1% HA + 5% LP), and VI (AGC + 5% HA). Peak stress (A) and equilibrium stress (B) at each strain (30%, 60%, 75%, 90%). Equilibrium stress less that of constructs with no AGC (group I) (C) and secant modulus (D) at all strains relative to strain-adjusted sGAG concentration. * $p<0.05$ and ** $p<0.01$ vs group I. # <0.05 and ## $p<0.01$ vs group II.

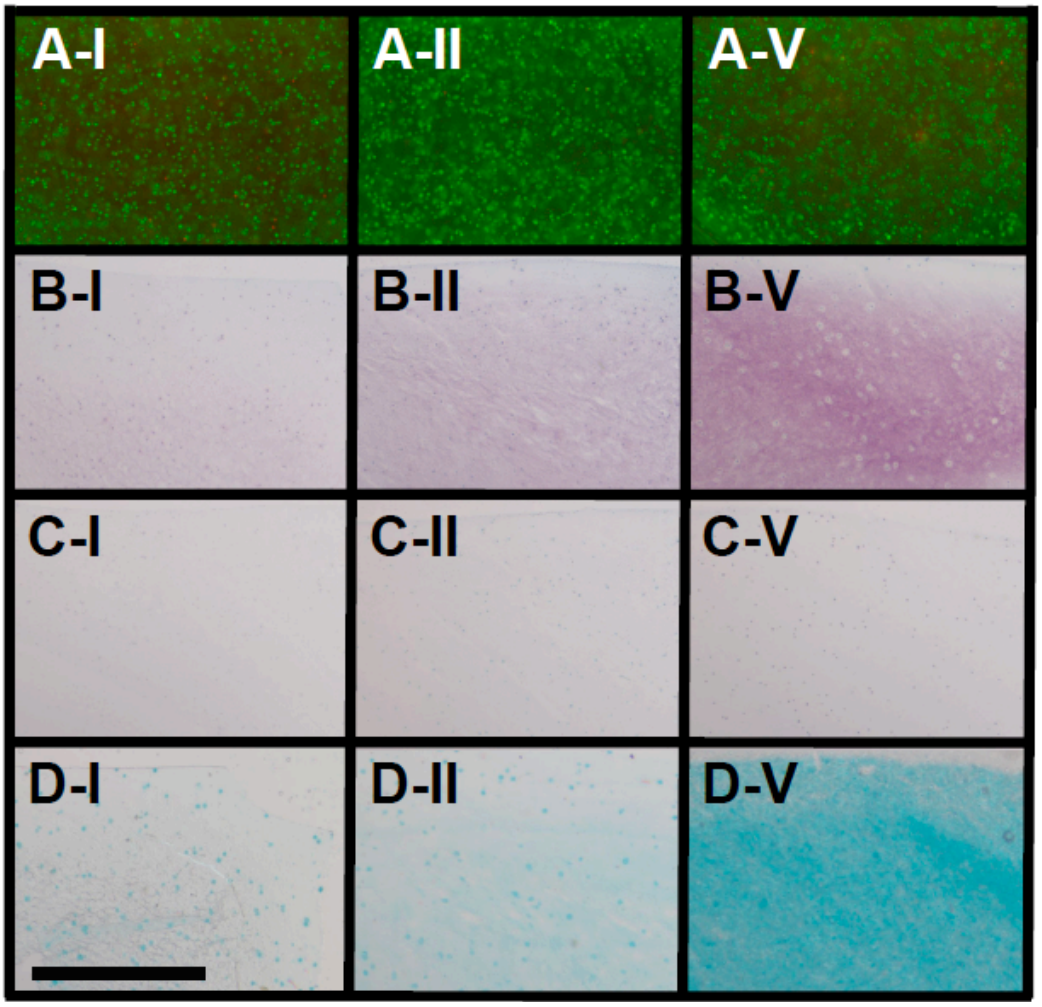

Figure 4.6: Histo- and immuno-chemical staining on constructs containing chondrocytes after 2 days of culture. Live/dead staining for cell viability (A). Collagen type I and II (B, C) immunochemical staining for chondrogenic function, and Alcian blue staining for sGAG distribution (D) on sections of constructs from groups I (control), II (AGC), and V (AGC + 1% HA + 5% LP). (bar=300 μm)

4.5 Discussion

The tissue engineering approach addressed in the present study was the creation of cartilaginous constructs by biomimetically harnessing the biochemical processes to assemble one of the key functional constituents of the native cartilage, PG aggregate. Biomimetic molecular reassembly of AGC with HA ± LP enhanced the AGC retention in hydrogel constructs (Fig. 4.2, 4.4), which in turn resulted in differential compressive properties of the constructs (Fig. 4.5). The addition of HA increased AGC retention in a dose-dependent manner, and the addition of LP to AGC+HA further enhanced AGC retention (Fig. 4.2, 4.4). Additionally, chondrocytes in the PG-containing constructs were able to maintain chondrogenic functions after a short-term culture (Fig. 4.6). These results support the general concept that a matrix disassembly and reassembly approach is feasible for the engineering of cartilaginous tissue as well as a number of other tissues containing PG and PG aggregates.

PG components from various sources may be utilized to assemble the matrix containing PG aggregates. This study used AGC from immature bovine calf cartilage, which has different GAG profiles in chain length and type (higher CS:KS ratio) than AGC from more mature cartilage [12]. While these differences may affect the fixed charge density of the tissue, the GAG content in cartilage is positively correlated with compressive modulus regardless of the level of maturation [52]. Since AGC monomers extracted from mature tissue maintain the ability to form aggregates *in vitro* [2] and PG aggregation is a highly conserved molecular mechanism across species, the approach described here is likely to be applicable to AGC from other sources, including human sources, and to other HA-binding PGs to create a

biomimetic matrix that can be used as a homograft. Recombinant forms of AGC and LP, which have been produced and demonstrated to maintain the ability to form aggregates [17, 33], along with commercially available HA, also may provide other sources of purified PG components.

Agarose was used in the present study as a hydrogel to retain PG components and aggregates, and as model for cartilage tissue engineering. Agarose is somewhat different than articular cartilage in that it lacks the biomechanical characteristics of the collagen network in the latter, providing a high resistance to PG swelling and allowing tissue pressurization. Since agarose has a relatively low tensile modulus, the constructs were fabricated with sGAG concentrations at free swelling state that were relatively low compared to those found in articular cartilage and were not significantly altered in dimension or wet weight by the inclusion of sGAG. However, with application of high compressive strains (e.g., to 90%), the agarose concentration reached ~200 mg/ml, and the sGAG concentration (~15 mg/ml tissue for group VI) is in the range of that in articular cartilage where electrostatic repulsion by sGAGs is marked [7] relative to the contribution of agarose to the compressive properties. The biomimetic assembly approach could be extended to PG concentrations approaching physiological levels with biomaterials with higher tensile stiffness closer to that of the target tissue.

Agarose can provide a reasonable approximation to the pore size of the collagen network in articular cartilage, and thus was useful to assess transport properties. The pore size of 2% agarose is estimated to be ~200 nm [35], similar to the ~100nm interfibrillar spacing of collagen fibrils in middle and deep zones of articular

cartilage [30]. Similar to cartilage, 2% agarose appears to allow for release of unbound AGC monomers and entrapment of AGC in PG aggregates.

The transport of the PG components out of the 2% agarose constructs in this study was consistent with a diffusion process. Based on the hydrodynamic radius (R_H) estimations in solution, AGC monomers (R_H=57 nm for 2.6 MDa AGC monomer) should be able to diffuse out slowly over time while much larger PG aggregates (R_H=~370 nm for PG aggregate with ~30 AGC monomers) should be almost immobile [16]. The high HA retention in the constructs may be due to large size of HA (~4 MDa), which is larger than those in native cartilage [23] but similar to those in synovial fluid [27]. The large size of HA also may enhance the AGC retention as compared to HA with smaller molecular weight due to the formation of larger PG aggregates. Since the very small LP molecules (~4-5 nm) can readily diffuse out and were present in higher molar ratio than AGC, the formation of LP-HA complexes without AGC likely aided in the high LP retention in the constructs [38, 39].

Such *in vitro* molecular engineering to pre-set AGC, HA, and LP levels of a matrix to a desired level may markedly quicken the tissue engineering process by avoiding the time normally needed for *de novo* matrix deposition by indwelling cells. AGC turnover in tissues generally takes a long time, with half life of PGs estimated to be ~150 days in adult dog articular cartilage [29] and 60-70 days in guinea pig costal cartilage [28] in *in vivo* studies, and 300-800 days in adult human articular cartilage in explant cultures [29]. Typically, traditional cartilage tissue engineering constructs take weeks if not months to culture and fabricate in order to reach near physiological levels of AGC accumulation by indwelling cells [31]. Since the relative amounts of HA or

LP to AGC can affect the level of AGC in aggregates [25, 49], the relative concentrations of AGC, HA and LP may be varied to modulate the retention of AGC in tissue-engineered constructs. Therefore, the ability to accelerate the formation of PG aggregates in the biomimetically-engineered tissue has the potential to save significant amount of time compared to the biological replenishment and redistribution of AGC.

The biomimetic basis of the approach described here, using native molecules and macromolecular structures, is likely to foster biocompatibility. Native PG molecules in cartilage have been suggested to have bioactive functions where they may play a role in binding of other matrix proteins and other biochemical factors, that regulate cell function [19]. In tissue engineering applications, scaffolds containing PG components have been shown to enhance chondrogenesis and matrix production by the indwelling cells, whether they are chondrocytes or stem cells [9, 45]. The use of native PG molecules in tissue-engineered constructs may foster a more native ECM turnover processes to take place within the constructs. The short-term culture of constructs containing immature chondrocytes along with assembled PG aggregates of the native AGC and LP along with HA indicated cell compatibility and chondrogenic activity. Longer-term culture and use of different cell types (in terms of maturity and differentiation state) would help to further elucidate the effect of the addition of assembled native PG components in tissue-engineered constructs.

Incorporating substantial quantities of native PG components into a collagenous matrix populated by chondrocytes has the potential to provide grafts with improved mechanical function. Higher sGAG concentration, as achieved from

enhanced AGC retention by aggregation with HA ± LP and from decreased volume from increasing compressive strain, positively related with compressive resistance apart from the contribution from the agarose. Previous studies with cultured chondrocytes encapsulated in agarose have shown higher compressive stress with increasing sGAG content with time in culture [6, 26]. Depletion of PG in immature cartilage has been shown to increase tensile strength [1] and may alter biomechanical properties in tissue-engineered constructs as well [36]. Studies of *in vitro* collagen fibril assembly have shown that the presence of PG, such as CS or AGC, alters size and rate of fibril formation and the mechanical properties of the resulting collagen-PG material as compared to collagen alone [15, 46]. Additionally, the presence of PG in a tissue-engineered construct may aid in the retention of newly synthesized collagen monomers from the indwelling cells (Fig. 6). Thus, alterations in PG content in tissue or engineered constructs may significantly affect the biomechanical properties of the tissue or construct. By modulating the assembly of aggregated PG, which affects AGC retention, it may be possible to create the desired balance between PG and collagen components, in order to modulate the mechanical properties of the engineered construct.

This paper describes the utilization of biomimetic molecular reassembly of native molecules into macromolecular structures, using AGC with HA ± LP, to modulate AGC retention in hydrogel constructs, and as a result, the compressive properties of the constructs. *In vitro* assembling of key functional extracellular matrix constituents of native cartilage has the potential to improve retention of the matrix

constituents, modulate the biomechanical properties of the engineered construct, and significantly reduce the time to produce a mature ECM in tissue engineered constructs.

4.6 Acknowledgments

This chapter, in full, was published in *Tissue Engineering: Part C Methods*. The dissertation author is the primary investigator and thanks co-authors, Ms. Lissette M. Wilensky, Mrs. Barbara L. Schumacher, and Drs. Koichi Masuda, and Robert L. Sah for their contributions to this work. This work was supported by NIH, NSF, and a grant to University of California-San Diego, in support of Prof. Robert Sah, from the Howard Hughes Medical Institute through the HHMI Professors Program. Additional supports were received from a NSF Graduate Research Fellowship (EHH) and Amgen Scholars Program (LMW).

4.7 References

1. Asanbaeva A, Tam J, Schumacher BL, Klisch SM, Masuda K, Sah RL: Articular cartilage tensile integrity: Modulation by matrix depletion is maturation-dependent. *Arch Biochem Biophys* 474:175-82, 2008.

2. Bayliss MT, Howat S, Davidson C, Dudhia J: The organization of aggrecan in human articular cartilage. Evidence for age-related changes in the rate of aggregation of newly synthesized molecules. *J Biol Chem* 275:6321-7, 2000.

3. Benjamin M, Ralphs JR: Fibrocartilage in tendons and ligaments--an adaptation to compressive load. *J Anat* 193 (Pt 4):481-94, 1998.

4. Bryant SJ, Arthur JA, Anseth KS: Incorporation of tissue-specific molecules alters chondrocyte metabolism and gene expression in photocrosslinked hydrogels. *Acta Biomater* 1:243-52, 2005.

5. Buckwalter JA, Rosenberg LC, Tang L-H: The effect of link protein on proteoglycan aggregate structure: an electron microscopic study of the molecular architecture and dimensions of proteoglycan aggregates reassembled from the proteoglycan monomers and link proteins of bovine fetal epiphyseal cartilage. *J Biol Chem* 259:5361-3, 1984.

6. Buschmann MD, Gluzband YA, Grodzinsky AJ, Kimura JH, Hunziker EB: Chondrocytes in agarose culture synthesize a mechanically functional extracellular matrix. *J Orthop Res* 10:745-58, 1992.

7. Buschmann MD, Grodzinsky AJ: A molecular model of proteoglycan-associated electrostatic forces in cartilage mechanics. *J Biomech Eng* 117:179-92, 1995.

8. Carney SL, Muir H: The structure and function of cartilage proteoglycans. *Physiol Rev* 68:858-910, 1988.

9. Chung C, Burdick JA: Engineering cartilage tissue. *Adv Drug Deliv Rev* 60:243-62, 2008.

10. Darling EM, Athanasiou KA: Biomechanical strategies for articular cartilage regeneration. *Ann Biomed Eng* 31:1114-24, 2003.

11. Drury JL, Mooney DJ: Hydrogels for tissue engineering: scaffold design variables and applications. *Biomaterials* 24:4337-51, 2003.

12. Dudhia J: Aggrecan, aging and assembly in articular cartilage. *Cell Mol Life Sci* 62:2241-56, 2005.

13. Ellis DL, Yannas IV: Recent advances in tissue synthesis in vivo by use of collagen-glycosaminoglycan copolymers. *Biomaterials* 17:291-9, 1996.

14. Farndale RW, Buttle DJ, Barrett AJ: Improved quantitation and discrimination of sulphated glycosaminoglycans by use of dimethylmethylene blue. *Biochim Biophys Acta* 883:173-7, 1986.

15. Garg AK, Berg RA, Silver FH, Garg HG: Effect of proteoglycans on type I collagen fibre formation. *Biomaterials* 10:413-9, 1989.

16. Gribbon P, Hardingham TE: Macromolecular diffusion of biological polymers measured by confocal fluorescence recovery after photobleaching. *Biophys J* 75:1032-9, 1998.

17. Grover J, Roughley PJ: The expression of functional link protein in a baculovirus system: analysis of mutants lacking the A, B and B' domains. *Biochem J* 300 (Pt 2):317-24, 1994.

18. Han E, Bae WC, Hsieh-Bonassera ND, Wong VW, Schumacher BL, Gortz S, Masuda K, Bugbee WD, Sah RL: Shaped, stratified, scaffold-free grafts for articular cartilage defects. *Clin Orthop Relat Res* 466:1912-20, 2008.

19. Hardingham TE, Fosang AJ: Proteoglycans: many forms and many functions. *Faseb J* 6:861-70, 1992.

20. Hardingham TE, Muir H, Kwan MK, Lai WM, Mow VC: Viscoelastic properties of proteoglycan solutions with varying proporations present as aggregates. *J Orthop Res* 5:36-46, 1987.

21. Hascall VC: Interaction of cartilage proteoglycans with hyaluronic acid. *J Supramol Struct* 7:101-20, 1977.

22. Heinegard D, Sommarin Y: Isolation and characterization of proteoglycans. *Methods Enzymol* 144:305-19, 1987.

23. Holmes MWA, Bayliss MT, Muir H: Hyaluronic acid in human articular cartilage: age-related changes in content and size. *Biochem J* 250:435-41, 1988.

24. Hsieh-Bonassera ND, Wu I, Lin JK, Schumacher BL, Chen AC, Masuda K, Bugbee WD, Sah RL: Expansion and redifferentiation of chondrocytes from osteoarthritic cartilage: cells for human cartilage tissue engineering. *Tissue Eng Part A* 15:3513-23, 2009.

25. Kahn A, Taitz AD, Pottenger LA, Alberton GM: Effect of link protein and free hyaluronic acid binding region on spacing of proteoglycans in aggregates. *J Orthop Res* 12:612-20, 1994.

26. Kelly TA, Ng KW, Wang CC, Ateshian GA, Hung CT: Spatial and temporal development of chondrocyte-seeded agarose constructs in free-swelling and dynamically loaded cultures. *J Biomech* 39:1489-97, 2006.

27. Kvam C, Granese D, Flaibani A, Zanetti F, Paoletti S: Purification and characterization of hyaluronan from synovial fluid. *Anal Biochem* 211:44-9, 1993.

28. Lohmander S: Turnover of proteoglycans in guinea pig costal cartilage. *Arch Biochem Biophys* 180:93-101, 1977.

29. Maroudas A: Glycosaminoglycan turn-over in articular cartilage. *Philos Trans R Soc Lond B Biol Sci* 271:293-313, 1975.

30. Maroudas A: Physico-chemical properties of articular cartilage. In: *Adult Articular Cartilage,* ed. by MAR Freeman, Pitman Medical, Tunbridge Wells, England, 1979, 215-90.

31. Martin I, Miot S, Barbero A, Jakob M, Wendt D: Osteochondral tissue engineering. *J Biomech* 40:750-65, 2007.

32. Martin I, Obradovic B, Treppo S, Grodzinsky AJ, Langer R, Freed LE, Vunjak-Novakovic G: Modulation of the mechanical properties of tissue engineered cartilage. *Biorheology* 37:141-7, 2000.

33. Miwa HE, Gerken TA, Huynh TD, Flory DM, Hering TM: Mammalian expression of full-length bovine aggrecan and link protein: formation of recombinant proteoglycan aggregates and analysis of proteolytic cleavage by ADAMTS-4 and MMP-13. *Biochim Biophys Acta* 1760:472-86, 2006.

34. Morgelin M, Heinegard D, Engel J, Paulsson M: The cartilage proteoglycan aggregate: assembly through combined protein-carbohydate and protein-protein interactions. *Biophys Chem* 50:113-28, 1994.

35. Narayanan J, Xiong J-Y, Liu X-Y: Determination of agarose gel pore size: Absorbance measurements vis a vis other techniques. *Journal of Physics: Conference Series* 28:83-6, 2006.

36. Natoli RM, Responte DJ, Lu BY, Athanasiou KA: Effects of multiple chondroitinase ABC applications on tissue engineered articular cartilage. *J Orthop Res* 27:949-56, 2009.

37. Nicodemus GD, Giunta SM, Bryant SJ: Rational design of 3D hydrogels to capture and retain ECM molecules within mechanically stimulated PEG gels. *Trans Orthop Res Soc*:572, 2009.

38. Poole AR, Pidoux I, Reiner A, Tang L-H, Choi H, Rosenberg L: Localization of proteoglycan monomer and link protein in the matrix of bovine articular

cartilage: an immunohistochemical study. *J Histochem Cytochem* 28:621-35, 1980.

39. Rosenberg L, Tang L-H, Pal S, Johnson TL, Choi HU: Proteoglcyans of bovine articular cartilage: studies of the direct interaction of link protein with hyaluronate in the absence of proteoglycan monomer. *J Biol Chem* 263:18071-7, 1988.

40. Roughley PJ: Biology of intervertebral disc aging and degeneration: involvement of the extracellular matrix. *Spine (Phila Pa 1976)* 29:2691-9, 2004.

41. Roughley PJ: The structure and function of cartilage proteoglycans. *Eur Cell Mater* 12:92-101, 2006.

42. Sah RL, Grodzinsky AJ, Plaas AH, Sandy JD: Effects of tissue compression on the hyaluronate-binding properties of newly synthesized proteoglycans in cartilage explants. *Biochem J* 267:803-8, 1990.

43. Sajdera SW, Hascall VC: Proteinpolysaccharide complex from bovine nasal cartilage. A comparison of low and high shear extraction procedures. *J Biol Chem* 244:77-87, 1969.

44. Scott JE, Dorling J: Differential staining of acid glycosaminoglycans (mucopolysaccharides) by alcian blue in salt solutions. *Histochemie* 5:221-33, 1965.

45. Sechriest VF, Miao YJ, Niyibizi C, Westerhausen-Larson A, Matthew HW, Evans CH, Fu FH, Suh J-K: GAG-augmented polysaccharide hydrogel: a novel biocompatible and biodegradable material to support chondrogenesis. *J Biomed Mater Res* 49:534-41, 2000.

46. Stuart K, Panitch A: Influence of chondroitin sulfate on collagen gel structure and mechanical properties at physiologically relevant levels. *Biopolymers* 89:841-51, 2008.

47. Suh JK, Matthew HW: Application of chitosan-based polysaccharide biomaterials in cartilage tissue engineering: a review. *Biomaterials* 21:2589-98, 2000.

48. Tang L-H, Rosenberg L, Reeiner A, Poole AR: Proteoglycans from bovine nasal and articular cartilage: properties of a soluble form of link protein. *J Biol Chem* 254:10523-31, 1979.

49. Tang LH, Buckwalter JA, Rosenberg LC: Effect of link protein concentration on articular cartilage proteoglycan aggregation. *J Orthop Res* 14:334-9, 1996.

50. Tomioka M, Matsumura G: Effects of concentration and degree of polymerization on the rheological properties of methylcellulose aqueous solution. *Chem Pharm Bull (Tokyo)* 35:2510-8, 1987.

51. Valiyaveettil M, Mort JS, McDevitt CA: The concentration, gene expression, and spatial distribution of aggrecan in canine articular cartilage, meniscus, and anterior and posterior cruciate ligaments: a new molecular distinction between hyaline cartilage and fibrocartilage in the knee joint. *Connect Tissue Res* 46:83-91, 2005.

52. Williamson AK, Chen AC, Sah RL: Compressive properties and function-composition relationships of developing bovine articular cartilage. *J Orthop Res* 19:1113-21, 2001.

CHAPTER 5

COMPACTION ENHANCES EXTRACELLULAR MATRIX CONTENT AND MECHANICAL PROPERTIES OF TISSUE ENGINEERED CARTILAGINOUS CONSTRUCTS

5.1 Abstract

Many cell-based tissue-engineered cartilaginous constructs are mechanically softer than native tissue and have an imbalance among its extracellular matrix contents. The fabrication of cartilaginous constructs that more closely approximates the collagen (COL):glycosaminoglycan ratio and content of the normal cartilage may result in improved mechanical properties. The objectives of this work were to (1) determine the effect of addition of proteoglycans (PG), COL, or COL+PG on compressive properties of 2% agarose constructs and (2) determine the feasibility of mechanical compaction to 90% of thickness to concentrate matrix content in tissue engineered constructs and the effect of such compaction on the compressive properties of such constructs. The mechanical compaction method rapidly increased the PG and COL concentrations in the constructs, and the compacted constructs had higher compressive stiffness than the construct before compaction. Presence of COL+PG

improved the compressive properties of hydrogel constructs compared to PG or COL alone. Chondrocytes included in the constructs maintained high viability after compaction. These results support the general concept that the mechanical compaction method provides a novel method to rapidly enhance the extracellular matrix content and compressive properties of engineered cartilaginous constructs.

5.2 Introduction

Articular cartilage is a smooth, load-bearing connective tissue at the ends of long bones that are designed to last a lifetime [7]. The bulk of the dry weight (DW) in articular cartilage is composed of extracellular matrix (ECM), mainly collagens (COL) (~60% DW) and proteoglycans (PG) (25–35% DW) [7]. The PG are found as large aggregates of aggrecan (AGC) monomers that are non-covalently bound to a hyaluronan (HA) chain and link proteins (LP) [36]. The long and numerous chains of sulfated glycosaminoglycans (GAG) on an AGC monomer provide the fixed charged density (FCD) and the high osmotic pressure (π_{PG}) within the tissue that are responsible for its compressive resistance [28]. The collagen networks aid in the retention of the large PG aggregates and provide the restraining forces that counterbalance π_{PG} at rest or in compression and the high resistance in tension [28].

Due to the limited capacity of avascular articular cartilage for self-repair once damaged, several treatment strategies have tried to address the issue of cartilage repair and healing, including tissue engineering approaches [8]. Tissue engineering has been envisioned as a potential solution to circumvent the limitation of the donor cell and tissue source in current treatments, such as autologous chondrocyte implantation or osteochondral allo- or auto-grafts. However, many cell-based tissue-engineered constructs for articular cartilage are mechanically soft and have an imbalance between its extracellular matrix components. In normal cartilage, the COL content is typically ~2-10 times higher that of sGAG content in immature fetal bovine to adult human cartilage, respectively [42, 49], but the typical ratio of COL:GAG in engineered cartilage are 1:1 or less even after prolonged culture [10, 31, 47]. These constructs

usually have a fairly robust PG content that approaches physiological levels, but the COL content is usually substantially below those of native cartilage.

By modulating the accumulation of PG and COL molecules with various chemical (e.g. growth factors, cytokines), mechanical (e.g. dynamic compression, shear, tension, perfusion, pressure), and other biophysical factors (e.g. hypoxia, electric field), there have been efforts to create cell-based, tissue-engineered cartilaginous constructs with increased matrix content and more robust mechanical properties [22, 46]. These approaches typically take weeks, if not months, to achieve the concentrations that approach physiological levels.

More recently, efforts have been made to increase the matrix concentration by direct manipulation of the matrix. By biomimetic molecular reassembly and addition of assembled PG aggregates to a tissue engineered construct, the desired PG concentration was rapidly achieved and maintained over a 3-day incubation [18]. The addition and retention of assembled PG content increased the biomechanical properties of the engineered construct and reduced the time to produce a mature ECM. In another method, selective enzymatic degradation of PG in cartilage and engineered constructs resulted in increased COL concentration, COL:PG ratio, and tensile stiffness of the tissue [4, 6, 30]. This highlights the importance of the balance between COL and PG in mechanical function of the tissue and engineered constructs.

The fabrication of cartilaginous constructs that more closely approximates the COL:GAG ratio and content of the normal cartilage may allow for improved mechanical properties and more rapid implantation of such constructs into the mechanical demanding environment of an *in vivo* joint. Thus, the objectives of this

work were (1) to determine the effect of addition of PG, COL, or COL+PG on compressive properties of 2% agarose constructs, and (2) to determine the feasibility of mechanical compaction to concentrate matrix content in tissue engineered constructs and the effect of such compaction on the compressive properties of such constructs.

5.3 Materials and Methods

The effect of addition of PG, COL, or COL+PG and mechanical compaction on biochemical and compressive properties of tissue engineered constructs were studied. Constructs with varying ECM components were measured for their thickness and wet weight and were mechanically compacted to 90% of their initial thickness while measuring their peak stress (σ_{PEAK}) and equilibrium stress (σ_{EQ}). After 1 day, the compacted constructs were analyzed for their thickness, wet weight, tested under compression to obtain σ_{PEAK} and σ_{EQ}, and then analyzed for GAG, and COL content. The mechanical properties were analyzed further by considering only the ECM contribution to σ_{EQ} with subtraction of the agarose contribution, comparing the stress-compression curves of the initial and final compacted constructs, and comparing the PG contribution to predicted π_{PG} values.

Preparation of Proteoglycan Components and Collagen

AGC and LP were purified from bovine calf knee articular cartilage as described previously [18, 19, 38, 41]. Pharmaceutical grade HA was obtained as Healon® (4 MDa) (Abbott Medical Optics, Inc., Santa Ana, CA). The concentrated PG aggregate solution containing AGC + 1% HA + 5% LP was dialyzed (MWCO 8-10kDa) against PBS, pH 7.0 at 4°C for 18 hours to remove the guanidine-HCl in order to allow for aggregation, which was verified by S-1000 column chromatography [37].

The COL was prepared from bovine calf knee articular cartilage, based on a modification of a previously described method [11, 14]. The cartilage pieces were digested with 1 mg/ml trypsin from bovine pancreas in PBS, 0.9 mM $CaCl_2$, 0.5 mM $MgCl_2$, pH 7.1 overnight at room temperature with gentle mixing to remove PG. After

the digestion, the cartilage pieces were washed twice in PBS, followed with 2 mg/ml soybean trypsin inhibitor in PBS for 30 mins, and then washed twice in PBS. The digested cartilage samples were cryomilled with dry ice, suspended in PBS, and then filtered through 100 μm pore size filter. The filtrate was determined to contain mostly COL (>95%) and a very small sGAG content as assessed by hydroxyproline [50] and dimethylmethylene blue assay [13], respectively.

Formation of Tissue Engineered Constructs

Disk constructs (d=6.4mm, h=~3mm; n=4-5/group) were composed of 2% low-melting temperature agarose (SeaPlaque, Lonza, Rockland, ME) with variable amounts of PG and COL (Table 1): (Group I) control with no PG or COL, (Group II) PG only (2.5 mg/ml AGC + 1% HA (by weight of AGC) + 5% LP, (Group III) COL only (10 mg/ml COL), and (Group IV) COL+PG. The concentrations of 10 mg/ml of COL and 2.5 mg/ml of sGAG were chosen since COL:GAG ratio of 4:1 is close to the COL:GAG ratio found in bovine articular cartilage [49].

The concentrated matrix solutions were warmed to 40°C and mixed well with a concentrated solubilized agarose solution, for a final agarose concentration of 2%. The PG-agarose solutions were gelled into ~3 mm thick sheets at 4°C for at least one hour. Disk constructs were punched from the PG-agarose sheets and were placed into PBS, pH 7.0 containing protease inhibitors (PIs) (0.5 mM EDTA, 1 mM phenylmethylsulfonyl fluoride (PMSF), 5 mM benzamidine-HCl, 5 mM N-ethylmaleimide (NEM)) overnight at 4°C.

Mechanical Compaction of the Constructs

After the overnight incubation, the wet weights and the thickness of the constructs were measured. For the mechanical compaction of the constructs, the constructs were placed in a radially confining chamber between two porous platens filled with PBS + PIs and compressed to a final compression of 90% of the initial thickness using a mechanical spectrometer [18]. The constructs were compressed to 30%, 60%, 75%, and 90% of initial thickness with 1600 s of ramp compression followed by 2400 s relaxation to equilibrium. At each compression level, the σ_{PEAK} and σ_{EQ}, calculated from the measured load at end of ramp compression and at end of relaxation divided by the circular confining chamber area, were analyzed. After the mechanical compaction, the constructs then were incubated in PBS + PIs overnight at 4°C under free-swelling condition to allow for rehydration.

Biomechanical Analysis of the Compacted Constructs

Following the overnight incubation after mechanical compaction, the constructs were photographed and measured for wet weight and thickness. The constructs were tested in the same confined compression set up to 60%, 75%, and 90% compression of the *initial* thickness with 1600 s of ramp compression followed by 2400 s relaxation to equilibrium. At each compression level, the σ_{PEAK} and σ_{EQ} were analyzed and were compared to those taken during the initial mechanical compaction and to compacted constructs from other experimental groups.

Biochemical Analysis of Construct ECM Components

After final mechanical testing, the constructs were cut in half. One half was solubilized by proteinase K digestion at 60°C overnight and incubation at 70°C for 2

minutes. The constructs were analyzed for sGAG content by dimethylmethylene blue assay [13] and for COL content by hydroxyproline assay [50].

The other halves of the constructs were prepared for histology. The constructs were fixed in 4% paraformaldehyde for 3 hours, snap frozen with optimal cutting temperature compound (Sakura Finetek, Torrance, CA) in isopentane cooled with liquid nitrogen, and cryosectioned in the vertical orientation of the constructs at 30 μm thickness. The sections were assessed for sGAG with Alcian blue [39] and for collagen type II by immunohistochemistry [20]. Sections were imaged using brightfield microscopy (Eclipse TE300, Nikon, Melville, NY).

Comparison of Mechanical Properties of Initial and Compacted Constructs

The stress-compression relationship was plotted using the compression levels normalized to the measured thicknesses before compaction for initial constructs or mechanical testing for compacted constructs. At the last two compression levels of the compacted constructs, stresses were estimated from the stress-compression curves of the initial constructs. Then, the estimated stresses were compared to the measured σ_{EQ} for the compacted constructs from the same group.

Comparison of PG contribution to Predicted π_{PG} to Compressive Properties

In order to assess the matrix contribution to the σ_{EQ} apart from the agarose contribution, assuming the contributions from each components were additive, the stress ascribed to PG or COL or COL+PG only at each compression level was calculated by subtracting the σ_{EQ} of Groups II, III, and IV from the σ_{EQ} of the agarose only constructs (Group I) ($\sigma_{EQ} - \sigma_{EQ,I}$).

Using the previously described FCD–π_{PG} relationship [17], the π_{PG} during compression were estimated for the constructs from Groups II and IV. The π_{PG} was calculated from FCD_{EF} using experimentally obtained biochemical data and COL extrafibrillar (EF) water at each compression level and the FCD–π_{PG} relationship. The EF water varies with the COL content in this FCD–π_{PG} relationship. Then, the π_{PG} was compared to the σ_{EQ}– $\sigma_{EQ,I}$ of the corresponding group.

Compatibility of Compaction with Viable Chondrocytes

To determine the effect of construct formation and compaction on cell viability, disk constructs (d=6.4 mm, h=~3 mm) containing either no ECM (Group I) or COL+PG at 80% concentration (8 mg/ml COL and 2 mg/ml PG) (Group IV) with alginate-recovered chondrocytes (ARC) at $1.7x10^6$ cells/ml in 2% agarose were formed. The ECM concentration was decreased to accommodate the additional volume of chondrocytes in the constructs. Briefly, the ARC were prepared from bovine calf femoral condyle chondrocytes cultured in beads of 1.2% alginate for 8 days at 37°C in DMEM/F12 with additives (100 U/ml penicillin, 100 μg/ml streptomycin, 0.25 μg/ml fungizone, 0.1 mM MEM non-essential amino acids, 0.4 mM L-proline, 2 mM L-glutamine), 10% fetal bovine serum, and 25 μg/ml ascorbate and then released with their cell-associated matrix from alginate in 55mM sodium citrate [23, 29]. The constructs were cultured at 37°C in DMEM with additives, 10% FBS and 25 μg/ml ascorbate for 1 day and compacted to 90% as described above. Then, the compacted constructs after 1-day culture, along with uncompacted constructs to serve as controls, were assessed qualitatively by live/dead staining (Life Technologies, Carlsbad, CA) for chondrocyte viability.

Statistical Analysis

Data are presented as mean ± standard error of the mean (SEM). Thickness, wet weight, GAG/volume, COL/volume, σ_{PEAK}, σ_{EQ}, and σ_{EQ}–$\sigma_{EQ,I}$ were analyzed by repeated measures analysis of variance (ANOVA) with compaction as a repeated factor and experimental groups as a main factor. To determine the effect of compaction within one experimental group, paired t-tests were performed ($p<0.05$). To determine the effect of experimental groups for either initial or compacted constructs, ANOVA was performed and was followed by post-hoc Tukey test when significance was detected ($p<0.05$). The estimated σ_{EQ} for initial constructs at compression levels for compacted constructs and compacted σ_{EQ} were analyzed by unpaired t-tests ($p<0.05$). The π_{PG} and σ_{EQ}– $\sigma_{EQ,I}$ for each group at one compression level were analyzed by ANOVA with post-hoc Tukey test when significance was detected ($p<0.05$).

Table 5.1: Experimental groups

		final concentration [mg/ml]			
Group	**in 2% agarose gel**	**COL**	**sGAG**	**HA**	**LP**
I	**control**	--	--	--	--
II	**PG**	0	2.5	0.025	0.125
III	**COL**	10	--	--	--
IV	**COL + PG**	10	2.5	0.025	0.125

5.4 Results

The 2% agarose constructs containing PG, or COL, or both COL+PG (Group II-IV) were formed, with the COL-containing constructs (Group III and IV) appearing more white and opaque than constructs without COL (Group I and II) (Fig. 5.1). All constructs were able to withstand the mechanical compaction and the subsequent mechanical testing, maintaining macroscopic integrity (Fig. 5.1). Thicknesses and wet weights of the constructs were reduced to 39-56% ($p<0.001$) and 41-61% ($p<0.001$), respectively, of their initial values (Fig. 5.2). The ability of the constructs to maintain their compacted thickness was dependent on their initial formulation. Those constructs assembled with PG (Group II and IV) swelled overnight more than the constructs assembled without PG (Group I and III) to higher thicknesses and wet weights ($p<0.01$). The constructs with PG had similar thickness and wet weights ($p>0.7$) while the constructs without PG were also similarly compacted to each other ($p>0.4$).

Mechanical compaction and initial formulation affected the final PG and COL concentrations of the constructs (Fig. 5.3). The constructs that initially contained PG or COL (Groups II-IV) had similar content before and after the compaction and mechanical testing, maintaining most of their matrix content during the PBS+PIs incubations, mechanical compaction, and mechanical testing. When normalized to the construct volume before and after compaction, the sGAG concentration increased by ~1.8-1.9 fold in Group II and IV constructs to ~4.6-4.8 mg/cm^3 ($p<0.001$) while the COL concentration increased by ~1.8 fold for Group IV constructs to 15.8 mg/cm^3 ($p<0.01$) and ~2.5 fold in Group III constructs to 24.6 mg/cm^3 ($p<0.001$) after compaction as compared to before the compaction.

Histological assessment for sGAG and type II collagen distribution on cryosections of the constructs were consistent with the biochemical analysis (Fig. 5.4). The compacted constructs stained more intensely for both sGAG and type II collagen than the corresponding constructs at day 0. The sGAG and type II collagen staining for the compacted constructs were relatively even throughout the section when the constructs contained these ECM components. Sections from compacted constructs with PG (Group II and IV) stained strongly blue indicative of sGAG throughout the section (Fig. 5.4A-H). Likewise, sections from compacted constructs containing COL (Group III and IV) immunostained intensely positive for type II collagen (Fig. 5.4I-P).

The initial mechanical properties of the constructs during the compaction were dependent on the construct formulation (Fig. 5.5A-C). The σ_{PEAK} and σ_{EQ} increased with increasing compression levels for all constructs (Fig. 5.5A, B). The constructs containing PG or COL alone or COL+PG (Groups II, III, IV) had higher σ_{PEAK} than the agarose only constructs (Group I) (overall $p<0.001$). Also, the constructs with COL+PG (Group IV) had the higher σ_{PEAK} and σ_{EQ} than that of the constructs containing PG or COL alone (Groups II, III) at 60, 75, and 90% compression ($p<0.01$). The σ_{EQ}-$\sigma_{EQ,I,}$ the stress ascribed to the ECM components by subtracting the contribution from agarose (Group I), was higher for Group IV constructs than for Group II and III ($p<0.01$) (Fig. 5.5C).

The compacted constructs had similar σ_{PEAK} and σ_{EQ} values as during the initial compaction at 75% and 90% compression to the initial thickness ($p>0.4$) (Fig. 5.5D-F). The data for 60% compression level was not used as the Group I and III constructs were too thin to test reliably. The σ_{PEAK} and σ_{EQ} at 75% and 90%

compression were the lowest for Group I constructs and highest for Group IV constructs ($p<0.001$ vs Group I, $p<0.05$ vs Group II and III) (Fig. 5.5D, E). The σ_{EQ}-$\sigma_{EQ,I}$ for Group IV constructs were higher than those from Group II and III ($p<0.05$) (Fig. 5.5F).

When compression levels were normalized to the thicknesses of the compacted constructs rather than the initial constructs, the computed compressive stiffnesses were higher (Fig. 5.6). The highest compression level (90% compression relative to initial thickness) was equivalent to 75-83% compression relative to thicknesses of the compacted constructs. At these compression levels, the compacted constructs had higher σ_{EQ} than the estimated σ_{EQ} for the initial constructs by 170-560% ($p<0.05$).

The predicted PG contribution to the σ_{EQ}, calculated from the FCD_{EF}–π_{PG} relationship, was consistent with σ_{EQ}-$\sigma_{EQ,I}$ values obtained experimentally (Fig. 5.7). At 90% compression of the initial thickness, the estimated π_{PG} contribution to the σ_{EQ} were similar to the σ_{EQ}-$\sigma_{EQ,I}$ for the initial and final constructs from Group II (16.1 kPa, 26.8 kPa, and 22.3 kPa for π_{PG}, initial and final σ_{EQ}-$\sigma_{EQ,I}$, respectively) ($p>0.3$) and IV (55.8 kPa, 55.5 kPa, 55.1 kPa) ($p>0.99$). The estimated π_{PG} at 75% compression of the initial thickness were not as similar ($p<0.07$) as the FCD values were very small (<0.05 mEq/g water) where the model is less accurate.

Alginate-recovered chondrocytes in the constructs remained mostly viable before and after mechanical compaction to 90% of construct thickness (Fig. 5.8). Formation of construct with ECM components was compatible with chondrocytes as most of the ARCs were viable in uncompacted constructs (Fig. 5.8A, B, E, F). After compaction, the viability of ARC was slightly lower than uncompacted constructs but

still qualitatively high for Group I constructs and remained fairly high in the constructs with COL+PG (Group IV) (Fig. 5.8C, D, G, H).

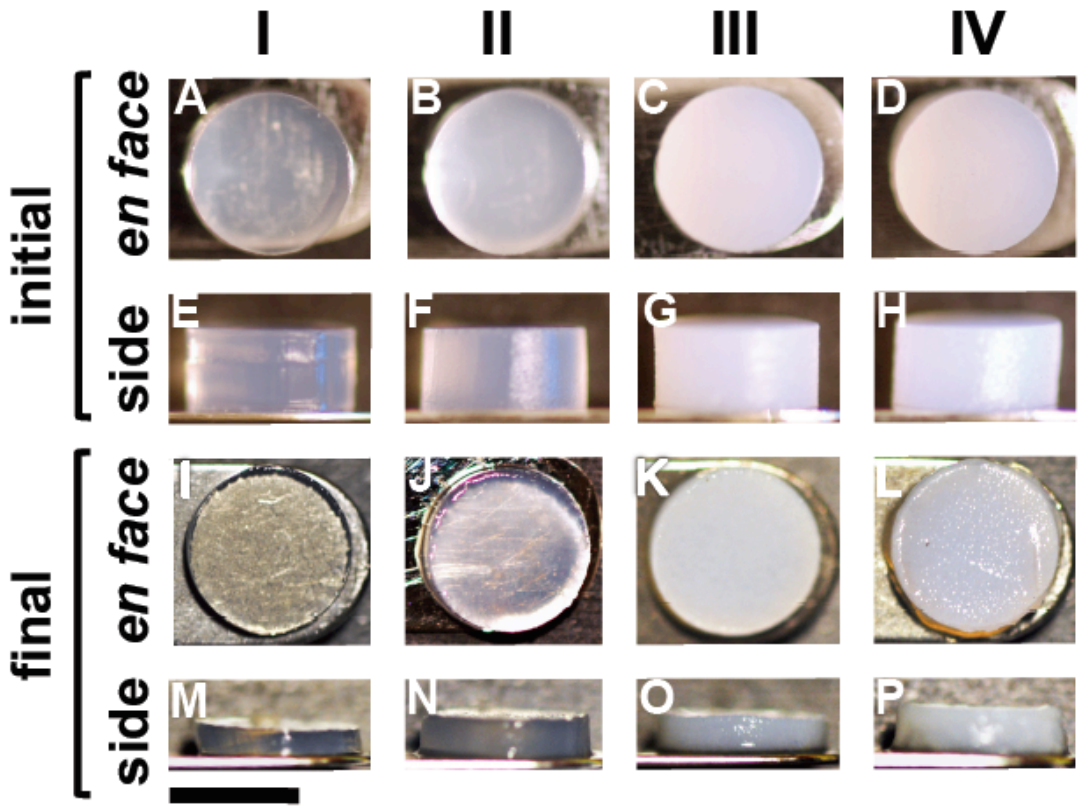

Figure 5.1: Macroscopic images of the constructs. The engineered cartilaginous constructs from Groups I (control) (A, E, I, M), II (PG) (B, F, J, N), III (COL) (C, G, K O), and IV (COL+PG) (D, H, L, P) before (initial) (A-H) and one day after compaction (final) (I-P). (bar= 5mm)

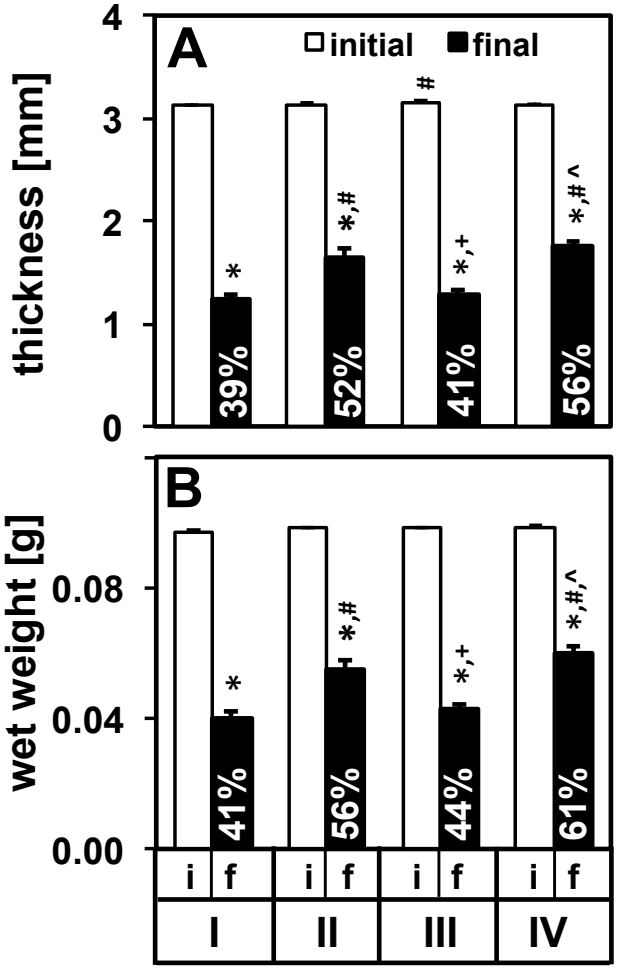

Figure 5.2: Dimension of constructs. Thickness (A) and wet weight (B) before (initial) and one day after mechanical compaction (final) of the constructs from Groups I-IV. The percentages of the final thickness and wet weight compared to initial values are noted. (* $p<0.001$ vs initial constructs of corresponding group. $p<0.01$ # vs Group I, + vs Group II, ^ vs Group III of corresponding time point)

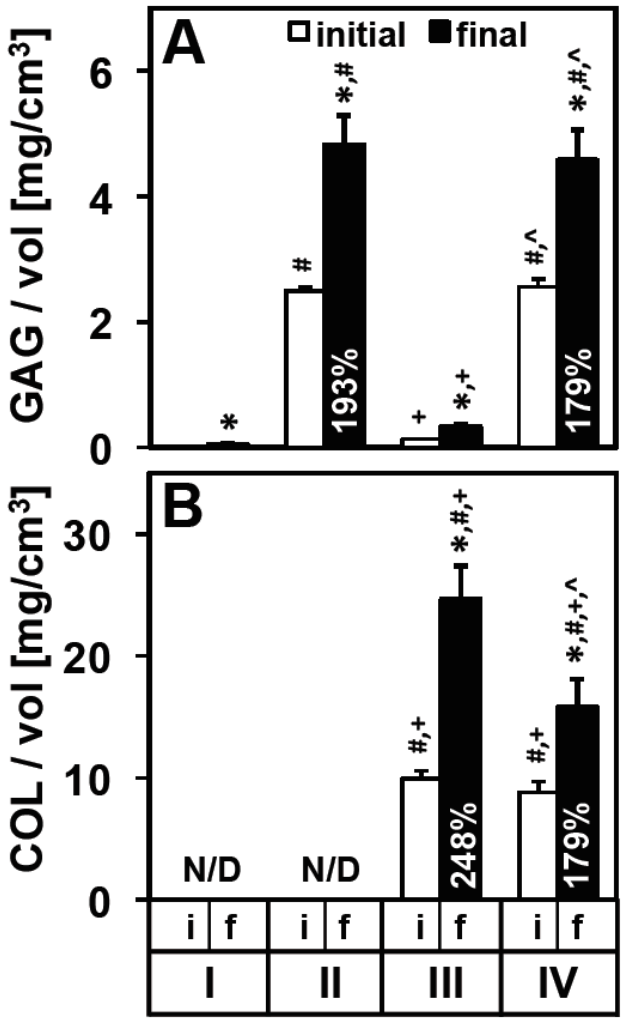

Figure 5.3: Biochemical content of constructs. GAG (A) and collagen (B) concentration normalized to the volume of the constructs from Groups I-IV before (initial) and a day after mechanical compaction (final). The percentages of the final GAG and COL concentrations compared to the initial values are noted. (N/D = not detectable. * $p<0.01$ vs initial constructs of corresponding group. $p<0.01$ # vs Group I, + vs Group II, ^ vs Group III of corresponding time point)

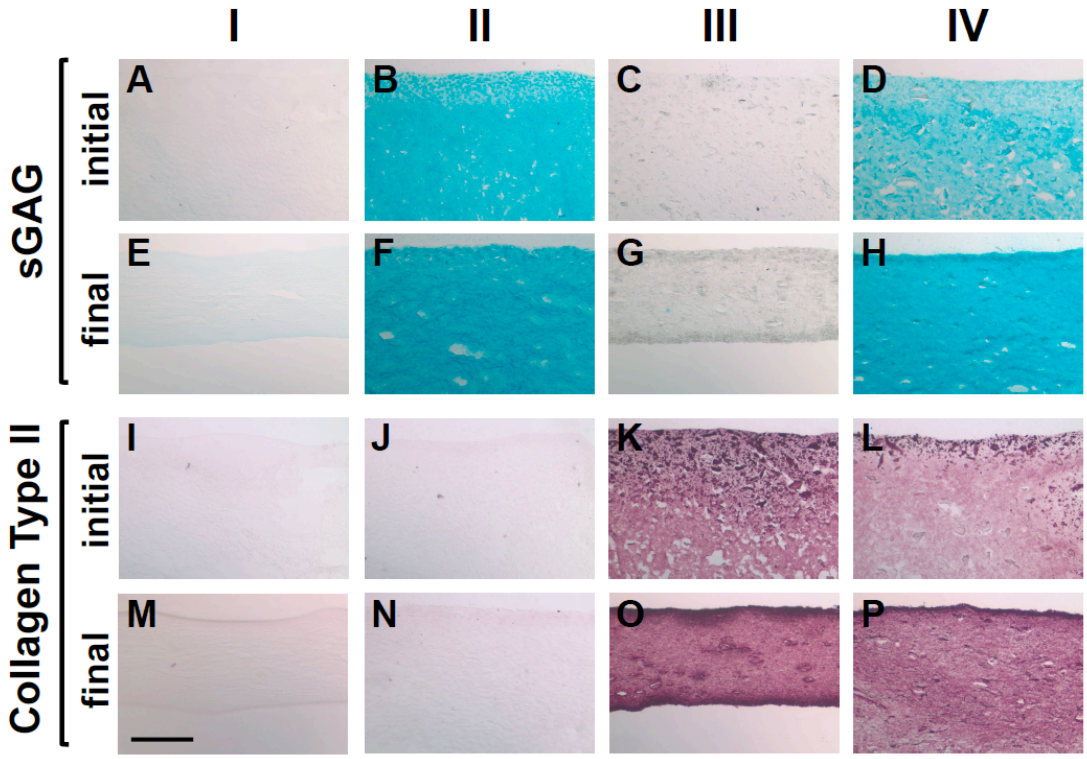

Figure 5.4: Staining of constructs for sGAG and collagen type II. The constructs from Groups I (control) (A, E, I, M), II (PG) (B, F, J, N), III (COL) (C, G, K O), and IV (COL+PG) (D, H, L, P) before (initial) (A-D, I-L) and one day after compaction (final) (E-H, M-P) stained with Alcian blue for sGAG (A-H) and immunostained for collagen type II (I-P). (bar= 500μm)

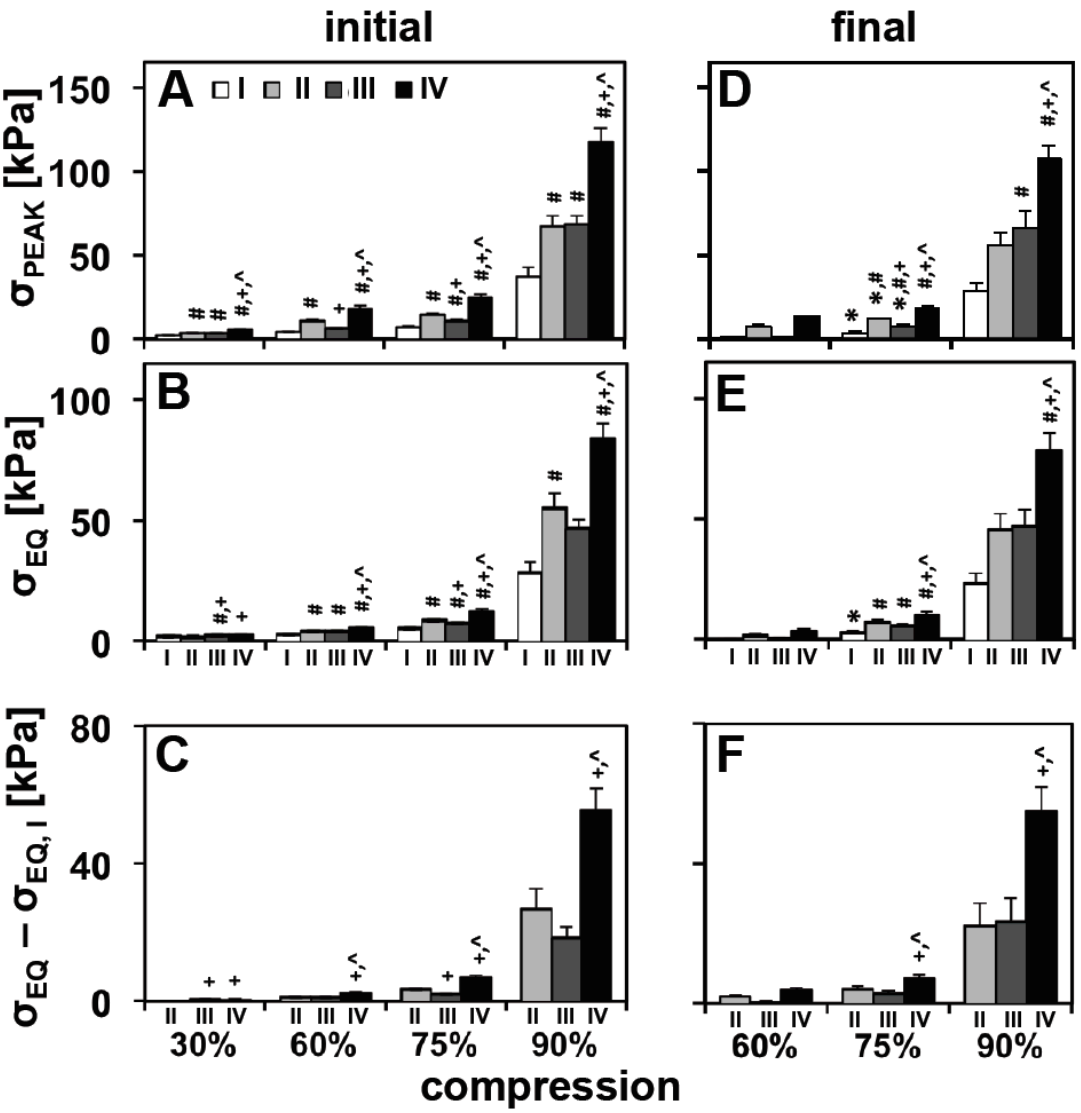

Figure 5.5: Compressive properties of the constructs during and after compaction. Peak (A, D) and equilibrium (B, E) stress of the constructs along with equilibrium stresses without the agarose contribution (Group I) (C, F) during initial compaction (A-C) at 30%, 60%, 75%, and 90% compression and after compaction (D-F) at 60%, 75%, and 90% compression of the initial thickness. (* $p<0.05$ vs initial constructs of corresponding group. $p<0.05$ # vs Group I, + vs Group II, ^ vs Group III of corresponding time point)

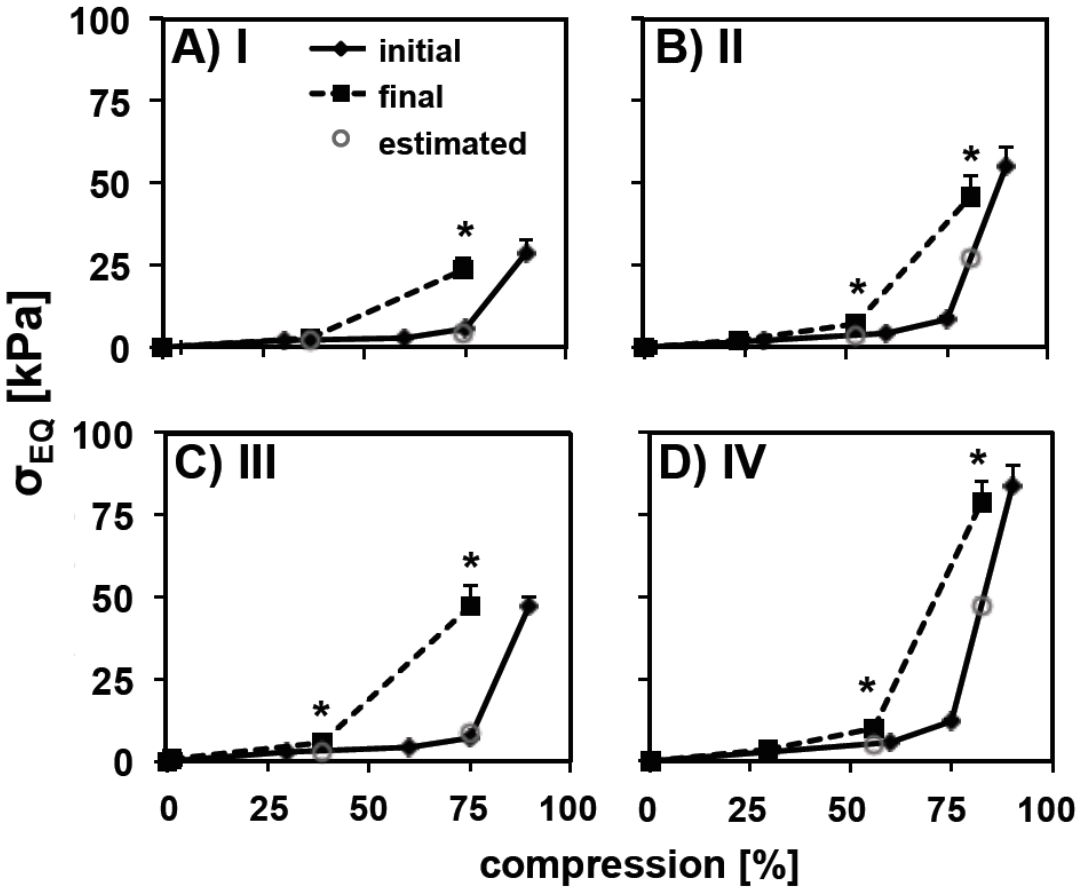

Figure 5.6: Stress-compression relationship of the constructs during and after compaction. Stress-compression curves of constructs during compaction (initial) and after compaction (final) from Groups I (A), II (B), III (C), and IV (D) after normalization to construct thickness before testing. At the last two compression levels of the final constructs, estimated stresses from the stress-compression curves of the initial constructs (estimated) are shown. (* $p<0.05$ final vs estimated σ_{EQ})

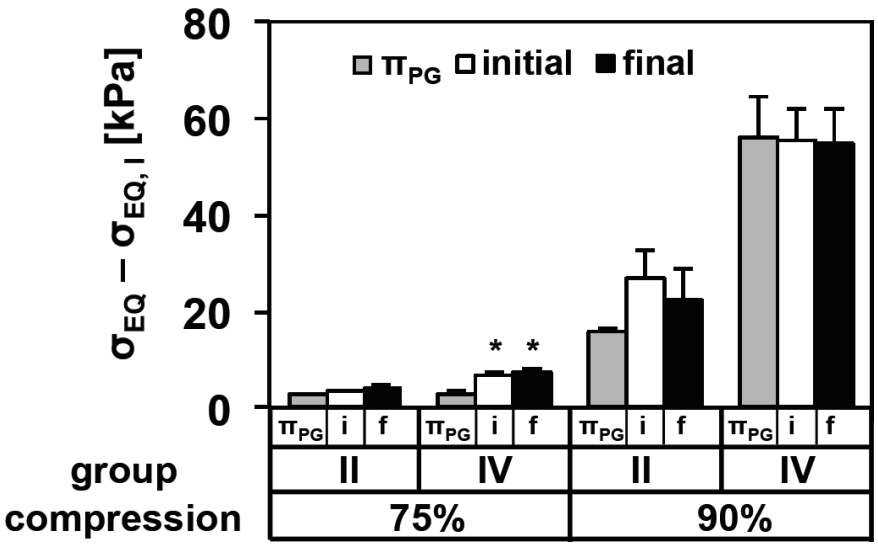

Figure 5.7: Prediction of PG contribution to compressive properties by π_{PG}. Comparison of predicted π_{PG} and experimentally obtained equilibrium stresses minus the agarose contribution ($\sigma_{EQ}-\sigma_{EQ,I}$) at 75% and 90% compressions of the initial thickness for Groups II and IV. (* $p<0.05$ vs π_{PG})

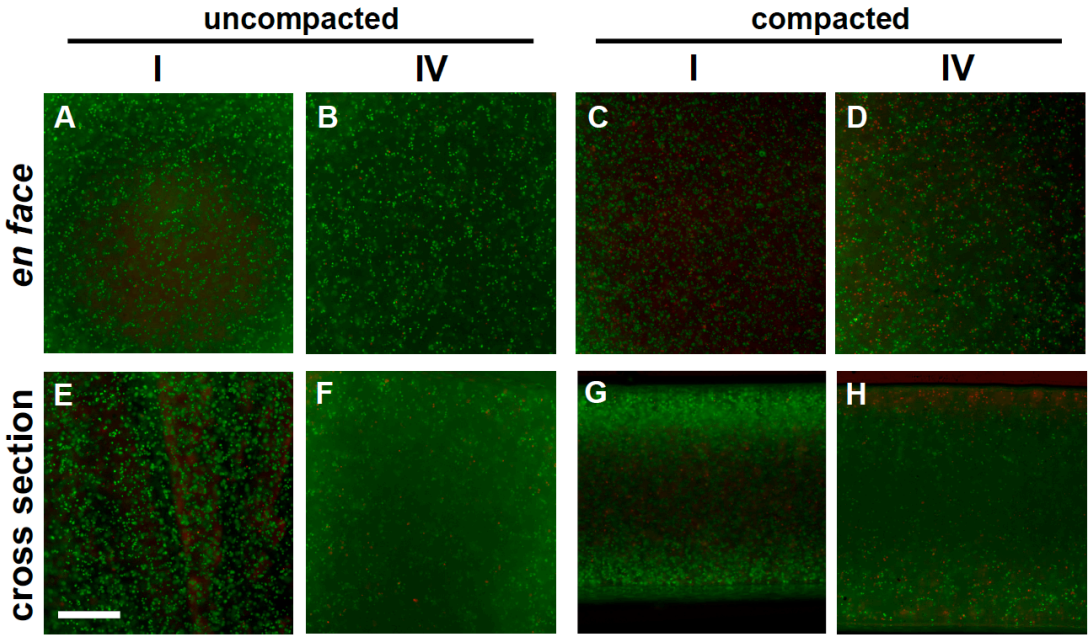

Figure 5.8: Live/dead staining of chondrocytes in uncompacted and compacted constructs. *En face* (A-D) and cross sectional (E-H) views of alginate-recovered chondrocytes in constructs from Groups I (control) (A, C, E, G) and IV (COL+PG) (B, D, F, H) without compaction (uncompacted) (A-D) or 1 day after compaction (compacted) (C-H). (bar= 500μm)

5.5 Discussion

Presented here is a novel method by the application of mechanical compaction to rapidly increase the extracellular matrix concentration and associated mechanical properties in cartilaginous constructs. Mechanical compaction increased the PG and COL concentrations (Fig. 5.3) as well as the compressive stiffness (Fig. 5.6). The presence of COL+PG improved the compressive properties of hydrogel constructs compared to PG or COL alone (Fig. 5.5), highlighting the contribution of COL content to compressive properties of engineered constructs. At 90% compression of the initial thickness, the predicted π_{PG} from FCD_{EF} from the PG content closely approximated the matrix contribution to the measured σ_{EQ} of the constructs (Fig. 5.7). Alginate-recovered chondrocytes remained mostly viable after compaction (Fig. 5.8), demonstrating the applicability of the method to cell-containing constructs. These results support the general concept that mechanical compaction provides a novel method to rapidly enhance the extracellular matrix content and compressive properties of engineered cartilaginous constructs.

The presence of both COL and PG in the appropriate proportions appears to play an important role in the compressive mechanical function of the engineered cartilaginous constructs. In addition to the space filling effect of the COL fibrils, the water associated with the COL fibrils, or the intrafibrillar (IF) water, is inaccessible to the large PG molecules [5]. This IF water exclusion results in a higher effective FCD and π_{PG} for the constructs with COL+PG compared to constructs with only PG. Thus, even with similar GAG concentrations, the presence and level of COL content in an engineered construct can alter the amount of PG contribution to the compressive

properties. Additionally, as COL plays an important role in restraining the π_{PG} in native cartilage, methods to increase COL content and to improve the COL:GAG ratio would be important in improving the biochemical composition and mechanical function of the engineered constructs.

The retention of most of the initial matrix content in the constructs after compaction and subsequent mechanical testing (see Appendix F) suggests that most of the compaction was due to fluid loss. In typical cell-based engineered constructs, the constructs tend to be highly hydrated with over 80% water content [30], due to the limited restraining forces provided by the low COL content, and result in compressive modulus only on the order of tens of kPa [24, 32]. Recently, efforts to improve construct mechanical properties by selective enzymatic degradation of PG in engineered constructs after weeks of culture have decreased the water content of the engineered tissue along with an increase in COL concentration [6, 30]. Others include cell-mediated compaction or contraction of the scaffold, which may increase the mechanical strength of the material but typically are associated with more fibroblastic phenotypes [15, 26, 45]. Other approaches include functionalizing the scaffold or composing the scaffold wholly with the desired matrix proteins [12, 34, 46], which increase the initial matrix concentration of the construct. Here, an 80% increase in COL concentration was achieved rapidly in a few days by a matrix assembly and mechanical dehydration method, demonstrating the utility of this time-saving approach.

During mechanical compaction, the gel network of the agarose constructs may have undergone restructuring with compaction since the constructs did not recover to

their initial thicknesses. The swelling of the PG-containing constructs (Groups II and IV) beyond the thickness of agarose only or COL-containing constructs (Groups I and III) after compaction indicates the presence of swelling pressure exerted by PG that was restrained with the increased thickness in the agarose gel network. A mechanism for providing higher restraining force with a smaller increase in construct thickness after compaction may be useful in further retention of the compacted state of the constructs and to further increase the matrix concentrations.

The compaction of the construct altered its geometry (i.e. thickness) and has the potential to be coupled with applying more complex three-dimensional shape to the constructs (Fig. 5.9). The surface congruity of an implanted graft to the surrounding native cartilage has been shown to be important in the viability of such constructs [25] and likely for tissue engineered constructs as well. Recently there have been efforts to shape cartilaginous constructs using molding techniques [16, 21, 48]. Using molds with anatomical contours, the compaction method has the potential to mechanically impose a shape to the constructs or further maintain and improve the shaping fidelity of an already shaped constructs, which may facilitate fabrication of grafts for large cartilage defects with complex surface contours.

Maintenance of high cell viability in compacted constructs demonstrates that the compaction method can be extended to cell-containing constructs. The cell-associated matrix on the alginate-recovered chondrocytes may have acted as a protective layer against the compressive and fluid shear stresses during compaction [3, 33]. While the present study involved short-term culture of constructs containing immature chondrocytes, a longer-term culture and use of different cell types may

further elucidate the effect of compaction and addition of native ECM components in tissue-engineered constructs.

The compaction of cartilaginous constructs with the appropriate COL:GAG ratio at a fraction of the targeted concentration may allow for rapidly achieving a more physiological matrix concentration. Working with lower concentration of COL and PG will allow for extracellular matrix manipulations at more manageable concentrations, as high concentrations of PG are very viscous and difficult to handle. The typical COL:GAG ratios found in engineered constructs are 1:1 or less, which is far below those found in native tissue of 3-4:1 in bovine calf and adult cartilage [49] and 3-10:1 human adult cartilage [2, 42]. Thus, pre-assembling of an engineered construct with a more physiological COL:GAG ratio and compacting to increased matrix concentrations may lead to rapid fabrication of a more mechanically functional engineered construct for treatment of articular cartilage defects.

The compaction method described here has the potential to significantly reduce the time to fabricate mechanically functional cartilaginous constructs. Typical tissue engineering methods requires weeks if not months of culture for the resident cells to produce enough extracellular matrix. Such constructs may not initially contain the appropriate balance of COL to PG or enough of matrix molecules, presence of which are known to foster chondrogenic phenotypes and cell compatibility [1, 9, 44]. Previous works have noted changes in rates of COL fibril formation in the presence of PG, highlighting the challenges in tissue engineered constructs to increase COL content when there is already a high PG content present [27, 35, 40, 43]. Thus, adding

pre-formed macromolecular units into the constructs, such as COL fibrils and PG aggregates, may circumnavigate these limitations.

The methods presented here may provide a new assembly paradigm for cartilage tissue engineering (Fig. 5.9). The matrix macromolecules first can be pre-assembled into PG aggregates and fibrillar COL (Fig. 5.9A) and then mixed into an appropriate COL:GAG ratio to form a hyper-hydrated construct (Fig. 5.9B). Such constructs can undergo mechanical dehydration by compaction to squeeze out excess fluid (Fig. 5.9C) and can be shaped into an appropriate physiological contour, in sequence or simultaneously (Fig. 5.9D). This assembly approach may facilitate a more rapid engineering of mechanically functional cartilaginous constructs that are ready for implantation into a cartilage defect to re-establish joint function.

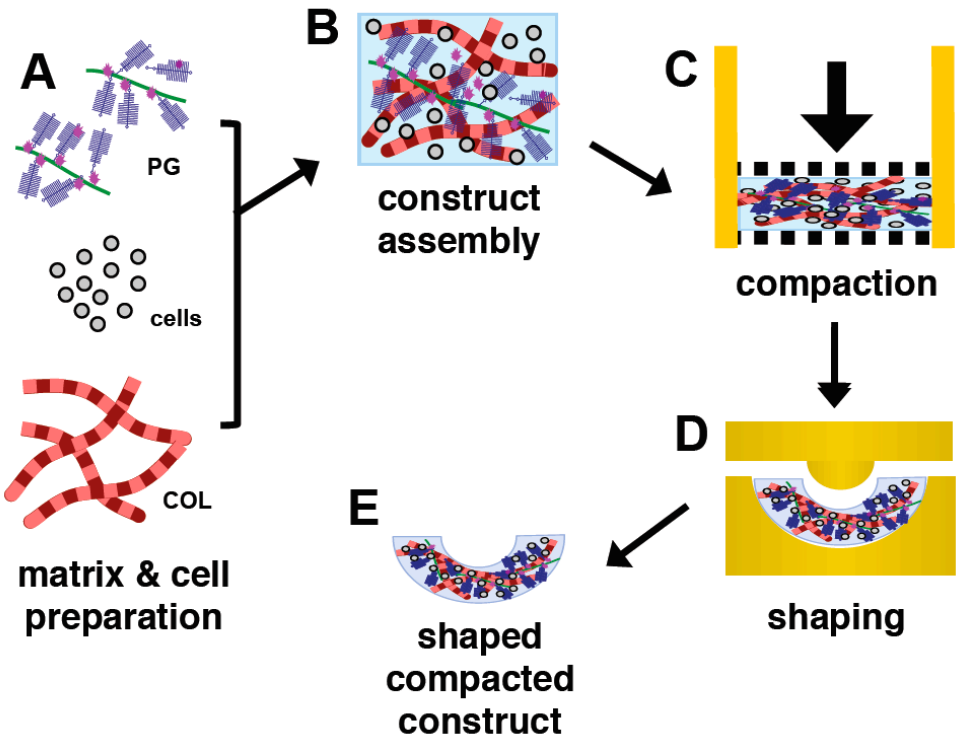

Figure 5.9: Schematic of application of matrix and cell preparation (A), matrix assembly in constructs (B), compaction (C), and shaping (D, E) methods for rapid engineering of cartilaginous constructs

5.6 Acknowledgments

The dissertation author is the primary investigator and thanks co-authors, Chenghao “Charles” Ge, Dr. Albert C. Chen, Barbara L. Schumacher, and Dr. Robert L. Sah for their contributions to this work. This work was supported by National Institutes of Health, National Science Foundation, and a grant to University of California-San Diego, in support of Prof. Robert Sah, from the Howard Hughes Medical Institute through the HHMI Professors Program. Additional support was received from a NSF Graduate Research Fellowship (EHH).

5.7 References

1. Aigner T, Stove J: Collagens-major component of the physiological cartilage matrix, major target of cartilage degeneration, major tool in cartilage repair. *Adv Drug Deliv Rev* 55:1569-93, 2003.

2. Akizuki S, Mow VC, Muller F, Pita JC, Howell DS, Manicourt DH: Tensile properties of human knee joint cartilage: I. influence of ionic conditions, weight bearing, and fibrillation on the tensile modulus. *J Orthop Res* 4:379-92, 1986.

3. Alexopoulos LG, Setton LA, Guilak F: The biomechanical role of the chondrocyte pericellular matrix in articular cartilage. *Acta Biomater* 1:317-25, 2005.

4. Asanbaeva A, Tam J, Schumacher BL, Klisch SM, Masuda K, Sah RL: Articular cartilage tensile integrity: Modulation by matrix depletion is maturation-dependent. *Arch Biochem Biophys* 474:175-82, 2008.

5. Basser PJ, Schneiderman R, Bank RA, Wachtel E, Maroudas A: Mechanical properties of the collagen network in human articular cartilage as measured by osmotic stress technique. *Arch Biochem Biophys* 351:207-19, 1998.

6. Bian L, Crivello KM, Ng KW, Xu D, Williams DY, Ateshian GA, Hung CT: Influence of Temporary Chondroitinase ABC-Induced Glycosaminoglycan Suppression on Maturation of Tissue-Engineered Cartilage. *Tissue Eng Part A*, 2009.

7. Buckwalter JA, Mankin HJ: Articular cartilage. Part I: tissue design and chondrocyte-matrix interactions. *J Bone Joint Surg Am* 79-A:600-11, 1997.

8. Buckwalter JA, Mankin HJ: Articular cartilage. Part II: degeneration and osteoarthrosis, repair, regeneration, and transplantation. *J Bone Joint Surg Am* 79-A:612-32, 1997.

9. Chang CH, Liu HC, Lin CC, Chou CH, Lin FH: Gelatin-chondroitin-hyaluronan tri-copolymer scaffold for cartilage tissue engineering. *Biomaterials* 24:4853-8, 2003.

10. Chen AC, Masuda K, Nakagawa K, Wong VW, Pfister BE, Thonar EJ, Sah RL: Tissue engineered cartilage from adult human chondrocytes: biomechanical properties and function-composition relationships. *Trans Orthop Res Soc* 28:945, 2003.

11. Chen AC, Nguyen TT, Sah RL: Streaming potentials during the confined compression creep test of normal and proteoglycan-depleted cartilage. *Ann Biomed Eng* 25:269-77, 1997.

12. Elder BD, Eleswarapu SV, Athanasiou KA: Extraction techniques for the decellularization of tissue engineered articular cartilage constructs. *Biomaterials* 30:3749-56, 2009.

13. Farndale RW, Buttle DJ, Barrett AJ: Improved quantitation and discrimination of sulphated glycosaminoglycans by use of dimethylmethylene blue. *Biochim Biophys Acta* 883:173-7, 1986.

14. Frank EH, Grodzinsky AJ, Koob TJ, Eyre DR: Streaming potentials: a sensitive index of enzymatic degradation in articular cartilage. *J Orthop Res* 5:497-508, 1987.

15. Galois L, Hutasse S, Cortial D, Rousseau CF, Grossin L, Ronziere MC, Herbage D, Freyria AM: Bovine chondrocyte behaviour in three-dimensional type I collagen gel in terms of gel contraction, proliferation and gene expression. *Biomaterials* 27:79-90, 2006.

16. Han EH, Bae WC, Hsieh-Bonassera ND, Wong VW, Schumacher BL, Gortz S, Masuda K, Bugbee WD, Sah RL: Shaped, stratified, scaffold-free grafts for articular cartilage defects. *Clin Orthop Relat Res* 466:1912-20, 2008.

17. Han EH, Chen SS, Klisch SM, Sah RL: Proteoglycan osmotic swelling pressure contribution to compressive properties of articular cartilage. *submitted.*

18. Han EH, Wilensky LM, Schumacher BL, Chen AC, Masuda K, Sah RL: Tissue engineering by molecular disassembly and reassembly: biomimetic retention of mechanically functional aggrecan in hydrogel. *Tissue Eng Part C Methods* 16:1471-9, 2010.

19. Heinegard D, Sommarin Y: Isolation and characterization of proteoglycans. *Methods Enzymol* 144:305-19, 1987.

20. Hsieh-Bonassera ND, Wu I, Lin JK, Schumacher BL, Chen AC, Masuda K, Bugbee WD, Sah RL: Expansion and redifferentiation of chondrocytes from osteoarthritic cartilage: cells for human cartilage tissue engineering. *Tissue Eng Part A* 15:3513-23, 2009.

21. Hung CT, Lima EG, Mauck RL, Taki E, LeRoux MA, Lu HH, Stark RG, Guo XE, Ateshian GA: Anatomically shaped osteochondral constructs for articular cartilage repair. *J Biomech* 36:1853-64, 2003.

22. Klein TJ, Malda J, Sah RL, Hutmacher DW: Tissue engineering of articular cartilage with biomimetic zones. *Tissue Eng Part B* 15:143-57, 2009.

23. Klein TJ, Schumacher BL, Blewis ME, Schmidt TA, Voegtline MS, Thonar EJ-MA, Masuda K, Sah RL: Tailoring secretion of proteoglycan 4 (PRG4) in tissue-engineered cartilage. *Tissue Eng* 12:1429-39, 2006.

24. Klein TJ, Schumacher BL, Schmidt TA, Li KW, Voegtline MS, Masuda K, Thonar EJ-MA, Sah RL: Tissue engineering of stratified articular cartilage from chondrocyte subpopulations. *Osteoarthritis Cartilage* 11:595-602, 2003.

25. Koh JL, Wirsing K, Lautenschlager E, Zhang LO: The effect of graft height mismatch on contact pressure following osteochondral grafting. A biomechanical study. *Am J Sports Med* 32:317-20, 2004.

26. Lee CR, Breinan HA, Nehrer S, Spector M: Articular cartilage chondrocytes in type I and type II collagen-GAG matrices exhibit contractile behavior in vitro. *Tissue Eng Part B Rev* 6:555-65, 2000.

27. Lowther DA, Natarajan M: The influence of glycoprotein on collagen fibril formation in the presence of chondroitin sulphate proteoglycan. *The Biochemical journal* 127:607-8, 1972.

28. Maroudas A: Balance between swelling pressure and collagen tension in normal and degenerate cartilage. *Nature* 260:808-9, 1976.

29. Masuda K, Sah RL, Hejna MJ, Thonar EJ-MA: A novel two-step method for the formation of tissue-engineered cartilage by mature bovine chondrocytes: the alginate-recovered-chondrocyte (ARC) method. *J Orthop Res* 21:139-48, 2003.

30. Natoli RM, Responte DJ, Lu BY, Athanasiou KA: Effects of multiple chondroitinase ABC applications on tissue engineered articular cartilage. *J Orthop Res* 27:949-56, 2009.

31. Ng KW, Kugler LE, Doty SB, Ateshian GA, Hung CT: Scaffold degradation elevates the collagen content and dynamic compressive modulus in engineered articular cartilage. *Osteoarthritis Cartilage* 17:220-7, 2009.

32. Ng KW, Saliman JD, Lin EY, Statman LY, Kugler LE, Lo SB, Ateshian GA, Hung CT: Culture Duration Modulates Collagen Hydrolysate-Induced Tissue Remodeling in Chondrocyte-Seeded Agarose Hydrogels. *Ann Biomed Eng* 35:1914-23, 2007.

33. Ng L, Hung HH, Sprunt A, Chubinskaya S, Ortiz C, Grodzinsky A: Nanomechanical properties of individual chondrocytes and their developing

growth factor-stimulated pericellular matrix. *Journal of biomechanics* 40:1011-23, 2007.

34. Nicodemus GD, Bryant SJ: Cell encapsulation in biodegradable hydrogels for tissue engineering applications. *Tissue engineering Part B, Reviews* 14:149-65, 2008.

35. Oegema TR, Laidlaw J, Hascall VC, Dziewiatkowski DD: The effect of proteoglycans on the formation of fibrils from collagen solutions. *Arch Biochem Biophys* 170:698-709, 1975.

36. Roughley PJ: The structure and function of cartilage proteoglycans. *Eur Cell Mater* 12:92-101, 2006.

37. Sah RL, Grodzinsky AJ, Plaas AH, Sandy JD: Effects of tissue compression on the hyaluronate-binding properties of newly synthesized proteoglycans in cartilage explants. *Biochem J* 267:803-8, 1990.

38. Sajdera SW, Hascall VC: Proteinpolysaccharide complex from bovine nasal cartilage. A comparison of low and high shear extraction procedures. *J Biol Chem* 244:77-87, 1969.

39. Scott JE, Dorling J: Differential staining of acid glycosaminoglycans (mucopolysaccharides) by alcian blue in salt solutions. *Histochemie* 5:221-33, 1965.

40. Stuart K, Panitch A: Influence of chondroitin sulfate on collagen gel structure and mechanical properties at physiologically relevant levels. *Biopolymers* 89:841-51, 2008.

41. Tang L-H, Rosenberg L, Reeiner A, Poole AR: Proteoglycans from bovine nasal and articular cartilage: properties of a soluble form of link protein. *J Biol Chem* 254:10523-31, 1979.

42. Temple MM, Bae WC, Chen MQ, Lotz M, Amiel D, Coutts RD, Sah RL: Age- and site-associated biomechanical weakening of human articular cartilage of the femoral condyle. *Osteoarthritis Cartilage* 15:1042-52, 2007.

43. Toole BP, Lowther DA: The effect of chondroitin sulphate-protein on the formation of collagen fibrils in vitro. *The Biochemical journal* 109:857-66, 1968.

44. Varghese S, Hwang NS, Canver AC, Theprungsirikul P, Lin DW, Elisseeff J: Chondroitin sulfate based niches for chondrogenic differentiation of mesenchymal stem cells. *Matrix Biology* 27:12-21, 2008.

45. Veilleux NH, Yannas IV, Spector M: Effect of passage number and collagen type on the proliferative, biosynthetic, and contractile activity of adult canine

articular chondrocytes in type I and II collagen-glycosaminoglycan matrices in vitro. *Tissue Eng Part B Rev* 10:119-27, 2004.

46. Vinatier C, Mrugala D, Jorgensen C, Guicheux J, Noel D: Cartilage Engineering: A Crucial Combination of Cells, Biomaterials and Biofactors. *Trends Biotechnol* 27:307-14, 2009.

47. Vunjak-Novakovic G, Martin I, Obradovic B, Treppo S, Grodzinsky AJ, Langer R, Freed LE: Bioreactor cultivation conditions modulate the composition and mechanical properties of tissue-engineered cartilage. *J Orthop Res* 17:130-9, 1999.

48. Williams GM, Lin JW, Sah RL: Cartilage reshaping via in vitro mechanical loading. *Tissue Eng Part B Rev* 13:2903-11, 2007.

49. Williamson AK, Chen AC, Sah RL: Compressive properties and function-composition relationships of developing bovine articular cartilage. *J Orthop Res* 19:1113-21, 2001.

50. Woessner JF: The determination of hydroxyproline in tissue and protein samples containing small proportions of this imino acid. *Arch Biochem Biophys* 93:440-7, 1961.

CHAPTER 6

CONCLUSIONS

6.1 Summary of Findings

The overall motivation of this dissertation was to contribute to the engineering of mechanically functional aggrecan-laden cartilaginous grafts by elucidating the roles of proteoglycans and its interaction with collagen to the compressive properties of articular cartilage and developing novel methods for shaping, assembling, and concentrating matrix-laden cartilaginous constructs. Specifically, the objectives of this work were to 1) to develop a novel combination of molding and stratification to form a cartilaginous graft of appropriate three-dimensional shape, 2) to elucidate the role of aggrecan and its interaction with collagen in the compressive biomechanical properties of native articular cartilage, as it varies with age and depth, 3) to develop engineered constructs with tunable aggrecan retention by *in vitro* assembly, and 4) to present a mechanical compaction method to enhance the extracellular matrix content of engineered constructs.

The application of a more defined FCD_{EF}–π_{PG} relationship to native cartilage demonstrated that FCD_{EF} and π_{PG} change with growth, age and depth of the tissue (Chapter 3). Accounting for CS:KS variation and exclusion of collagen IF water

appeared to accurately predict π_{PG} for bovine and human cartilage of various stages and depth under compression. Even with similar GAG/WW, mature cartilage from bovine calf, adult and human young sources had higher FCD_{EF} and π_{PG} than immature (bovine fetal) or normal aged (human old) tissue due to COL content variations, and this effect was amplified with compression. The π_{PG} were close to σ_{EQ} in all bovine cartilage in development and human Young cartilage but only approximated half of σ_{EQ} in the human Old cartilage, suggesting a larger collagen role in compression in Old cartilage. The strain, FCD_{EF}, π_{PG}, and σ_{CN} profiles revealed depth-related variations in human cartilage that changed significantly with aging, which suggest a loss of a functional superficial layer in macroscopically normal old cartilage. These results demonstrate that the FCD_{EF}–π_{PG} relationship defined here can provide a powerful tool in studying PG contribution to the biomechanical properties of cartilage with development, age, and depth based on biochemical data. These findings in native tissue provided the motivation for novel methods of assembly cells and matrix components in engineered constructs to modulate shape, AGC retention, and matrix content.

In treatment of larger cartilage defects with more complex surface contours, the shape of the implanted graft and its match with the surrounding native cartilage is important to the success of such graft. Building on previously described alginate-recovered chondrocyte (ARC) method to fabricate stratified, scaffold-free constructs, a combination of a molding technique with the stratification method was applied to fabricate cartilaginous constructs with appropriate three-dimensional shape and structure (Chapter 2). The shaped constructs in saucer and cup shapes with one and

two surfaces molded, respectively, had surface contours that were different from those of the control disk constructs and from each other with distinct radii of curvature. These results demonstrate molding fabrication can generate constructs that are shaped and fabricated from only chondrocytes and their biosynthetic products. While the matrix products accumulated fairly similarly regardless of the shape of the construct, demonstrating the shaping does not adversely affect chondrocyte functions, the GAG and COL content were far below those found in native cartilage, approximately 2 fold lower for GAG/WW and 20 fold for COL/WW. Additionally, this molding technique was adapted to create shaped cartilaginous constructs with biomimetic stratification of superficial zone chondrocyte atop middle/deep zone chondrocytes. These shaped cartilaginous constructs with biomimetic stratification demonstrate the potential to facilitate treatment of larger cartilage defects where recreation of surface contour is important.

To address one of the challenges in cartilage tissue engineering of low matrix content as compared to native tissue, an assembly approach to rapidly build up matrix content was taken. Addition of assembled PG aggregates, consisting of AGC with hyaluronan and link proteins, to hydrogel constructs increased AGC retention, increased the construct compressive properties, and maintained chondrogenic phenotype (Chapter 4). Cartilaginous constructs were created by biomimetically harnessing the biochemical processes to assemble one of the key functional constituents of the native cartilage, the PG aggregate. Biomimetic molecular reassembly of AGC with HA ± LP enhanced the AGC retention in hydrogel constructs in a dose dependent manner for HA, and this enhanced retention resulted in increased

compressive stiffness of the constructs. Additionally, chondrocytes in the PG-containing constructs were able to maintain chondrogenic function after a short-term culture, secreting type II collagen but little type I collagen. Thus, the concept of a matrix reassembly approach is feasible for the engineering of cartilaginous tissue and can be extended to collagen to achieve a more physiological COL:GAG ratio that are associated with improved mechanical properties than in typical cell-based engineered constructs.

To further enhance the matrix density, especially the COL:GAG ratio, and the construct mechanical properties, a mechanical compaction method was applied to the constructs containing pre-assembled matrix of collagen and PG aggregates. The mechanical compaction method rapidly increased the COL and PG concentrations in the constructs, and the compacted constructs had higher compressive mechanical properties than the construct before compaction (Chapter 5). Presence of COL+PG improved the compressive properties of hydrogel constructs compared to constructs with either PG or COL alone, highlighting the importance of the interaction between PG and COL to tissue mechanical properties discussed in Chapter 3. The compacted constructs had higher compressive stiffness than the initial constructs before compaction. These results support the general concept that that mechanical compaction method may provide cartilaginous constructs with rapidly increased extracellular matrix concentrations and with higher compressive properties.

6.2 Future Directions

The extension of the FCD_{EF}–π_{PG} model developed here to study depth-varying properties of developing cartilage and degenerating cartilage as well as cartilage from various sites may provide further insight into cartilage biomechanics and role of matrix components and organization in its mechanical function. Immature cartilage is typically described and modeled as fairly isotropic tissue compared to more mature cartilage with less distinct zonal properties such as GAG content variations and collagen orientation [6, 14]. As such, the FCD_{EF} and π_{PG} of such immature tissues may show a more tempered depth variations than more developed tissues [7]. In such tissues, the contribution of collagen to compressive properties may be different in magnitude or in its variation with depth due to lower collagen concentration and less organized and less crosslinked network. In degeneration, the tensile properties of such tissues are known to decrease in all layers along with increased collagen degradation [13]. For such degenerated cartilage, the strain, FCD_{EF}, π_{PG}, and σ_{CN} profiles with depth of may vary significantly from normal cartilage, and the differences may further elucidate the mechanical failures in such tissues and provide insight into the mechanobiology of diseased tissues and possible mechanical mechanisms of degeneration. The FCD_{EF}–π_{PG} model also can be used along with experiments at low strains to further elucidate the mechanisms of strain softening that have been observed [2, 11].

Further modeling of the transport of aggrecan within a hydrogel may provide design criteria for the appropriate pore size of the matrix, which may be a collagenous

matrix, to enhance aggrecan retention whether in monomeric form or in aggregate form. In order to model this appropriately, the reaction rates of aggrecan, HA, and link protein, in pairs or in a combination of all three, binding needs to be further elucidated.

Agarose was used in these studies as a hydrogel to hold together the extracellular matrix components together into constructs. While agarose provides an excellent and clean system to study proof of concepts and various biochemical, biomechanical, and biophysical responses to the applied stimuli of shaping, compaction or assembly, the use of native matrix components as the sole scaffold would be more desirable as it more closely mimics the native tissue.

There are a number of efforts underway to study the application of decellularized matrix, either as an intact tissue scaffold or as milled powders or gels, as tissue engineering scaffolds, exploiting the native scaffold proteins components and structural organization [4]. For larger decellularized tissue scaffolds, cells may have difficulties migrating into the scaffold in order facilitate repair and healing [12]. These scaffolds usually maintain the various endogenous chemokines and growth factors through the preparation process. While this may be favorable in providing the cells a nutrient-rich milieu to differentiate and growth, the batch-to-batch variations with such scaffold and the lack of precise control of content and assembly may provide potential challenges to widely and rapidly translating such technologies.

The development of native extracellular matrix components as the sole scaffold is would be useful in an assembly approach to cartilage tissue engineering. The two main matrix components of cartilage, proteoglycans and collagens, have been

recombinantly expressed and produced [5, 8, 9], and may provide a more reliable and more reproducible scaffold sources combined with the methods presented here. Alternatively, the matrix molecules can be extracted and purified from either from tissue sources or a large cell culture, as proteoglycan aggregate components (AGC, HA, and link proteins) and collagen tropocollagen are secreted matrix products. Harnessing the ability of the matrix components to assemble into higher order structures extracellularly in absence of cells [1, 10] would be useful in fabrication of scaffolds containing only native matrix components. Upon the fabrication of such constructs, the methods discussed in this dissertation such as shaping and compaction can be applied for a more mechanically robust and more biomimetically structured construct.

The combination of the methods presented here may provide a new assembly paradigm for cartilage tissue engineering (Fig. 6.1). The matrix macromolecules first can be pre-assembled into PG aggregates and fibrillar collagens and then mixed into an appropriate COL:GAG ratio to form a hyper-hydrated construct. Such constructs can undergo mechanical dehydration by compaction to squeeze out excess fluid and can be shaped into an appropriate physiological contour, in sequence or simultaneously. This assembly approach may facilitate a more rapid engineering of mechanically functional cartilaginous constructs that are ready for implantation into a cartilage defect to re-establish joint function.

The application of the mechanical compaction method to constructs containing chondrocytes may be useful. A preliminary compaction study using a 1% agarose construct with freshly isolated chondrocytes and 2 mg/ml aggrecan with 5% HA

indicated that the chondrocytes remained viable and maintained biosynthetic activity for days after compaction. Alternatively, alginate recovered chondrocyte (ARC) may be used as these cells are more protected by their accumulated pericellular matrix.

Cartilaginous constructs with the appropriate COL:GAG ratio at a fraction of the targeted concentration may be mechanically compacted to rapidly achieve a more physiological matrix concentration. This will allow for extracellular matrix manipulations at more manageable concentrations, as high concentrations of PG are very viscous and difficult to handle. Since the typical COL:GAG ratios found in engineered constructs range from 1:3 to 1:1, which is far below those found in native tissue of 4:1 in bovine calf and adult cartilage [14] and 10:1 human adult cartilage [3], pre-setting an engineered construct to a more physiological COL:GAG ratio and compacting to increased matrix concentrations may lead to a more mechanically functional engineered construct for treatment of articular cartilage defects.

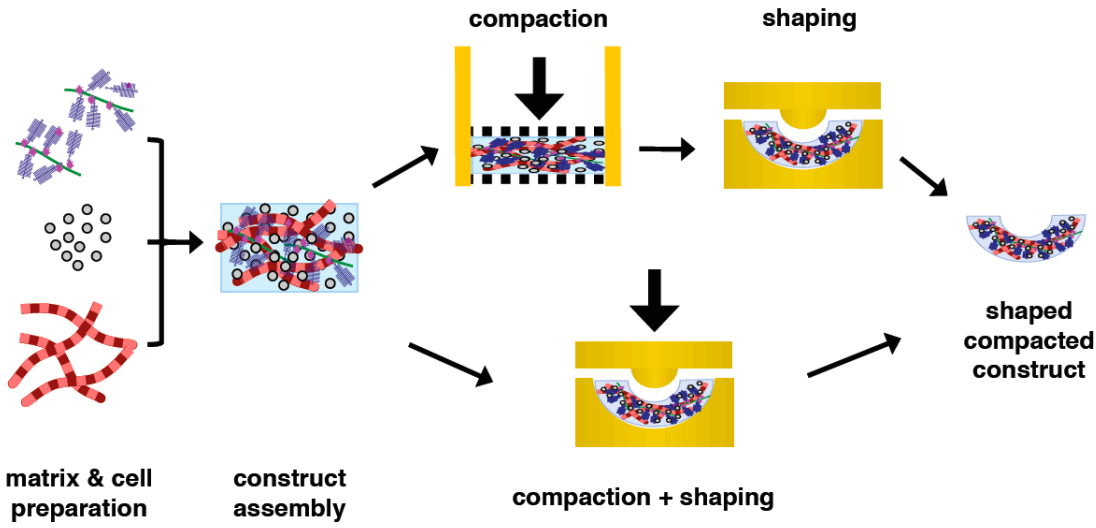

Figure 6.1: Schematic of application of matrix assembly, compaction, and shaping methods for rapid engineering of cartilaginous constructs

6.3 References

1. Bayliss MT, Howat S, Davidson C, Dudhia J: The organization of aggrecan in human articular cartilage. Evidence for age-related changes in the rate of aggregation of newly synthesized molecules. *J Biol Chem* 275:6321-7, 2000.

2. Chahine NO, Wang CC, Hung CT, Ateshian GA: Anisotropic strain-dependent material properties of bovine articular cartilage in the transitional range from tension to compression. *J Biomech* 37:1251-61, 2004.

3. Falcovitz YH. Compressive properties of normal human articular cartilage: age, depth and compositional dependencies [M.S.]. La Jolla: University of California, San Diego; 2000.

4. Gilbert TW, Sellaro TL, Badylak SF: Decellularization of tissues and organs. *Biomaterials* 27:3675-83, 2006.

5. Grover J, Roughley PJ: The expression of functional link protein in a baculovirus system: analysis of mutants lacking the A, B and B' domains. *Biochem J* 300 (Pt 2):317-24, 1994.

6. Julkunen P, Harjula T, Iivarinen J, Marjanen J, Seppanen K, Narhi T, Arokoski J, Lammi MJ, Brama PA, Jurvelin JS, Helminen HJ: Biomechanical, biochemical and structural correlations in immature and mature rabbit articular cartilage. *Osteoarthritis Cartilage* 17:1628-38, 2009.

7. Klein TJ, Chaudhry M, Bae WC, Sah RL: Depth-dependent biomechanical and biochemical properties of fetal, newborn, and tissue-engineered articular cartilage. *J Biomech* 40:182-90, 2007.

8. Miwa HE, Gerken TA, Huynh TD, Flory DM, Hering TM: Mammalian expression of full-length bovine aggrecan and link protein: formation of recombinant proteoglycan aggregates and analysis of proteolytic cleavage by ADAMTS-4 and MMP-13. *Biochim Biophys Acta* 1760:472-86, 2006.

9. Nokelainen M, Helaakoski T, Myllyharju J, Notbohm H, Pihlajaniemi T, Fietzek PP, Kivirikko KI: Expression and characterization of recombinant human type II collagens with low and high contents of hydroxylysine and its glycosylated forms. *Matrix Biol* 16:329-38, 1998.

10. Notbohm H, Nokelainen M, Myllyharju J, Fietzek PP, Muller PK, Kivirikko KI: Recombinant human type II collagens with low and high levels of hydroxylysine and its glycosylated forms show marked differences in fibrillogenesis in vitro. *J Biol Chem* 274:8988-92, 1999.

11. Schinagl RM, Gurskis D, Chen AC, Sah RL: Depth-dependent confined compression modulus of full-thickness bovine articular cartilage. *J Orthop Res* 15:499-506, 1997.

12. Secretan C, Bagnall KM, Jomha NM: Effects of introducing cultured human chondrocytes into a human articular cartilage explant model. *Cell Tissue Res* 339:421-7.

13. Temple-Wong MM, Bae WC, Chen MQ, Bugbee WD, Amiel D, Coutts RD, Lotz M, Sah RL: Biomechanical, structural, and biochemical indices of degenerative and osteoarthritic deterioration of adult human articular cartilage of the femoral condyle. *Osteoarthritis Cartilage* 17:1469-76, 2009.

14. Williamson AK, Chen AC, Sah RL: Compressive properties and function-composition relationships of developing bovine articular cartilage. *J Orthop Res* 19:1113-21, 2001.

APPENDIX A

TITLE DETERMINATION OF FCD AND TRUE CS AND KS VALUES FROM BIOCHEMICAL ASSAYS

A.1 Introduction

FCD_{EF} can be defined using molecular weights of CS (MW_{CS}) and KS (MW_{KS}) in g/mol, weights of CS (m_{CS}) and KS (m_{KS}) in grams, mol-charges of CS and KS (z_{CS}, z_{KS}), and EF water ($m_{EF,H2O}$) in grams. Equation 1 for FCD_{EF} can be re-written in terms of moles of CS and KS (mol_{CS}, mol_{KS}), where $mol_{CS} = m_{CS}/ MW_{CS}$, with extrafibrillar water ($m_{EF,H2O}$) and mol-charges of CS and KS (z_{CS}, z_{KS}), as follows:

$$FCD_{EF} = \frac{\left(mol_{CS} * z_{CS}\right) + \left(mol_{KS} * z_{KS}\right)}{m_{EF,H2O}} * \frac{1000\text{mEq}}{1\text{mol} - \text{charge}} \qquad \text{(A1)}$$

This also can be written in terms of extrafibrillar concentrations of CS and KS ($c_{CS,EF}$, $c_{KS,EF}$) where $c_{CS,EF} = m_{CS}/ m_{EF,H2O}$, as:

$$FCD_{EF} = \left(\left(c_{CS,EF} * \frac{z_{CS}}{MW_{CS}}\right) + \left(c_{KS,EF} * \frac{z_{KS}}{MW_{KS}}\right)\right) * \left(\frac{1000\text{mEq}}{1\text{mol} - \text{charge}}\right) \qquad \text{(A2)}$$

The methods used to estimate the weights of CS (m_{CS}) and KS (m_{KS}) should be carefully considered to make sure that the estimations are correct. The two common

methods of GAG estimations are dimethylmethylene blue (DMMB) assay, usually using a standard of sodium salts of chondroitin sulfate, and uronic acid assay, typically using glucuronolactone as the standard.

A.2 Adjustments for DMMB Assay

The use of sodium salts of CS, such as shark cartilage CS, (Sigma, product number: C4384) in DMMB assay standards requires accounting for the differences in the CS sodium salts and the CS and KS chains in the sample. Some considerations include the weight contributions from 1) contaminants in the sodium CS salt, including extra sodium ions and water, 2) hydrogens on the sulfate and carboxyl groups that may be missing depending on the pH of the solvent, and 3) the glycosidic linkages, which result in the loss of one H_2O molecule between two CS disaccharides, that become more important with the length of GAG chains. The mol-charge differences between CS and KS also should be considered.

From the NCBI PubChem database, CS sodium salt from Sigma (compound ID 23679063, SID 24892689) has a molecular weight of 499.37695 g/mol based on a molecular formula of $C_{14}H_{22}NNaO_{15}S$, with the carboxyl group containing a H and one sodium salt interacting with the sulfate group (Table A1). However, this sodium CS salt usually is found in a long chain of disaccharides in the compound as the average molecular weight of the CS-6 from shark cartilage (Miles Laboratories) has been estimated to be ~63 kDa by PAGE, or ~130 disaccharides [6]. Thus, most of the CS disaccharides in the sodium CS salt are lacking the water molecule that is lost with

glycosidic linkages. From the Certificate of Analysis from Sigma, the CS sodium salt typically also contains some impurities (~14-15%), including ~6-7% water (certificate of analysis and [3]). The purity of the CS in sodium CS salt as assessed by FT-NMR is typically ~85%, accounting for CS without the sodium, as sodium is considered an impurity and present at a higher than 1:1 molar ratio with the CS disaccharide (closer to 1 part CS:1.6 Na). Thus, the molecular weight of the CS in the CS salt (MW_{NaCS}) is closer to 458.37 g/mol = 499.37695 – 18.015 (from a water molecule) – 22.99 (from sodium salt).

The CS disaccharide found in a CS chain in cartilage is given by the formula of $C_{14}H_{19}NO_{14}S$, less one sodium, one hydrogen (from carboxyl group), and one water molecule (from glycosidic linkages) compared to the molecular structure for sodium CS salt (PubChem database) (Table A1). The carboxyl group is typically charged at physiological pH as carboxyl group in CS has a very low pKa ~3.6. Thus, the CS disaccharide found in a chain of CS has a molecular weight of 457.36 g/mol given by its molecular formula.

Calculated in a likewise fashion, the keratan sulfate disaccharide in a KS chain in cartilage is given by the formula of $C_{14}H_{22}NO_{13}S$ and a molecular weight of 444.39 g/mol (Table A1).

Previous works noted the MW of CS and KS to be 513 and 464, respectively [3, 7, 9] but did not note the impurities that may be present in the CS Na salt in the standards if DMMB assay was performed.

Typically, DMMB assay is used to detect sulfated GAG, such as CS and KS, in cartilage samples by a charge-based colorimetric reaction with the standards

containing sodium CS salt. Due to the impurities in sodium CS salt and differences in molecular weight amongst sodium CS salt, CS, and KS and the charge difference between CS and KS, conversions need to be performed to obtain an accurate FCD and amounts of CS and KS in the sample.

The conversion between the mass of sodium CS salt from DMMB assay ($m_{NaCS,\ DMMB}$) into moles is as follows:

$(k*m_{NaCS,\ in\ DMMB}) / MW_{NaCS}$ = moles of CS from DMMB assay (A3)

where k = % (w/w) of CS in NaCS salt used (~0.85)

This can be used directly to calculated FCD as follows:

FCD_{EF} = (moles of CS from DMMB assay/$m_{EF,H2O}$)*(2 mol-charge/mol CS)*(1000 mEq/1 mol-charge) (A4)

FCD_{EF} = (($k*m_{NaCS,\ DMMB}$)/MW_{NaCS}/$m_{EF,H2O}$)*(2 mol-charge/mol CS)*(1000 mEq/1 mol-charge) (A5)

For a sample containing both CS and KS in molar proportion of x and y, where x = moles of CS/(moles of CS + moles of KS) and y = moles of KS/(moles of CS + moles of KS) and x+y=1,

mole of CS in DMMB assay = (1/x)*mole of CS + (1/2y)*mole of KS (A6)

moles of CS = [x/(x+0.5*y)]*moles of CS in DMMB assay (A7)

moles of KS = [y/(x+0.5*y)]*moles of CS in DMMB assay (A8)

These moles can be used directly to calculate FCD or mass of CS and KS.

m_{CS} = moles of CS * MW_{CS} = [x/(x+0.5*y)]* moles of CS in DMMB * MW_{CS} (A9)

$$m_{KS} = \text{moles of KS} * MW_{KS} = [y/(x+0.5*y)]* \text{moles of CS in DMMB} * MW_{KS} \quad \text{(A10)}$$

A.3 Adjustments for Uronic Acid Assay

The uronic acid assay as first described by Dische [5] and later improved by Bitter and Muir [1] uses its reaction with carbazole to colorimetrically detect the uronic acid. In this assay, the glycosaminoglycans are broken into monosaccharides by sulfuric acid and heat, and carbazole is added for colorimetric reaction. This assay typically uses glucuronolactone ($C_6H_8O_6$, MW = 176.124 g/mol) in the standards (Table A1).

CS contains a form of uronic acid, D-glucuronate, as one of the sugars in its disaccharide unit. KS does not contain any uronic acid and is not detected by the uronic acid assay. The glucuronate sugar ($C_6H_7O_6$) found in CS has molecular weight of 175.12 g/mol, which is very similar to that of glucuronolactone (175.12/176.124 = 0.9943) (Table A1). As compared to a NaCS salt, the ratio of NaCS to D-glucuronate is 499.38/175.12 = 2.8516, which matches the value for dry weight: uronic acid ratio given in Table 1 of [4]. For aggrecan monomers, this ratio of dry weight: uronic acid was 3.29. A comparison of these ratios indicates that ~86.6% of an aggrecan monomer from rat chondrosarcoma is CS (2.85/3.29 = 0.86626).

The PG concentrations from [10], as presented in Figure 4 of [2], is from rat chondrosarcoma, which is known to contain no KS in the skeletal system [8]. Thus,

the PG concentrations were converted to FCD with a correction for the ratio between D-glucuronate and glucuronolactone.

$c_{PG} = m_{PG} / m_{H2O}$ in [g/ml] (A12)

m_{PG} * (uronic acid/dry weight ratio) = $m_{\text{uronic acid}}$, where the UA/DW ratio is 1/3.29 = 0.30395 (A13)

$m_{\text{uronic acid}} / MW_{\text{UA in glucuronolactone}}$ = moles of uronic acid (A14)

1 mole of uronic acid = 1 mole D-glucuronate in CS (A15)

moles uronic acid = moles D-glucuronate in CS*(1 mole CS/1 mole D-glucuronate) = moles CSmoles CS*(z_{CS}/mole CS) = fixed charge of CS

(A16)

$$FCD = c_{PG} * \left(\frac{UA}{DW}\right) * \frac{1\text{mole glucuronolactone}}{MW_{glucuronolactone(UAstd)}} * \frac{1\text{mole D-glucuronate}}{1\text{mole glucuronolactone}} * \frac{1\text{mole CS}}{1\text{mole D-glucuronate}} * \frac{z_{CS}}{1\text{mole CS}} * \left(\frac{1000\text{mEq}}{1\text{mol-charge}}\right)$$

(A17)

$$FCD = c_{PG} * \left(\frac{1}{3.29}\right) * \frac{1\text{mole glucuronolactone}}{176.124} * \frac{1\text{mole D-glucuronate}}{1\text{mole glucuronolactone}} * \frac{1\text{mole CS}}{1\text{mole D-glucuronate}} * \frac{2\text{mol-charge}}{1\text{mole CS}} * \left(\frac{1000\text{mEq}}{1\text{mol-charge}}\right)$$

(A18)

FCD = 3.45156* c_{PG} (A19)

Table A.1: Chondroitin sulfate and keratan sulfate structure, molecular formula, and molecular weight.

GAG	disaccharide structure	molecular formula	molecular weight [g/mol]
sodium CS salt (with H on carboxyl group)	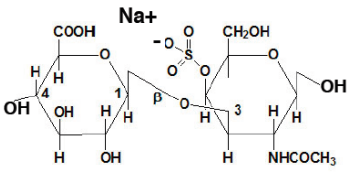	$C_{14}H_{22}NNaO_{15}S$	499.38
sodium CS salt in a chain (with H on carboxyl group)	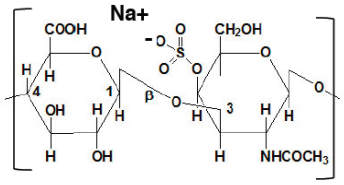	$C_{14}H_{20}NNaO_{14}S$	481.36
CS salt in a chain, without sodium (with H on carboxyl group)	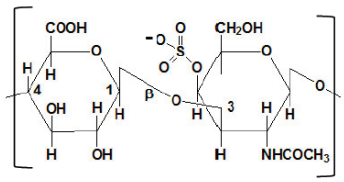	$C_{14}H_{20}NO_{14}S$	458.37
CS in a chain in solution (without H on carboxyl)	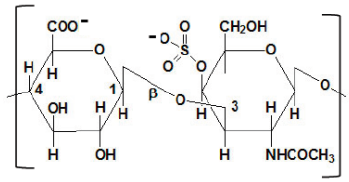	$C_{14}H_{19}NO_{14}S$	457.36
KS in a chain	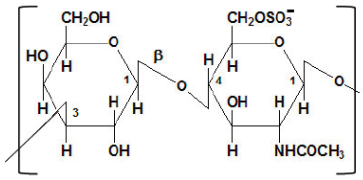	$C_{14}H_{22}NO_{13}S$	444.39
D-glucuronate in CS	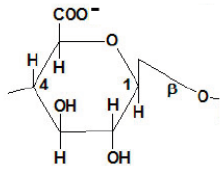	$C_6H_7O_6$	175.12
glucurunolactone	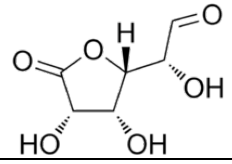	$C_6H_8O_6$	176.12

A.4 References

1. Bitter T, Muir HM: A modified uronic acid carbazole reaction. *Anal Biochem* 4:330-4, 1962.

2. Buschmann MD, Basser PJ, Grodzinsky AJ: A microstructural model for swelling pressure and compressive modulus of tissues containing charged GAG chains: comparison to Donnan theory. *ASME Advances in Bioengineering* BED-24:80-3, 1993.

3. Chahine NO, Chen FH, Hung CT, Ateshian GA: Direct measurement of osmotic pressure of glycosaminoglycan solutions by membrane osmometry at room temperature. *Biophys J* 89:1543-50, 2005.

4. Comper WD, Williams RP: Hydrodynamics of concentrated proteoglycan solutions. *J Biol Chem* 262:13464-71, 1987.

5. Dische Z: A new specific color reaction of hexuronic acids. *J Biol Chem* 167:189-98, 1947.

6. Nader HB, Ferreira TM, Paiva JF, Medeiros MG, Jeronimo SM, Paiva VM, Dietrich CP: Isolation and structural studies of heparan sulfates and chondroitin sulfates from three species of molluscs. *J Biol Chem* 259:1431-5, 1984.

7. Narmoneva DA, Wang JY, Setton LA: Nonuniform swelling-induced residual strains in articular cartilage. *J Biomech* 32:401-8, 1999.

8. Venn G, Mason RM: Absence of keratan sulphate from skeletal tissues of mouse and rat. *Biochem J* 228:443-50, 1985.

9. Venn MF, Maroudas A: Chemical composition and swelling of normal and osteoarthritic femoral head cartilage. I. Chemical composition. *Ann Rheum Dis* 36:121-9, 1977.

10. Williams RP, Comper WD: Osmotic flow caused by polyelectrolytes. *Biophys Chem* 36:223-34, 1990.

APPENDIX B

ANALYSIS OF FCD_{EF}, π_{PG}, AND σ_{CN} OF BOVINE PATELLO-FEMORAL GROOVE CARTILAGE

B.1 Materials and Methods

Data from a previous study were used [1]. Bovine cartilage from patello-femoral groove (PFG) of fetal, calf, and adult cows were tested under confined compression and analyzed as described for bovine femoral condyle cartilage (see Methods in main paper). The GAG/WW, COL/WW, and σ_{EQ} data were used to calculated the FCD_{EF}, π_{PG}, and σ_{CN} under compression.

B.2 Results

The GAG/WW were similar with growth in bovine PFG cartilage while COL/WW increased with growth (Fig. B.1; $p<0.05$ for Adult vs Fetal and Calf). The FCD_{EF} was generally higher for Calf and Adult cartilage than for Fetal cartilage under corresponding compression levels (Fig B.2A; $p<0.05$ for Adult vs Fetal at 15% and 30% compression). The π_{PG} closely approximated σ_{EQ} for all growth stages at all compression levels and trended higher for Calf and Adult cartilage than Fetal cartilage

(Fig. B.2B-D; $p<0.05$ for Adult vs Fetal). The σ_{CN} for bovine tissues were generally low and moved from tension at reference state to compression with applied compression. The CN pre-stress, or σ_{CN} at 0% compression, was higher for Adult cartilage than for Fetal cartilage ($p<0.05$). There was no effect of site (PFG vs condyle) on the FCD_{EF}, π_{PG}, and σ_{CN} at each compression level.

B.3 Discussion

The increases in FCD_{EF} and π_{PG} with bovine growth in PFG cartilage were consistent and similar to those observed in bovine femoral condyle cartilage. Even with similar GAG/WW content, the increase in FCD_{EF} and π_{PG} with growth suggest that the interaction between the PG and CN is important in the compressive properties of articular cartilage.

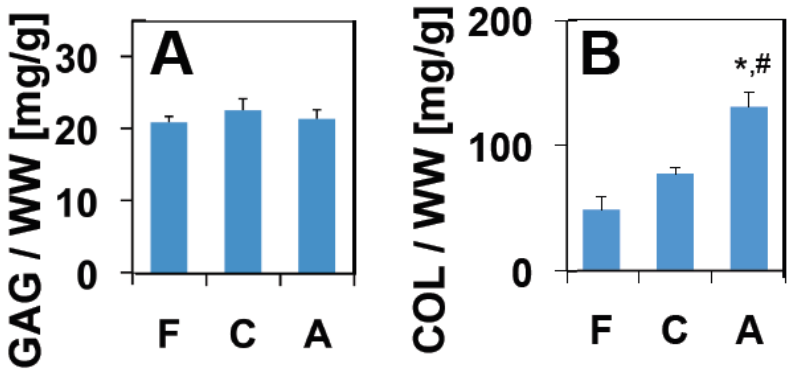

Figure B.1: GAG/wet weight (A) and collagen/wet weight (B) of bovine patello-femoral cartilage (Fetal, Calf, Adult). (* $p<0.001$ vs fetal; # $p<0.001$ vs calf)

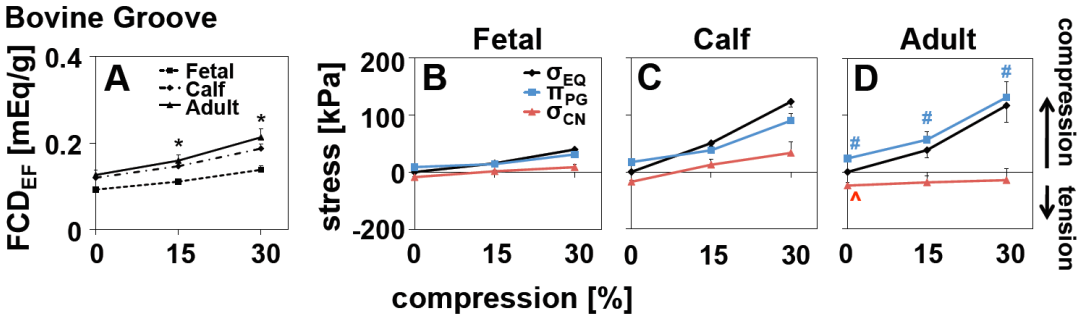

Figure B.2: FCD_{EF} (A) and π_{PG} along with σ_{EQ} and σ_{CN} (B-D) for bovine fetal (A, B), calf (A, C), and adult (A, D) patello-femoral cartilage. (* for FCD_{EF}, # for π_{PG}, ^ for σ_{CN}, $p<0.05$ vs fetal)

B.4 Reference

1. Williamson AK, Chen AC, Sah RL: Compressive properties and function-composition relationships of developing bovine articular cartilage. *J Orthop Res* 19:1113-21, 2001.

APPENDIX C

EFFECT OF DEPTH IN HUMAN CARTILAGE ON TOTAL AND EXTRAFIBRILLAR WATER CONTENT

C.1 Results

The total water content varied with depth ($p<0.05$ at 0%, 20%, and 30% compression) but was similar at corresponding depths in Young and Old cartilage ($p>0.15$) (Fig. C.1A, B).

The EF water content was trended higher in the superficial layer than the deeper layers at reference state for both Young and Old cartilage (Fig. C.1C,D; $p<0.01$). With the application of compression, the EF water content in the superficial layers decreased, but to lower EF water levels in Young cartilage than the Old cartilage.

C.2 Discussion

The larger decrease in EF water in the superficial layer for Young cartilage is likely the result of the higher strains observed in this layer than for Old cartilage.

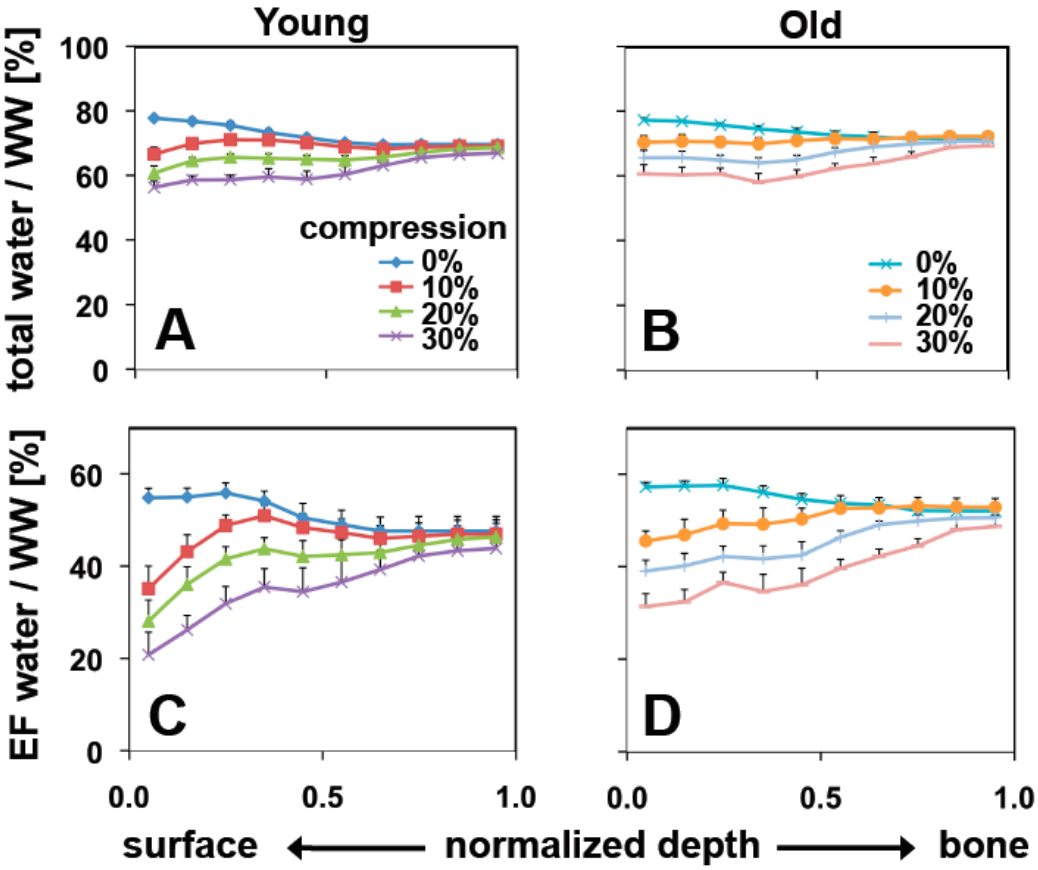

Figure C.1: Proportion of total water (A, B) and EF water (C, D) to total wet weight for human Young (A, C) and Old (B, D) cartilage with initial normalized depth of the tissue at each compression level (0%, 10%, 20%, 30%).

APPENDIX D

ANALYSIS OF RELEASED HA CONTENT IN PBS

D.1 Materials and Methods

To quantify the released HA content from PBS from days 1, 2, and 3 separately, PBS from group VI (AGC + 5% HA) was digested overnight at 60°C with 0.5 mg/ml proteinase K to remove possible interference from HA binding regions of aggrecan in the HA assay. The samples were incubated with 1 mM AEBSF for 2 hours at 37°C to inhibit proteinase K and assayed using HA test kit (Corgenix, Broomfield, CO) [1].

D.2 Results and Discussion

The release of HA into the PBS was similar for days 1, 2, and 3. The amount of HA released into the PBS was very small compared to the amount retained in the constructs (<10%). The HA used here is a relatively large molecule (~$4x10^6$ Da), which would become larger upon formation of aggregates with AGC. Thus, HA would likely be released very slowly into the PBS in comparison to unbound AGC monomers. Therefore, the PBS was pooled from days 1-3 due to a small and similar release of HA over days 1-3 in comparison to sGAG release.

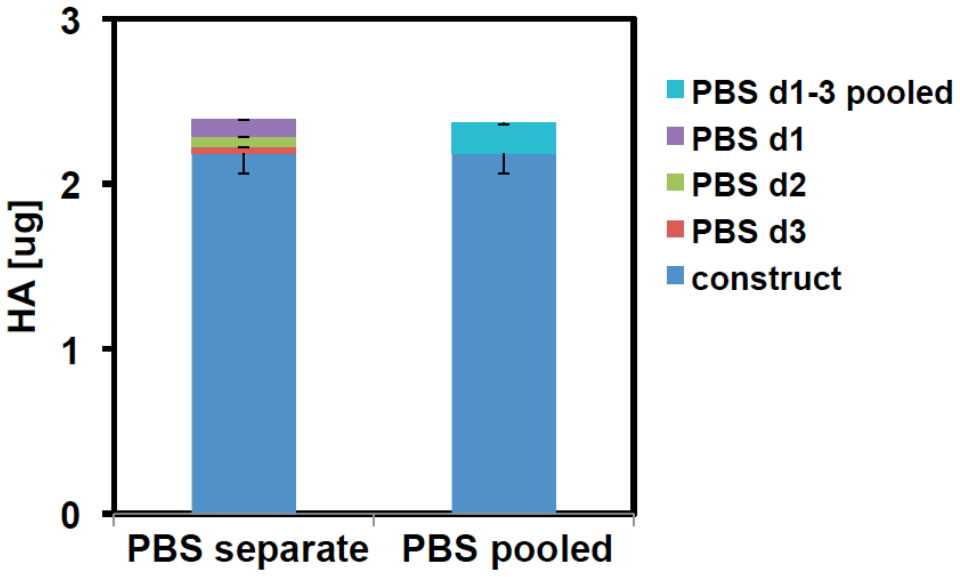

Figure D.1: HA content analysis on PBS and constructs Group VI (AGC + 5% HA) with PBS from days 1-3 separately or pooled together.

D.3 Reference

1. Asanbaeva A, Tam J, Schumacher BL, Klisch SM, Masuda K, Sah RL: Articular cartilage tensile integrity: Modulation by matrix depletion is maturation-dependent. *Arch Biochem Biophys* 474:175-82, 2008.

APPENDIX E

ANALYSIS OF CONFINED COMPRESSION TESTING SET-UP

E.1 Materials and Methods

Disk constructs (d=9.6mm) containing either no AGC (group I) or 2 mg/ml AGC with 5% HA (group VI) in 2% agarose with thickness of either 1.5mm or 3mm were prepared as described in the manuscript. Confined compression tests were performed on a stack of two 1.5mm thick constructs or one 3mm thick construct from groups I and VI (n=2-3 stacks) at day 0 using the same compression testing protocol as described in the manuscript. Unconfined compression tests were also performed on 3mm-thick, group I constructs (n=2), with the construct in between two non-porous platens and without a radially confining chamber, using the same testing protocol as the confined test. Photographs of the constructs were taken before and after compression testing. At each strain, the equilibrium stress was analyzed for differences in stacking setups (stacks of 1 or 2 constructs) by ANOVA with post-hoc Tukey test when significant variation ($p<0.05$) was detected.

E.2 Results and Discussion

The agarose constructs were able to withstand the high strains without fracturing in the confining chambers that limit radial expansion of the constructs. The constructs tested in an unconfined compression test resulted in failures of the constructs, with large cracks through the whole construct (Fig. E.1A).

From the confined compression tests, the equilibrium stresses at each of the strains were not significantly different for a stack of two constructs or a stack of one construct with the same sGAG contents (Fig. E.1B; $p>0.05$). Therefore, stacking of two constructs of similar sGAG content for the confined compression test should not pose a significant hindrance in interpretation of the data from this uniaxial confined compression test set up.

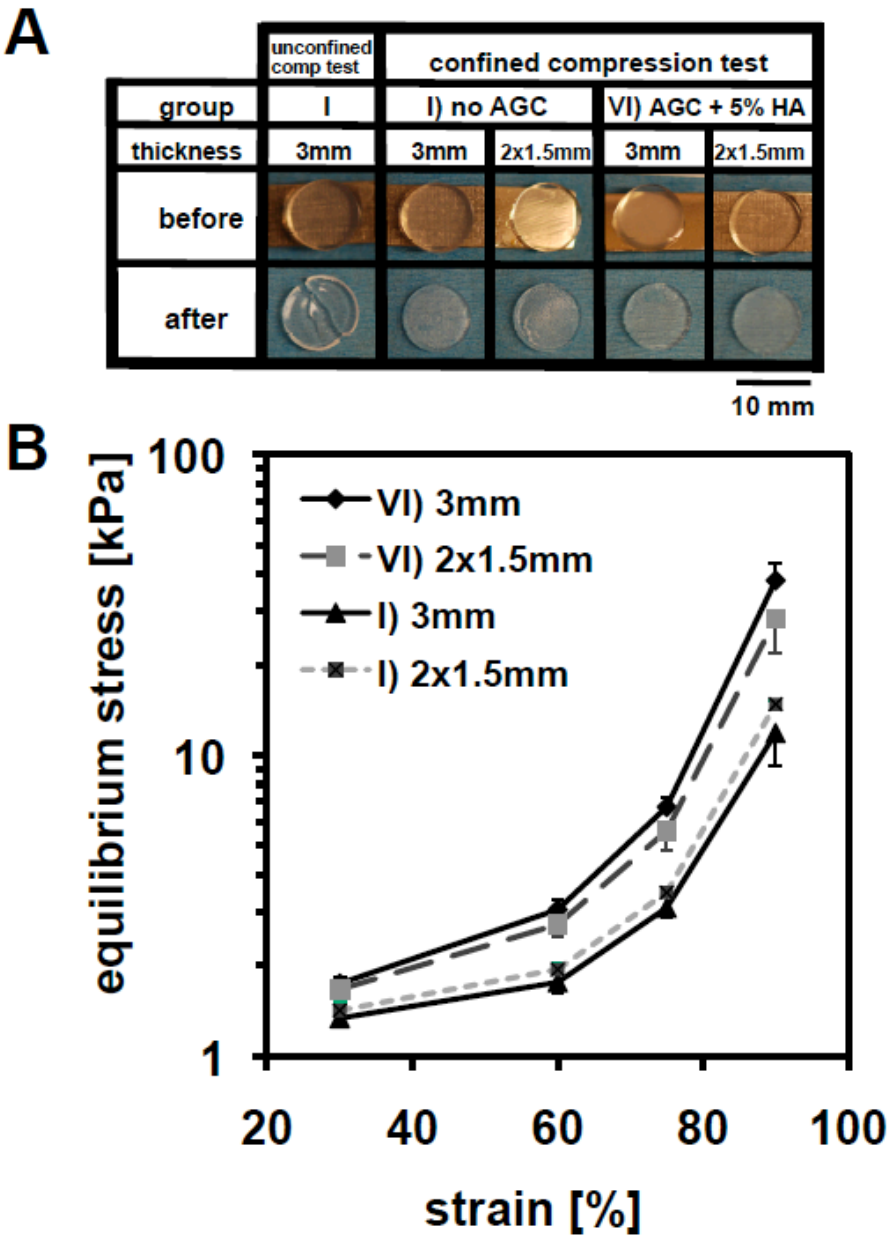

Figure E.1: Analysis of confined compression tests of constructs from Groups I (control) and VI (AGC + 5% HA), in either stacked (two constructs of 1.5mm thickness) or unstacked (one construct of 3mm thickness) set ups. Photographs of constructs before and after unconfined or confined compression tests (A). Equilibrium stresses at each strain for the group I and VI constructs in stacked or unstacked set ups (B, $p>0.05$ for all samples, n=2-3)

APPENDIX F

ANALYSIS OF RETENTION OF INITIAL MATRIX CONTENT AFTER COMPACTION

F.1 Materials and Methods

Smaller disk constructs (d=2mm, h=~3mm; n=3/group) from each of the experimental group were prepared and analyzed for matrix content at day 0. The constructs were solubilized by proteinase K digestion at 60°C overnight and incubation at 70°C for 2 minutes. The constructs were analyzed for sGAG content by dimethylmethylene blue assay [1] and for COL content by hydroxyproline assay [3]. The matrix contents of the constructs at day 0 were compared to that of the final constructs after compaction. Data are presented as mean ± standard error. Unpaired t-tests were performed to compare the matrix content in day 0 constructs and final compacted constructs.

F.2 Results and Discussion

The constructs retained of most of the initial matrix content after compaction and subsequent mechanical testing (Fig. S1). The constructs from Group II retained

~80% of the initial GAG content from day 0 after compaction and subsequent mechanical testing ($p=0.1$). The constructs from Group III retained 76% of the initial COL content from day 0 ($p=0.07$). The constructs from Group IV retained 78% of the initial GAG content and 73% of the initial COL content from day 0 ($p<0.05$).

Previous study found that ~10% of the PG is released into the PBS during the first day of PBS incubation [2]. This suggests that most of the matrix content was retained in the constructs and most of the compaction was due to fluid loss.

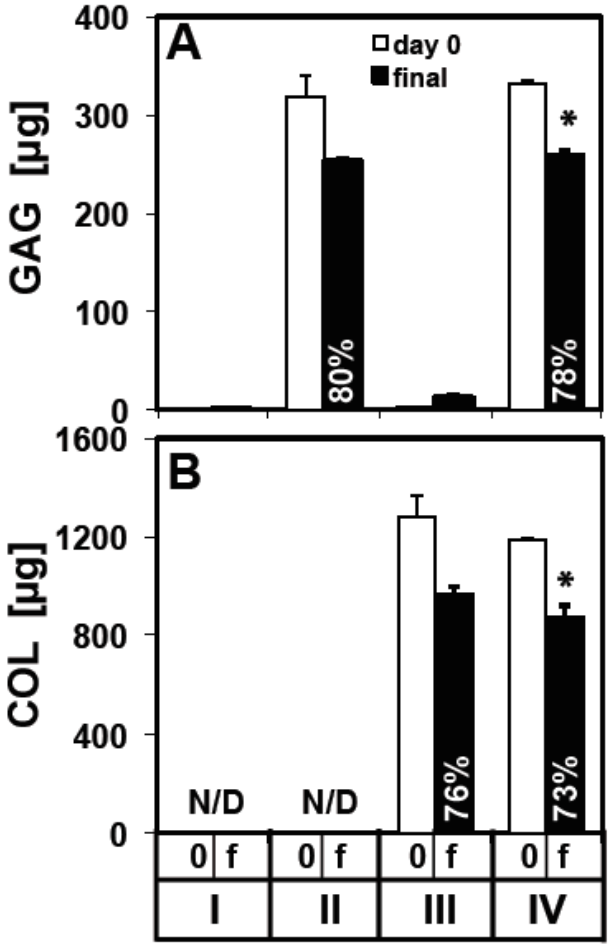

Figure F.1: Matrix content of day 0 constructs and final compacted constructs. The GAG content (A) and COL content (B) of day 0 constructs (0) and final compacted constructs (f) for Groups I (control), II (PG), III (COL), IV (COL+PG). The percent of retained matrix content from day 0 are noted. (* $p<0.05$ vs day 0 construct)

F.3 References

1. Farndale RW, Buttle DJ, Barrett AJ: Improved quantitation and discrimination of sulphated glycosaminoglycans by use of dimethylmethylene blue. *Biochim Biophys Acta* 883:173-7, 1986.

2. Han EH, Wilensky LM, Schumacher BL, Chen AC, Masuda K, Sah RL: Tissue engineering by molecular disassembly and reassembly: biomimetic retention of mechanically functional aggrecan in hydrogel. *Tissue Eng Part C Methods* 16:1471-9, 2010.

3. Woessner JF: The determination of hydroxyproline in tissue and protein samples containing small proportions of this imino acid. *Arch Biochem Biophys* 93:440-7, 1961.